

**DEVELOPMENT AND APPLICATION OF COUNTERFLOW  
METHODS: GEITP, GEITP-CZE, TGF, TGDF**

---

A Thesis  
Submitted  
to the Temple University Graduate Board

---

In Partial Fulfillment  
of the Requirements for the Degree of  
MASTERS OF ARTS, CHEMISTRY

---

By  
**Nejea I. Davis**  
May, 2011

Thesis Committee Members:

Dr. Jonathan G. Shackman, Thesis Advisor, Former Associate Professor, Temple University, Chemistry Department

Dr. Susan Jansen-Varnum, Committee Chair, Professor, Temple University, Chemistry Department

Dr. Robert Stanley, Committee Member, Professor, Temple University, Chemistry Department

©  
Copyright  
2011

by

Nejea I. Davis  

---

All Rights Reserved

## **ABSTRACT**

Extensive research on amino acids, and even other biochemical assays usually present in low concentration and volume face challenges using known analytical techniques for analysis of traces amounts. Some limiting factors are the achievable efficiency, sensitivity (resulting from instrument limit of detection and/or experimental methods), volume requirement, and total analysis time. Counterflow electrofocusing techniques combining forces of electrophoresis and bulk flow (pressure driven flow and/or electroosmotic flow) provides a basis for the development of alternative detection techniques geared towards improving peak efficiency, sensitivity and time. The work presented gives a vivid description of recently developed capillary counterflow techniques: gradient elution isotachopheresis (GEITP) using UV detection, GEITP coupled to Capillary Zonal Electrophoresis (GEITP-CZE), temperature gradient focusing (TGF), and temperature gradient denaturing focusing (TGDF).

A first demonstration of GEITP using UV detection was applied to enrichment and separation of tyrosine and tryptophan under optimized conditions. Primarily, separation is achieved as the result of the difference in electrophoretic velocity of analytes in a discontinuous buffer system. First, a plug of sample is allowed to preconcentrate (or enrich) between high mobility leading electrolyte (LE) and low mobility trailing electrolyte (TE) under controlled hydrodynamic pressure and continuous injection. This preconcentration is initiated outside the capillary in a conductivity bubble of analyte, TE, LE and spacer ions. Although analytes focus according to their

electrophoretic velocity, the inclusion of spacer molecule in sample matrix was instrumental in achieving separation with tradeoff between analyte's resolution and enrichment. Gradient produced results from reduction in pressure as sample is loaded on column. Separation using this technique is a one step process.

A hybrid method marking the first successful coupling of GEITP to CZE with laser induced fluorescence detection was used for separation of six fluorescently labeled amino acids (which formulates the Mars-7). An eleven minute separation was achieved under optimized conditions.

A proof-of-concept demonstration of TGF with LIF detection showed focusing and separation of fluorescein and carboxyfluorescein dye molecules, and carboxyfluorescein-labeled glutamate and aspartate. The generation of null focusing point (which is different for each ion) along the thermal separation column (set between 80-20°C) was produced in collaboration with continuous sample injection, discontinuous buffer system and balancing of counterflows (electrophoresis and bulk flow). Preliminary results showed stability in instrument.

The TGDF method carried out on a TGF apparatus is a modification to the known temperature gradient gel electrophoresis (TGGE) and denaturing gradient gel electrophoresis (DGGE) methods. In principle, TGDF primarily achieves focusing and separation on a thermal separation column (set between 20 to 80 °C) as a result of conformational changes. This method is currently being developed for the detection and simultaneous separation of single and double stranded DNA. Preliminary results show enrichment of wildtype and mutant synthetic DNA strands (containing twenty-four base pairs in sequence, 24mer) in different buffer matrices.

## **ACKNOWLEDGMENTS**

I am profoundly grateful to the ALMIGHTY God amidst the odds and personal struggles for life, opportunity, will-power, health and strength in completing this work, and yet, another milestone in my life.

I express heartfelt thanks, and sincere appreciation to my research advisor Dr. Jonathan Graham Shackman, Former Associate Professor, Chemistry Department, for his valuable supervision, patience, and scholarly enlightenment that was necessary in completing this phase of my graduate studies. The guidance provided throughout this process was indeed insightful, introduced me to a new approach of research, and prepared me for the scientific world. Thanks for giving me the opportunity to research in your lab. It was truly a great and interesting experience; the knowledge attained, challenges, and lessons learned can only be valuable for future pursuits.

Sometimes it is not how long you know someone, but the quality of the friendship is what matters. I say special thanks to my undergraduate advisor, Dr. Susan Jansen-Varnum, Dr. Allan Thomas, Dr. Roy Keyer, and Dr. Stephen Cox, for their mentorship, friendship, encouragement, discussions, and upliftment through this journey. Your kind words and concern got me through tough times when my confidence was weak, and spirit broken. I am delighted to know you all. Most of all, I thank you all for believing in my potential.

To my graduate committee members: Dr. Jonathan G. Shackman, Dr. Susan Jansen-Varnum and Dr. Robert Stanley, I say thanks for consenting to serve on my committee even with your busy schedules.

The fulfillment of this degree would not have been possible without the financial support from the National Science Foundation Louis Stokes Alliances for Minority Participation (NSF-LSAMP) Bridge-to-the-Doctorate Fellowship, and Chemistry Department Teacher's Assistantship, Temple University. I say thanks for the opportunity and support.

Finally, I thank my parents, good friends and colleagues, especially Andro Marc Pierre-Louis and all my well-wishers for moral support, inspiration and good wishes. I also say thanks to my lab colleague, Manasa Mamunooru, with whom I collaborated with on all research projects.

## **DEDICATION**

This thesis is dedicated to my parents, Mr. Isaac S. Davis, Sr., and Ms. Edith V. McIntosh, my deceased Grandmother, Amanda Jane Randall Montgomery and Mrs. Willette Porte for their love and moral support. Also, to the Louis Stokes Alliance for Minority Participation (LSAMP) for financial support and the opportunity for educational advancement.

## PREFACE

This thesis describes alternative electrophoretic based analytical methods: Gradient Elution Isotachopheresis (GEITP), GEITP coupled to Capillary Zonal Electrophoresis (GEITP-CZE), Temperature Gradient Focusing (TGF), and Temperature Gradient Denaturing Focusing (TGDF), developed by the Shackman lab. Counterflow electrofocusing is effectively used to concentration analytes at a dynamic equilibrium point. These methods can be exploited for: studying a wider range of sample type, trace analysis, improving sample resolution and sensitivity, microfluidics options, and making other quantitative studies. A reference section climaxes each chapter.

The discussions in chapter 1, is directed to a selective discussion of fundamental concepts of separation necessary for understanding counterflow electrofocusing. Here, a concise explanation of the following concepts: capillary electrophoresis (or capillary zonal electrophoresis), isotachopheresis (ITP), and counterflow electrofocusing are discussed in part. The focus of each concept is on general description technique, basic principles, instrumentation and applications. However, a general review of Fick's law of diffusion and the mass transport phenomena will be presented to give a background on the counterflow concept.

In chapter 2, a two-fold discussion of research work based on recently developed counterflow technique, GEITP, would be presented. GEITP combines continuous sample injection against a discontinuous buffer interface with a hydrodynamically controlled

bulk counterflow in a capillary or microchannel. In part one, the research work focuses on the analysis of slow mobility amino acids, tryptophan and tyrosine, using GEITP as a stand-alone method with a universal detection system. Also, these analytes were separated from artificial cerebrospinal fluid to demonstrate the applicability of GEITP. Parametric and optimized conditions employed showed comparable limits of detection and very rapid analysis time. In part two, using the hybrid technique, GEITP-CZE with laser induced fluorescence detection, enrichment and separation of six amino acids (glutamate, aspartate, glycine, alanine, valine, and serine) showing femtomolar limit of detection would be discussed in details.

In chapter 3, the TGF method is briefly described and demonstrated. TGF operates by creating a pseudo-equilibrium point (or focusing point) for each analyte ion along a thermal microchannel resulting from counteraction between bulk flow and electrophoresis. A summary of theoretical description of the method will be presented to show how temperature, velocity, and concentration can be determined in a system under TGF conditions. A brief results section would show a demonstration of the TGF method for focusing and separation of fluorescein and carboxyfluorescein dye molecules, and carboxyfluorescein-labeled glutamate and aspartate.

In chapter 4, an inconclusive research on the separation and enrichment of single and double DNA strands using the TGDF method would be summarized. Although TGDF functions on the same operational scheme and instrumentation as TGF, the concept is slightly different. For TGDF, focusing is based on analyte's (DNA) conformational change. A summary of different buffer systems used in this study would be presented. The conditions and results presented here are not optimized and cannot be

completely justified because of irreproducibility issues. However, the experiments herein can be use as a guide for continuation and evaluation of this project.

## TABLE OF CONTENTS

	PAGE
ABSTRACT.....	iv
ACKNOWLEDGMENTS .....	vi
DEDICATION.....	viii
PREFACE.....	ix
LIST OF TABLES .....	xvi
LIST OF FIGURES .....	xvii
CHAPTER 1: FUNDAMENTAL CONCEPTS	
1.1 CAPILLARY ELECTROPHORESIS .....	1
1.1.1. INTRODUCTION .....	1
1.1.2. BASIC PRINCIPLES AND THEORY .....	2
<i>1.1.2.1. ELECTROPHORESIS</i> .....	2
<i>1.1.2.2. ELECTROOSMOTIC FLOW (EOF)</i> .....	4
<i>1.1.2.3. NET MOBILITY</i> .....	7
<i>1.1.2.4. JOULE HEATING</i> .....	7
<i>1.1.2.5. EFFICIENCY AND RESOLUTION</i> .....	9
<i>1.1.2.6. INJECTION MODES</i> .....	10
1.1.3. INSTRUMENTATION .....	13
1.1.4. MODES OF OPERATION.....	14
1.1.5. REFERENCES CITED.....	16

1.2. ISOTACHOPHORESIS .....	18
1.2.1. INTRODUCTION .....	18
1.2.2. BASIC PRINCIPLES AND THEORY .....	19
<i>1.2.2.1. BASIC ITP PROCESS</i> .....	19
<i>1.2.2.2. KOHLRAUSCH REGULATING FUNCTION IN ITP</i> .....	22
<i>1.2.2.3. RESOLUTION IN ITP</i> .....	23
1.2.3. INSTRUMENTATION .....	24
1.2.4. COUNTERFLOW IN ITP .....	24
1.2.5. MODES OF OPERATION.....	25
1.2.6. REFERENCES CITED.....	25
1.3. COUNTERFLOW ELECTROFOCUSING .....	29
1.3.1. GENERAL OVERVIEW .....	29
1.3.2. BASIC THEORY .....	32
1.3.3. REFERENCES CITED.....	37
 CHAPTER 2: GRADIENT ELUTION ISOTACHOPHORESIS	
2.1. GRADIENT ELUTION ISOTACHOPHORESIS WITH DIRECT UV ABSORPTION DETECTION FOR SENSITIVE AMINO ACID ANALYSIS .....	40
2.1.1. ABSTRACT.....	40
2.1.2. INTRODUCTION .....	41
2.1.3. EXPERIMENTAL.....	47
<i>2.1.3.1. CHEMICALS AND REAGENTS</i> .....	47
<i>2.1.3.2. INSTRUMENTATION</i> .....	47
2.1.4. RESULTS AND DISCUSSION.....	48
<i>2.1.4.1. EFFECT OF CAPILLARY I.D. ON ENRICHMENT</i> .....	48

2.1.4.2. <i>COMPARISON OF LE VERSUS ELECTRIC FIELD ADJUSTMENT OF CURRENT</i> .....	56
2.1.4.3. <i>APPLICATION TO AMINO ACID ANALYSES</i> .....	61
2.1.5. CONCLUSION.....	64
2.1.6. REFERENCES CITED.....	66
2.2. GRADIENT ELUTION ISOTACHOPHORESIS COUPLED TO CAPILLARY ZONE ELECTROPHORESIS FOR SENSITIVE AMINO ACID ANALYSES.....	69
2.2.1. ABSTRACT.....	69
2.2.2. INTRODUCTION .....	70
2.2.3. EXPERIMENTAL.....	73
2.2.3.1. <i>CHEMICALS AND REAGENTS</i> .....	73
2.2.3.2. <i>INSTRUMENTATION</i> .....	74
2.2.4. RESULTS AND DISCUSSION.....	76
2.2.4.1. <i>GEITP-CZE OPERATION</i> .....	76
2.2.4.2. <i>HYDRODYNAMIC FLOW EFFECTS DURING CZE</i> .....	78
2.2.4.3. <i>LE EFFECTS ON ENRICHMENT</i> .....	80
2.2.4.4. <i>INITIAL PRESSURE EFFECTS ON ENRICHMENT</i> .....	83
2.2.4.5. <i>GEITP DURATION EFFECTS</i> .....	85
2.2.4.6. <i>APPLICATION TO AMINO ACID MIXTURES</i> .....	87
2.2.5. CONCLUSION.....	89
2.2.6. REFERENCES CITED.....	90
 CHAPTER 3: TEMPERATURE GRADIENT FOCUSING	
3.1. ABSTRACT.....	93
3.2. INTRODUCTION .....	94

3.3. THEORY OF TGF.....	97
3.4. EXPERIMENTAL.....	99
3.4.1. <i>CHEMICALS AND REAGENTS</i> .....	99
3.4.2. <i>INSTRUMENTATION</i> .....	100
3.5. RESULTS AND DISCUSSION.....	102
3.5.1. <i>TGF CONCEPT AND OPERATION</i> .....	102
3.5.2. <i>TGF SEPARATION OF CARBOXYFLUORESCHEIN AND           FLUORESCHEIN</i> .....	105
3.5.3. <i>TGF SEPARATION OF AMINO ACIDS</i> .....	107
3.6. CONCLUSION.....	107
3.7. REFERENCES CITED.....	109

#### CHAPTER 4: TEMPERATURE GRADIENT DENATURING FOCUSING

4.1. ABSTRACT.....	112
4.2. INTRODUCTION.....	113
4.3. THEORY OF TGF.....	117
4.4. EXPERIMENTAL.....	119
4.4.1. <i>CHEMICALS AND REAGENTS</i> .....	119
4.4.2. <i>INSTRUMENTATION</i> .....	122
4.5. RESULTS AND DISCUSSION.....	123
4.5.1. <i>CONCEPT AND OPERATION OF TGDF</i> .....	123
4.5.2. <i>OHM'S LAW PLOT</i> .....	125
4.5.3. <i>TGDF ENRICHMENT</i> .....	128
4.5.4. <i>EVALUATING TRENDS IN MIGRATION TIME</i> .....	130
4.5.5. <i>DETERMINATION AND COMPARISON OF BUFFER           SYSTEMS</i> .....	132
4.5.6. <i>SEPARATION IN BSA</i> .....	134

4.5.7. <i>HARDWARE MODIFICATION</i> .....	136
4.6. CONCLUSION.....	138
4.7. REFERENCES CITED.....	139
BIBLIOGRAPHY.....	148

## LIST OF TABLES

<u>Table</u>	<u>Page</u>
<b>Table 1.3.1</b> Summary of counterflow techniques presented.....	31
<b>Table 2.1.1.</b> Selected CE-based methods for Trp and Tyr measurements .....	46
<b>Table 2.1.2.</b> Experimental parameters to assess affect of capillary I.D. on enrichment.....	51
<b>Table 2.1.3.</b> Experimental parameters to compare current adjustment by LE or electric field .....	57
<b>Table 2.2.1.</b> Amino Acid Detection Limits <sup>a</sup> .....	88
<b>Table 3.1.</b> List of TGF advantages and disadvantages of TGF.....	96
<b>Table 4.1.</b> DNA oligonucleotides .....	121
<b>Table 4.2.</b> Summary of comparison .....	133

## LIST OF FIGURES

<u>Figure</u>	<u>Page</u>
<p><b>Figure 1.1.1.</b> Electroosmotic Flow. Cations, <math>\oplus \rightarrow</math> and anions, <math>\ominus \rightarrow</math> are circles with + or - sign attached to arrowhead indicating direction of flow; neutrals, <math>\bullet</math> are filled circles; and ionized silanol groups are represented by the circles with - sign, <math>\ominus</math>. The voltage potential in each reservoir is shown by the large circles without arrowhead: anode, <math>\oplus</math> and cathode, <math>\ominus</math>.</p>	6
<p><b>Figure 1.1.2.</b> CE injection modes. (a) electrokinetic injection is driven by EOF resulting in a flat profile. (b) hydrodynamic injection is driven by pressure gradient resulting in a laminar (parabolic) flow profile.</p>	12
<p><b>Figure 1.1.3.</b> Capillary tube.</p>	12
<p><b>Figure 1.1.4.</b> Schematic of CE operation. (a) Hydrodynamic injection of sample plug into capillary. (b) Solution in source vial is replaced with buffer and high voltage (~30kV) is simultaneously applied. Depending on the analyte's charge, net flow is either toward anode or cathode. Species are detected in order of charge and electrophoretic mobility (anions (-), neutrals (N), and cations (+)).</p>	15
<p><b>Figure 1.2.1.</b> Schematic of Anionic Isotachopheresis (ITP) mode. (a) Typical stacking stages occurring in ITP are as follows: <b>i.</b> the capillary is filled with LE solution; <b>ii.</b> under a constant electric field a slug of undifferentiated analyte ions zone begin to migrate (by electrophoresis) with high mobility LE ions ahead of the slug; <b>iii.</b> ionic zones begin to form as migration proceeds and field strength changes as zone length overlaps; <b>iv.</b> same as <b>iii</b> but zone formation more defined; not shown is possible zone overlap between A and LE ions and B and TE ions (<b>iii-iv</b>); <b>v.</b> pseudo steady state results in discrete zones moving at same speed. (b) Non-steady state (analogous to (a) <b>iii</b> and <b>iv</b>); LE ions force slug to stack in direction towards high field. Stacking order of ions: LE&gt;A&gt;A+B (intermediate zone)&gt;B&gt;TE; low mobility ions (TE) experience highest field strength. (c) analogous to (a)<b>v</b>; established pseudo-steady state profile of field strength as a function of electrophoretic velocity. Stacking order and field strength profiles same as (b) but no intermediate zones only discrete zones.</p>	21
<p><b>Figure 1.3.1</b> Counterflow schematic.</p>	33
<p><b>Figure 1.3.2.</b> One dimensional diffusion.</p>	33

**Figure 2.1.1.** Instrumentation and concept of GEITP. (a) Schematic of instrument used for performing GEITP with UV detection. A 15 cm capillary connected a pressure controlled and grounded reservoir containing 750  $\mu\text{L}$  of leading electrolyte (LE) solution to a 100  $\mu\text{L}$  sample reservoir maintained at high voltage. Detection was performed 6 cm from sample inlet. (b) In GEITP the initial bulk flow (hydrodynamic and electroosmotic, EOF) is high enough that LE is pushed into the sample reservoir. (c) It is hypothesized that the LE creates an ionic interface upon which analytes and trailing electrolyte (TE) are enriched as the counter-flow is reduced. (d) As the hydrodynamic flow is further reduced, the interface and analyte zones are pulled into the capillary forming enriched zones based on order of electrophoretic mobility where they will be detected on-capillary. Zone resolution can be achieved using non-detectable spacer ions. ....44

**Figure 2.1.2.** Examples of flow-through (FT) and GEITP-UV detection. (A) FT in a 30  $\mu\text{m}$  I.D. capillary of 1, 2, 4, and 8 mM Trp obtained by step-changing the applied pressure from 7000 Pa to -7000 Pa at the start of data collection. (B) GEITP-UV of 100, 200, 300, and 400  $\mu\text{m}$  Trp. 15 cm capillary (30  $\mu\text{m}$  I.D.); 6 cm separation length; -400 V/cm; -58.6 Pa/s acceleration; LE: 50 mM acetate balanced to pH 9.5 with ETA; TE, 0.1 M NaOH with 0.2% (v/v) ampholyte. ....51

**Figure 2.1.3.** Effect of capillary I.D. on GEITP enrichment. See Table 2.1.2 for individual separation conditions. (a) FT and GEITP calibration curves using 75  $\mu\text{m}$  I.D. capillary. (b) 50  $\mu\text{m}$  I.D. capillary calibration curves with the same acceleration and current density ( $a$  and  $J$ ), pressure step and current density ( $\Delta P$  and  $J$ ), acceleration and current ( $a$  and  $i$ ), and pressure step and current ( $\Delta P$  and  $i$ ) as used for the 75  $\mu\text{m}$  I.D. capillary in (a). (c) Same as (b) using 30  $\mu\text{m}$  I.D. capillary. (d) Comparison of sensitivity enrichment over FT *versus* capillary I.D. (e) Comparison of N *vs.* capillary I.D. All error bars are 1 SD ( $n = 3$ ). ....55

**Figure 2.1.4.** Comparison of LE *vs.* electric field strength ( $E$ ) adjustment of current. See Table 2.1.3 for individual separation conditions. (a) Calibration curves of GEITP enrichment using various concentrations of acetate as LE (all balanced to pH 9.5 with ETA). (b) Calibration curves of GEITP enrichment using fields of -400, -682, and -780 V/cm to generate equivalent initial currents as generated using 50, 100, and 150 mM acetate LE at -400 V/cm. (c) Comparison of sensitivity enrichments when current was adjusted by either LE or field strength. (d) Comparison of plate number when current was adjusted by either LE or field strength. All error bars are 1 SD ( $n = 3$ ).....58

**Figure. 2.1.5.** Monitoring current in GEITP. (a) Ohm's law plots of 50, 100, and 150mM acetate balanced to pH 9.5 with ETA present in both the sample and pressure controlled reservoirs. No pressure was applied during the current measurement. All error bars are 1 SD ( $n = 3$ ). (b) Examples of current changes during the course of GEITP using 50mM acetate LE at -400 V/cm, 150mM LE at -400 V/cm, and 50mM LE at -720 V/cm. TE, 0.1M NaOH with 0.2% (v/v) ampholyte. The power supply had a maximal output of 300  $\mu\text{A}$ . ....60

**Figure 2.1.6.** Optimized amino acid analyses by GEITP. (a) FT and GEITP calibration curves for Trp and Tyr. 15 cm capillary (30  $\mu\text{m}$  I.D.); 6 cm separation length; -400 V/cm; -58.6 Pa/s acceleration; LE: 250 mM acetate balanced to pH 9.5 with ETA; TE: 0.1 M NaOH with 0.2% (v/v) ampholyte. Error bars are 1 SD ( $n = 3$ ). Example electropherograms showing the separation of 2  $\mu\text{M}$  Tyr and 500 nM Trp samples (b) in only TE and (c) in 1:20 aCSF:TE.....63

**Figure 2.2.1.** Instrumentation for and concept of GEITP-CZE. A) The capillary format utilized 11 cm of capillary connecting a pressure controlled and grounded 750  $\mu\text{L}$  reservoir containing leading electrolyte (LE) to a 100  $\mu\text{L}$  open-atmosphere reservoir containing sample and trailing electrolyte (TE). Detection was performed by laser-induced fluorescence (LIF) microscopy 6 cm from the sample inlet. (B) In-house instrumental set-up. (C) The stages to perform GEITP-CZE are as follows: (i) Initially, LE is dispersed into sample reservoir by relatively high bulk flow, a combination of hydrodynamic ( $\Delta P$ ) and EOF ( $\mu_{\text{EOF}}$ ) flows. Anionic analyte mobility ( $\mu_a$ ) is toward the microcolumn outlet. (ii) As pressure is reduced, analytes form ITP zones at the ionic interface and are enriched between LE and TE. (iii) Pressure is further reduced, and enriched zones are introduced onto the microcolumn. (iv) Applied pressure and voltage are discontinued. LE replaces the TE and sample solution. (v) Voltage and static hydrodynamic flow toward the outlet are applied. Because of the presence of TE, a short stage of tITP occurs. (vi) Once LE enters the TE zone, CZE conditions are present and analytes separate based on their respective electrophoretic mobilities. ....77

**Figure 2.2.2.** Effect of hydrodynamic flow on CZE resolution. (A) Example electropherograms of 500 pM Gly/Ala mixtures introduced by GEITP and separated by CZE at various pressures. Peaks marked Dye were due to unreacted conjugate and side reaction products. LE, 50 mM citrate balanced with tris (pH 8.5); TE, 250 mM tris-borate (pH 8.5); -600 V/cm; GEITP initial, 2000 Pa; GEITP final, -4000 Pa; gradient, -500 Pa/s. (B) Plot of resolution versus square root of average migration times ( $t_{\text{m,avg}}$ ). Error bars are 1 standard deviation ( $n = 3$ ). ....79

**Figure 2.2.3.** Effect of LE on enrichment with constant GEITP parameters: A) Gly enrichment (relative to 50 mM LE, as described in the text) as LE concentration increased. Error bars are 1 standard deviation ( $n = 3$ ). LE, citrate balanced with tris (pH 8.5); TE, 250 mM tris-borate (pH 8.5); -600 V/cm; GEITP initial: 2000 Pa; GEITP final: -4000 Pa; gradient, -250 Pa/s; CZE pressure, normalized to  $t_{\text{m}} = 150 \pm 10$  s. (B) Example currents observed at the LE concentrations used in part A. The middle, zero-current region was the point of solution exchange. ....82

**Figure 2.2.4.** Effect of initial GEITP pressure on enrichment. (A) Example electropherograms of 50 pM Gly introduced by GEITP with varying start pressures but constant gradients and pressure differentials (initial minus final pressure). Peaks marked Dye were due to unreacted conjugate and side reaction products. LE, 200 mM citrate balanced with tris (pH 8.5); TE, 250 mM tris-borate (pH 8.5); -600 V/cm; GEITP pressure differential, 6000 Pa; gradient, -250 Pa/s; CZE pressure, normalized to  $t_m = 150 \pm 10$  s. (B) Measured Gly peak heights and areas as the start pressure varied. (C) Measured Gly peak plates as the start pressure varied. Error bars for parts B and C are 1 standard deviation ( $n = 3$ ). (D) Example currents observed as the start pressure varied. The middle, zero-current region was the point of solution exchange. ....84

**Figure 2.2.5.** Effect of GEITP duration on enrichment. With a constant initial and final pressure for GEITP, the gradient steepness was reduced to increase the enrichment time. Plot shows increasing Gly enrichment (relative to the shortest time, 12 s, as described in the text) as GEITP duration increased. Error bars are 1 standard deviation ( $n = 3$ ). LE, 50 mM citrate balanced with tris (pH 8.5); TE, 250 mM tris-borate (pH 8.5); -600 V/cm; GEITP initial, 2000 Pa; GEITP final, -4000 Pa; CZE pressure, -2500 Pa. ....86

**Figure 2.2.6.** Capillary GEITP-CZE analysis of six carboxyfluorescein-labeled amino acids. The sample consisted of (in picomolar): 6.25 Asp, 6.25 Glu, 12.5 Gly, 25 Ala, 25 Ser, and 62.5 Val. Peaks marked Dye were due to unreacted conjugate and side reaction products. LE, 50 mM citrate balanced with tris (pH 8.5); TE, 250 mM tris-borate (pH 8.5); -600 V/cm; GEITP initial, 1000 Pa; GEITP final, -1000 Pa; gradient, -10 Pa/s; CZE pressure, -600 Pa. ....88

**Figure 3.1.** TGF instrumentation and concept. **A.** Assembly of the capillary format of TGF. 8.0 cm of capillary (1.9 cm from the sample inlet) connecting a pressure controlled and grounded 750  $\mu$ L reservoir containing background buffer to a 100  $\mu$ L open-air reservoir containing sample and background electrolyte matrix. Detection was performed by laser-induced fluorescence (LIF) microscopy. **B.** Photograph of the in-house instrument set-up. **C.** Schematic of TGF in a microcolumn. **D.** Establishment of conductivity due to temperature change across a microcolumn. For a given electrolyte, the relationship may be as shown or reversed. **E.** Illustration of the three major forces involved in focusing.<sup>20,28</sup> The convective or bulk velocity incorporates both hydrodynamic and EOF velocities. Focusing occurs at the equilibrium point where electrophoretic and convective velocities balance. ....104

**Figure 3.2.** Example of flow-through (FT) of carboxyfluorescein (FAM). **A.** FT in a 25  $\mu$ m I.D. capillary of 10, 35, 100, and 300 nM FAM obtained by step-changing the applied pressure from 10,000 Pa to -10000 Pa at the start of data collection. **B.** TGF calibration curve of 10, 35, 100, and 300 nM FAM. 8.0 cm capillary (25  $\mu$ m I.D.); -1000 V/cm; -10 Pa/s acceleration; buffer: 0.5 M Tris-Borate balanced to pH 8.29. **C.** Example electropherogram showing separation of carboxyfluorescein (FAM) and fluorescein. TGF separation of 10 nM F and FAM in 8.0 cm capillary

(25  $\mu\text{m}$  I.D.); -1000 V/cm; -10 Pa/s acceleration; buffer: 0.5 M Tris-Borate balanced to pH 8.29. ....106

**Figure 3.3.** Separation of aspartate (Asp) and glutamate (Glu). Calibration curves for 10, 100, 250, and 500 nM Asp (**A**) and Glu (**B**) in 8.0 cm capillary (25  $\mu\text{m}$  I.D.); -1000 V/cm; -10 Pa/s acceleration; buffer: 0.5 M Tris-Borate balanced to pH 8.29. **C.** Example electropherogram of TGF separation and focusing of Asp and Glu. ....108

**Figure 4.1.** TGDF Concept. **A.** TGDF instrument. Assembly of the capillary format of TGF. 7.0 cm of capillary (1.4 cm from the sample inlet) connecting a pressure controlled and grounded 750  $\mu\text{L}$  reservoir containing background buffer to a 100  $\mu\text{L}$  open-air reservoir containing sample and background electrolyte matrix. Detection was performed by laser-induced fluorescence (LIF) microscopy. **B.** Schematic of TGDF in a microcolumn. **C.** Establishment of temperature gradient. **D.** Three major forces controlling focusing. The bulk velocity incorporates both hydrodynamic and EOF velocities. Focusing occurs at the equilibrium point where electrophoretic and bulk velocities balance to zero. **A-D** same as TGF. **E.** Focusing of dsDNA as it denatures. DNA to the left of the focus point has a higher electrophoretic mobility ( $\mu$ ) and will overcome the counter-flow ( $v_{CF}$ ) to move to the right. Should the DNA travel past the focus zone,  $\mu$  continues to decrease and counter-flow forces it back into the focus zone. **F.** Recovery of melted DNA. As the focused zone approaches the dsDNA melting temperature, the likelihood for full melting increases. If the ssDNA reanneals faster than it migrates through the gradient, focusing can be restored. The continuous presence of labeled DNA (probe) increases the chances of recombination. Grey arrows show relative net velocities. ....126

**Figure 4.2.** Ohm's Plot. Plot of 50 mM Tricine-NaOH balance with 10 mM NaCl to pH 8.3; field strength range -100 to -1800 V/cm (in 100V/cm increments); 8.0 cm capillary (25  $\mu\text{m}$  i. d.). ....127

**Figure 4.3.** Enrichment Rates. Example electropherogram of 10 nM dsDNA (24mer WT\*/Wt; See Table 1 for DNA properties) focused on both hot (~80 °C) and cold (~20 °C) sides at -10, -5, -2.5 Pa/s acceleration rates, respectively. Running buffer: 50 mM Tricine-NaOH balance with 20 mM NaCl to pH 8.15; field strength, -250 V/cm; -2000 Pa start pressure; 8.0 cm capillary (25  $\mu\text{m}$  i. d.); temperature gradient between 80 °C - 20 °C (at 15 °C /mm). ....129

**Figure 4.4.** Trends in migration time. **A.** Example electropherogram of 10 nM dsDNA-24mer (WT\*/Wt; WT\*/mut) and 5 nM mixture of duplexes focused on cold side at different temperature gradients: 80/20 °C, 80/30 °C, 80/40 °C. Experiment conducted on 8.0 cm capillary (25  $\mu\text{m}$  i. d.). Conditions: -1400 Pa start  $\Delta P$ ; -5 Pa/s acceleration; -350 V/cm field strength; PMT = 0.600V. Running buffer: 50 mM Tricine-NaOH balance with 20 mM NaCl to pH 8.17. **B.** Example electropherogram of 2.5 nM dsDNA-24mer (WT\*/Wt; GCWT\*/gcwt) and 5 nM mixture of duplexes focused on cold side at different temperature gradients: 80/15 °C, 80/20 °C, 80/30 °C, 80/40 °C. Experiment conducted on 7.0 cm capillary (25  $\mu\text{m}$  i. d.). Conditions:

2700 Pa start  $\Delta P$ ; -20 Pa/s acceleration; -600 V/cm field strength; PMT = 0.600V.  
Running buffer: 0.5 M Tris borate balance with 20 mM NaCl to pH 8.3.....131

**Figure 4.5.** Separation in BSA. **A.** Plot of migration time versus concentration of BSA. **B.** Example electropherogram of 10 nM WT\*/Wt-24mer, 10 nM GCWT\*/gcwt-24mer, and 5 nM mixture of strands prepared in different concentrations of BSA (250 nM, 1, 50, 100, 150, and 200- $\mu$ M): Focusing was on the hot side at 55/20  $^{\circ}$ C temperature gradient. Experiment was conducted on 7.0 cm capillary (25  $\mu$ m i. d.) at constant: -10 Pa/s acceleration, start  $\Delta P$  = 1400 Pa, and -600 V/cm field strength; PMT = 0.475V. Running buffer was 0.5 M Tris borate balance with 20 mM NaCl to pH 8.3. . . . .135

**Figure 4.6.** Generation of pressure blocks. #1: Standard  $\Delta P$  block, PMMA material; holds between 750-860  $\mu$ L volume; #2: standard  $\Delta P$  block cured with glass vial, 4 ml in volume; #3: 6 ml large volume reservoir, non-PMMA material; #4: stage vial attached to 20 cm (25  $\mu$ m i. d.) capillary.....137

# CHAPTER 1

## FUNDAMENTAL CONCEPTS

### 1.1. CAPILLARY ELECTROPHORESIS

#### 1.1.1. Introduction

The development of new and improved techniques for sensitive analysis is a key focus of separation science. The capillary electrophoresis (CE) technique developed and introduced by Hjerten<sup>1,2</sup> in 1967 rapidly emerged as a widely used analytical separation technique. The popularity and advancement of the technique is credited to pioneering research efforts of many authors including Mikkers *et al.*,<sup>3,4</sup> Jorgenson and Lukas.<sup>5,6</sup> Thus, CE is no longer a single technique but has diverged as a family of related techniques which conducts electrophoresis in a capillary format.<sup>7</sup>

In recent years the CE method has developed into a high resolution separation technique making it a choice alternative to slab gels, and other chromatographic techniques including high performance liquid chromatography (HPLC) and gas chromatography (GC).<sup>8-12</sup> Although CE was primarily known for separating charged analytes, further modifications to the technique made it possible to separate neutral ions (indirectly using micellar electrokinetic capillary chromatography (MEKC)).<sup>13-14</sup> Some key features of CE are simplicity of operation, small volume requirement for sample and reagent, rapid separation (in minutes) aided by the high field strength ( $> 500 \text{ Vcm}^{-1}$ ) tolerance, small inner diameter (a key factor in efficiency enhancement), easy

automation, parallelization and applicability to diverse fields and analyte types. However, the major drawbacks of CE are low sensitivity (usually  $\mu\text{M}$  limits of detection), migration time drifts due to irreproducibility when using small injection volume, and the challenge of high throughput analysis in a single run. To improve CE sensitivity usually laser induced fluorescence detection is used, which requires that samples be derivatized or labeled with a fluorescence dye for sensitive detection.

CE either as a standalone, or hyphenated techniques has found application in many fields including biotechnology, environmental, pharmaceuticals, drug analysis, forensic, food and beverage, targeting a vast range of analytes (small and large molecules, enantiomers, inorganic ions (Reviewed in 15-25). Currently, other advances focus on transferring CE to microfluidics.<sup>24,25</sup> Notably, the parallelization of CE in experimental design was responsible for early completion of the human genome project.<sup>26,27</sup>

### **1.1.2. Basic principles and theory**

#### *1.1.2.1. Electrophoresis*

The development of the electrophoresis (ep) separation method in 1937 is credited to Arne Tiselius, a Swedish chemist, who later became the noble prize winner in 1948 for his development.<sup>28</sup> Electrophoresis was initially described for separation on a slab gel. Capillary electrophoresis operates on the basic principles of electrophoresis. A key distinction is that movement of ions under an applied electric field is carried out on a capillary rather than a slab gel.

Generally, an electrophoretic system requires on a homogeneous buffer system (usually in low mM concentration) and application of constant field strength. When voltage is applied to the system, current flows between the electrodes (cathode (-) and anode (+)) and the potential different between electrodes produces the electrical force (F) which facilitates the movement of ions. The direction of movement is dependent on the ion's charge. Anions will move toward the cathode while cations move toward the anode. As ions move, they experience frictional force due to viscosity of the buffer solution.

The overall velocity in due to voltage gradient known as the ion's electrophoretic mobility ( $\mu_{ep}$ ) is determined by the balancing between electrical and frictional forces. This relationship is derived as follows:

$$F = q \frac{dV}{dx} \quad (1)$$

and

$$F_d = f \frac{dx}{dt} \quad (2)$$

where  $q$  is charge ( $q=ze_o$ ),  $z$  is the analyte ion charge,  $e_o$  is the electron charge defined as ( $1.602 \times 10^{-19}$  Coulombs),  $dV/dx$  or  $E$  is the field strength (V/cm),  $f$  is the frictional coefficient ( $f=6\pi\eta r$ , in Newton or  $\text{kgms}^{-2}$ ), and  $dx/dt$  or  $v_{ep}$  is the ion's electrophoretic velocity ( $\text{ms}^{-1}$ ).<sup>2</sup> At equilibrium, both forces are balanced,

$$fv_{ep} = qE \quad (3)$$

Thus, the ion's electrophoretic mobility is expressed as,

$$\mu_{ep} = \frac{v_{ep}}{E} \quad (4)$$

Rearranging equation (4) gives a relationship for electrophoretic velocity (5),

$$v_{ep} = \mu_{ep}E \quad (5)$$

The drag force ( $F_d$ ) is particularly explained by the Navier-Stokes equation,<sup>29</sup>

$$F_d = 6\pi\eta rv \quad (6)$$

which assumes that ions are of spherical radius,  $r$  (in m), moving in a solution of viscosity,  $\eta$  (in  $\text{kgms}^{-1}$ ). Normally, larger molecules will have a larger radius and their drag force would increase causing ions to exhibit slower mobility. Also, electrostatic interaction between buffer and analyte ions can influence movement of ions. For a low ionic strength buffer the field strength is high and large amount of current is transferred to the analyte ions causing rapid movement as a result low heat is generated.

#### *1.1.2.2. Electroosmotic Flow (EOF)*

In CE, the movement of bulk fluid under electric field is facilitated by EOF.<sup>30</sup> When buffer solution (containing anions, cations and neutral molecules) is introduced on a preconditioned capillary column, the positively charged cations from the buffer solution attaches to the negatively charged ionized silanol ion ( $\text{SiO}^-$ ) on the capillary wall and forms an electrically charged bilayer. This bilayer is instrumental in moving the bulk solution containing buffer and analyte ions through the column, a process known as EOF (Fig. 1.1.1). In a system under electrical conduction the direction of migration of ions is usually from anode (site of oxidation) to cathode (site of reduction); thus, a net flow is generated in that direction. Conversely, the flow of current is from cathode to anode. So in an electrophoretic system, the cathode (-) attracts positive ions (cations) while anode

(+) draws negative ions (anions). Although both cations and EOF have positive (+) sign, EOF is generally much faster for suitable pH environment.

The EOF is subject to pH constraints to ensure control and reproducibility in results. The pH of the buffer controls the ionization of silanol group on the capillary wall and movement of EOF. When acidic buffer (usually  $\text{pH} < 3$ ) is used the silanol groups are not ionized making it impossible to form the double layer causing EOF to be effectively reduced. For buffers with pH greater than 3 (between pH 3-7), silanol groups are ionized and EOF predominates electrophoresis ( $\mu_{eo} \gg \mu_{ep}$ ); however, for  $\text{pH} > 9$ , EOF may be uncontrollable giving irreproducible results or no separation at all.

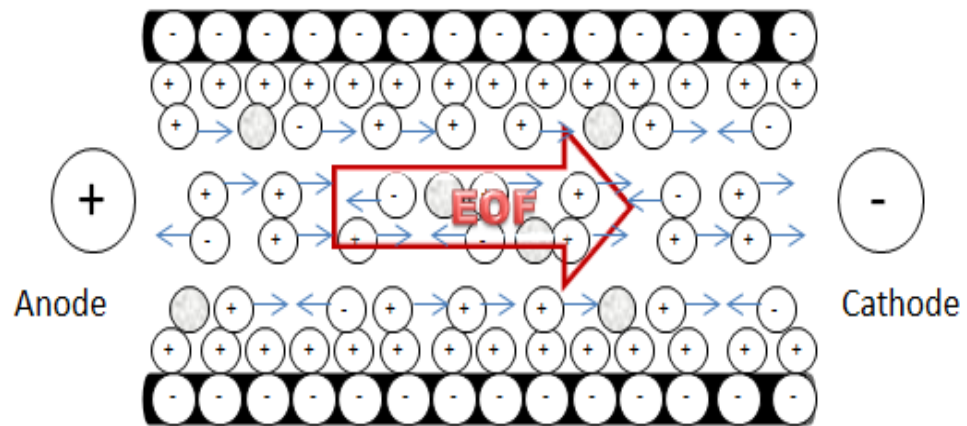


**Figure 1.1.1.** Electroosmotic Flow. Cations,  $\oplus \rightarrow$  and anions,  $\ominus \rightarrow$  are circles with + or - sign attached to arrowhead indicating direction of flow; neutrals,  $\bullet$  are filled circles; and ionized silanol groups are represented by the circles with - sign,  $\ominus$ . The voltage potential in each reservoir is shown by the large circles without arrowhead: anode,  $\oplus$  and cathode,  $\ominus$ .

### 1.1.2.3. Net Mobility

In a system undergoing electrophoresis, the total ion mobility ( $\mu_{tot}$ ) is the combination of electrophoretic mobility and electroosmotic mobility.<sup>29-31</sup>

$$\mu_{tot} = \mu_{ep} + \mu_{eo} \quad (7)$$

For any ion or species,  $\mu_{tot}$  is defined as the net speed with respect to field strength,  $E$ :

$$\mu_{tot} = \frac{v_{tot}}{E} = \frac{L_d/t_m}{V/L_t} = \frac{L_d L_t}{V t_m} \quad (8)$$

where  $L_d$  and  $L_t$  are the effective separation length from sample reservoir to the detector, and the total capillary length, respectively. The excess length ( $L_{br} = L_{tot} - L_d$ ) allows for connection to the buffer reservoir (br);  $t_m$  is the measure of time ion takes to reaches detector or the net mobility of the ion on-column, and  $V$  is the voltage at both reservoirs.

The electrophoretic velocity is influence by the ion's charge and size. Generally, smaller ions (have large surface density) move faster than larger ions because of the difference in their hydrodynamic radius and frictional forces. However, movement of ions with different charge would be slower for singly charged ions than for doubly charge ones (Fig. 1.1.4b).

### 1.1.2.4. Joule Heating

Eventhough CE has a high tolerance for high voltage (up to 30 kV) and field strength greater than  $500 \text{ Vcm}^{-1}$  it is still possible to experience joule heating. The high surface ratio especially in capillary with smaller inner diameter makes it easy to effectively dissipate heat. The Ohm's Law ( $V=IR$ ) is used to describe the relationship

between voltage potential and buffer resistance:

$$I = \frac{V}{R} \quad (9)$$

where  $V$  is voltage potential (measured in kilovolts, kV),  $I$  is the current (measured in microamperes,  $\mu\text{A}$ ) which is proportional to the heat generated, and  $R$  is the resistance (measured in Ohms,  $\Omega$ ).

Equation (9) can be written in terms of current density  $J$  (in A/cm),

$$J = \sigma E \quad (10)$$

to show proportionality between buffer conductivity,  $\sigma$  (in A/V) and electric field strength given by,<sup>35</sup>

$$E = I/A\sigma \quad (11)$$

where  $A$  is the cross-sectional area of the channel.

When constant voltage is applied to a system using low ionic strength buffer, there is a linear relationship between  $R$  and  $I$ . However, in a high ionic strength environment large amount of heat is generated leading to Joule heating ( $E$ ). This results in a non-linear relationship because of the resistance to flow. Nelson et al<sup>10</sup> developed the concept of the *Ohm's Law Plot* to determine the optimal range of field and voltage for a particular buffer system used in analysis. Measurements of a buffer (usually in mM concentration) at different intervals of voltage (kV) or field strength (V/cm) is made, and a plot of current ( $\mu\text{A}$ ) as a function of voltage or field strength is generated. The linear portion of the plot indicated a good working range and implies that heat is dissipated. The point of deviation from linearity is a good indicator of joule heating.

### 1.1.2.5. Efficiency and Resolution

From the van Deemter equation<sup>34</sup> ((12a) and (12b)) for plate height (H), peak broadens as the result of three types of flow rates: multiple flow paths or Eddy diffusion, (A-term,  $H_A$ ), longitudinal diffusion (B-term,  $H_D$ ), and mass transfer (C-term,  $H_M$ ),

$$H_{tot} = H_A + H_D + H_M \quad (12a)$$

Rewritten as,

$$H = A + \frac{B}{u_x} + C u_x \quad (12b)$$

In basic CE, analysis is carried out in a single buffer (or mobile phase) and the primary contribution to band broadening is from the B-term. As the A and C terms go to zero, the peak width decreases; thus, an overall reduction in  $H_D$  means more theoretical plates (translates in to high efficiency). Therefore,

$$H_D = \frac{B}{u_x} \quad (13)$$

The theoretical plates or measure of efficiency (measured at half height ( $N_{1/2}$ )) is a dimensionless parameter where  $w$  is the peak width and can be experimentally determined.

$$N_{1/2} = 5.54 \left( \frac{t_R^2}{w_{1/2}^2} \right) \quad (14)$$

Efficiency in CE is defined as,

$$N = \frac{\mu V L_d}{2 D L_t} \quad (15)$$

The high efficiency separation in CE results from more theoretical plates being produced when high voltage is applied. The analyte ion(s) will move faster spending less time on the column resulting in less rate of diffusion.

Resolution is proportional to  $N$  and  $L$  (column length).<sup>30,31</sup> In CE, resolution is described as,

$$R = \frac{1}{4} \frac{\mu_{ep}\sqrt{N}}{\mu_{tot}} \quad (16)$$

#### 1.1.2.6. Injection modes

CE sample loading on column is either by voltage (a) or pressure (b) resulting in different flow profiles (Fig. 1.1.2). For electrokinetic injection (Fig.1.1.2a), the application of voltage (up to 30 kV) drives solution on column. Since the voltage applied to the entire capillary is constant, a uniform flow of EOF velocity and a flat bulk fluid movement is achieved. The amount of moles of sample ions or analyte,  $X$ , injected is determined by the relationship below:

$$X = \mu_{tot} \left( E \frac{\kappa_b}{\kappa_s} \right) t \pi r^2 C \quad (17)$$

where  $\kappa_b$  and  $\kappa_s$  are buffer and sample conductivities, respectively,  $t$  is the injection time,  $C$  is the analyte's concentration, and the other variables were previously defined. This injection mode is responsible for the characteristic peak sharp profile in CE. However, peak can be distorted either when solution conductivity ( $\kappa_b$ ) exceeds that of the analyte ( $\kappa_s$ ), that is,  $\kappa_b > \kappa_s$  leading to peak tailing, or the reverse ( $\kappa_b < \kappa_s$ ) effect leads to peak fronting.<sup>31</sup>

For hydrodynamic injection (Fig. 1.1.2b), either a pressure source, or pressure difference ( $\Delta P$ ) between height of sample and buffer reservoirs operating on gravity is used for sample introduction on column. Together, frictional force (or drag force) and pressure (as in flow rate) influence the establishment of a flow gradient along the column. The pressure drop at wall is lower than in the center. This difference is responsible for

peak broadening which leads to loss in peak efficiency. Thus, hydrodynamic injection of sample results in parabolic or laminar flow profile. The Poiseuille equation can be used to predict the amount of sample loaded ( $V$  in mL) on column:<sup>29</sup>

$$V = \frac{\pi \Delta P r^4}{8 \eta_s L t} \quad (18)$$

where  $\eta_s$  is solution viscosity; all other variables were previously defined.

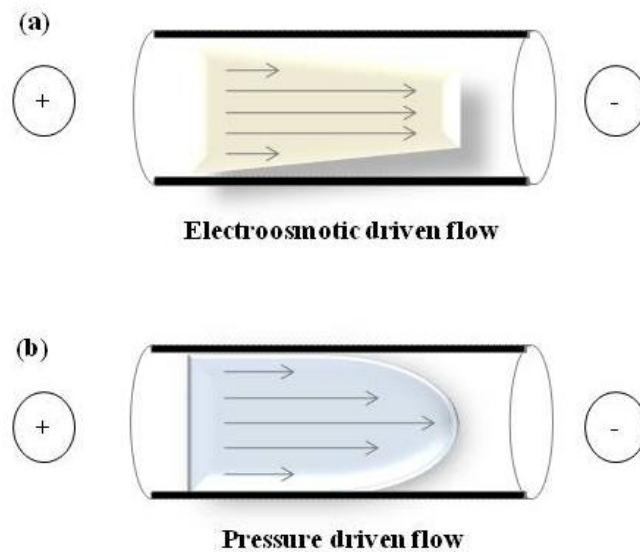


**Figure 1.1.2.** CE injection modes. (a) electrokinetic injection is driven by EOF resulting in a flat profile. (b) hydrodynamic injection is driven by pressure gradient resulting in a laminar (parabolic) flow profile.

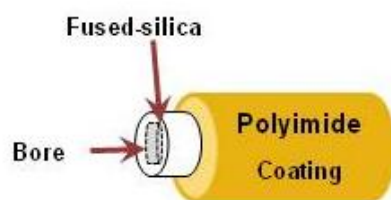


**Figure 1.1.3.** Capillary tube.

### 1.1.3. Instrumentation

The basic CE instrument consists of high voltage power supply, pressure controller or vacuum, capillary, reservoirs, conducting electrodes, detector and computer. The capillary tube is usually thin fiber of fused-silica (inner wall), outer coated with polyimide (Fig. 1.1.3); its inner diameter ranges from 15 to 100  $\mu\text{m}$ .

Each end of the capillary tube is inserted into a different reservoir (Fig. 1.1.4a). One reservoir is the source connected to the capillary inlet while the other is the destination vial connected to the capillary outlet. The reservoirs are equipped with electrode for electrical conduction. Electrodes can be made from inert materials (usually platinum wire) to prevent degradation or impurities which could interfere with conduction. To create an optical detection window (in millimeters) a portion of the capillary is burned to remove polyimide coating. Many detectors can be use for CE analysis including ultraviolet visible (UV-VIS), electrochemical, refractive index, contactless conductivity, chemiluminescence, mass spectrophotometer, fluorescence, laser-induced fluorescence (LIF) and more recently light emitting diode induced fluorescence (LEDF). Even though LIF detector is more often used for simplicity and sensitivity detection, a slow transition is towards LEDF for cost reduction and comparable (in some cases better) sensitivity.<sup>17</sup>

CE separation is described in the schematic shown in Fig. 1.1.4. Prior to first use, the capillary is conditioned with 0.1 M sodium hydroxide, deionized water, and buffer in ~5 minutes cycles, respectively. Initially a plug of the sample solution contained in source vial is injected onto the capillary either hydrodynamically (pressure or vacuum

injection) (Fig. 1.1.4a) or electrokinetically (Fig. 1.1.4b). Once the plug is injected on column, the sample is removed from the vial and replaced with background buffer solution. The voltage is turned on and separation is achieved based on the electrophoretic mobility of ions (Fig 1.1.2b). A computer equipped with necessary software is used to display the resulting electropherogram.

#### **1.1.4. Modes of Operation**

The rapid advancement of the CE technique is responsible for to sample resolution enhancement and/or affords separation of particular analyte type. CE is a general description for subclasses of techniques using the capillary format. Some common CE modes are capillary zonal electrophoresis (CZE), capillary gel electrophoresis (CGE), capillary isotachopheresis (cITP), capillary isoelectric focusing (cIEF), capillary electrochromatography (CEC or CE-HPLC), micellar electrokinetic chromatography (MEKC) (reviewed in 13-25). These modes are applicable to the separation of different types of ionic species making CE a versatile technique.

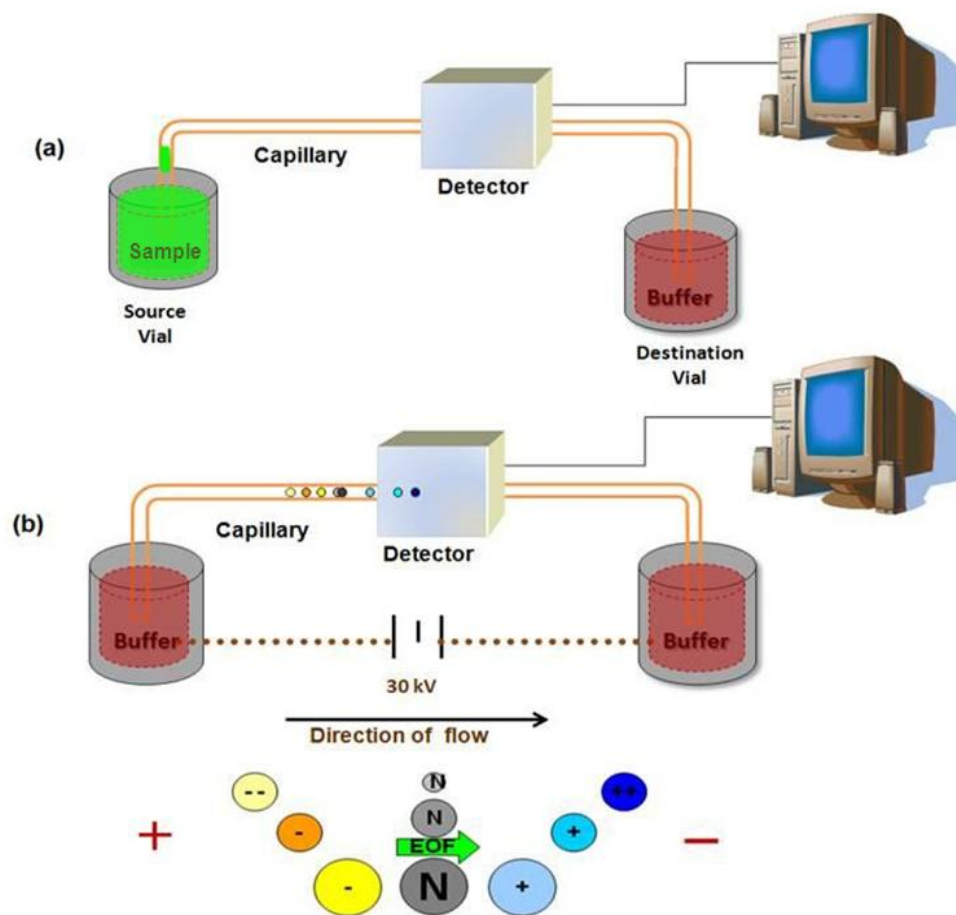


**Figure 1.1.4.** Schematic of CE operation. (a) Hydrodynamic injection of sample plug into capillary. (b) Solution in source vial is replaced with buffer and high voltage ( $\sim 30\text{kV}$ ) is simultaneously applied. Depending on the analyte's charge, net flow is either toward anode or cathode. Species are detected in order of charge and electrophoretic mobility (anions (-), neutrals (N), and cations (+)).

### 1.1.5. References Cited

1. Hjertén, S. *Chromatogr. Rev.* **1967**, *9*, 122-219.
2. Baker, D. R. *Capillary Electrophoresis*. John Wiley & Sons, Inc. New York, **1995**.
3. Mikkers, F.; Ringoir, S.; De Smet, R. *J. Chromatogr.* **1979**, *162*, 341-350.
4. Mikkers, F. E. P.; Everaerts, F. M.; Verheggen, T. P. E.; *J. Chromatogr. A* **1979**, *169*, 11-20.
5. Jorgenson, J. W.; Lukacs, K. D. *Anal. Chem.* **1981**, *53*, 1298-1302.
6. Jorgenson, J. W.; Lukacs, K. D. *Science* **1983**, *222*, 266-272.
7. Bruno, T. J. *Chromatographic and Electrophoretic Methods*, Prentice Hall, Englewood Cliffs, NJ, **1991**.
8. Hjertén, S. *J. Chromatogr. A* **1985**, *347*, 191-198.
9. Guttman, A. *Electrophoresis* **1995**, *16*, 611-16.
10. Cohen, A. S.; Karger, B. L. *J. Chromatogr.* **1987**, *397*, 409-417.
11. Hjertén, S. *J. Chromatogr.* **1983**, *270*, 1-6.
12. Majors, R. E. *LC-GC* **1997**, *15*, 412, 413, 416-420, 422.
13. Quirino, J. P.; Terabe, S. *J. Capillary Electrophor.* **1997**, *4*, 233-245.
14. Peric, I.; Kenndler, E. *Electrophoresis* **2003**, *24*, 2924-2934.
15. Terabe, S. *Annu. Rev. Anal. Chem.* **2009**, *2*, 99-120.
16. Kašička, V. *Electrophoresis* **2010**, *31*, 122-146.
17. Poinot, V.; Gavard, P.; Feurer, B.; Couderc, F. *Electrophoresis* **2010**, *31*, 105-121.
18. Herrero, M.; García-Cañas, V.; Simo, C.; Cifuentes, A. *Electrophoresis* **2010**, *31*, 205-228.

19. Ha, P. T. T.; Hoogmartens, J.; Van Schapdael, A. *J. Pharm. Biomed. Anal.* **2006**, *41*, 1-11.
20. Castro-Puyana, M.; Crego, A. L.; Marina, M. L. *Electrophoresis* **2010**, *31*, 229-250.
21. Klampfl, C.W. *Electrophoresis* **2009**, *30*, S83-91.
22. Dolnik, V. *Electrophoresis* **2008**, *29*, 143-156.
23. Kuhr, W. G.; Monnig, C. A. *Anal. Chem.* **1992**, *64*, 389-407.
24. Fu, L. M.; Leong, J. C.; Lin, C. F.; Tai, C. H.; Tsai, C. H. *Biomed. Microdevices* **2007**, *9*, 405-412.
25. Pang, H. M.; Kenseth, J.; Coldiron, S. *Drug Discov. Today* **2004**, *9*, 1072-1080.
26. Collins, F. S.; Morgan, M.; Patrinos, A. *Science* **2003**, *300*, 286-290.
27. Collins, F. S.; Patrinos, A.; Jordan, E.; Chakravarti, A.; Gesteland, R.; Walters, L. R. *Science* **1998**, *282*, 682-689.
28. Hjertén, S. *J. Chromatogr. Rev.* **1972**, *65*, 345-348.
29. Giddings, J.C. *Unified Separation Science*, Wiley, New York, **1991**.
30. Terabe, S.; Otsuka, K.; Ando, T. *Anal. Chem.* **1985**, *57*, 834-841.
31. Harris, D. C. *Quantitative Chemical Analysis*, 7<sup>th</sup> Ed. W.H. Freeman and Co., New York, NY, 2007.
32. Gareil, P. *Chromatographia* **1990**, *30*, 195-200.
33. Ghowri, K.; Foley, J. P.; Gale, R. J. *Anal. Chem.* **1990**, *62*, 2714-21.
34. Van Deemter, J. J.; Zuiderweg, F. J.; Klinkenberg, A. *Chem. Eng. Sci.* **1956**, *5*, 271-89.
35. Ross, D.; Locascio, L. E. *Anal. Chem.* **2002**, *74*, 2556-2564.

## 1.2. ISOTACHOPHORESIS

### 1.2.1. Introduction

Analytical method development depends heavily on instrumentation and applicability of technique to a wide range of sample type for making quantitative and qualitative analysis. The early introduction of isotachophoresis was described by many different nomenclatures (as reviewed in 1-3). The isotachophoresis (ITP) method functions primarily as a preconcentration technique which operates on a discontinuous buffer system to achieve resolution of discrete sample zone. This key feature makes it a useful tool to combine to other separation methods which can be employed in trace analyses. During the ITP process electric field drives sample ions along a separation column. A pseudo steady state condition results in sample ions forming discrete boundaries between leading and trailing ions according to their electrophoretic mobility. This stacking process is similar to the moving boundary concept developed by Arne Tiselius<sup>3</sup> where the amount of analyte ions present (although not separated) is related to the amount of zones formed.

ITP has found its niche with other electrophoretic methods including field amplified sample stacking (FASS), field amplified sample injection (FASI), pH junctions, sweeping, and focusing methods such as isoelectric, electric field gradient, and temperature gradient techniques (as reviewed in 4-18). Developments in the ITP technique employed analysis using gel, capillary and more recently microfluidics devices for making sensitive analysis.<sup>19-26</sup> Most importantly, it is used in combination with other methods primarily as a preconcentration step prior to separation.<sup>27-32</sup> Over the years the

ITP method has been applied to the analysis of wide range of ionic, biological, organic and inorganic substances in different fields of study.<sup>11-18</sup>

### **1.2.2. Basic Principles and Theory**

While electrophoresis separates ions based on their electrophoretic mobility in a constant applied field, ITP requires that a difference in field induced by the discontinuous buffer system be used to stack ions in discrete zones. ITP is an analytical method that allows analyte ions of intermediate mobilities to concentrate, and stack into discrete zones between a discontinuous buffer system, of high mobility leading electrolyte (LE) and low mobility trailing electrolyte (TE). The selection of TE and LE takes into consideration the choice of analyte to be analyzed. Generally the mobility of anions will increase as the pH increases from LE to TE, while cations increase as pH decreases TE to LE. An optimal current is constantly applied so that a compromise between analysis time and resolution do not result in inability to form steady state zones.

#### *1.2.2.1. Basic ITP process*

In a typical ITP analysis (reviewed in 33), initially the separation column is filled with high mobility LE solution (Fig. 1.2.1a(i)), so that it is ahead of the separation zone. When electric field (or pressure) is applied, analyte matrix is introduced on column and begins to migrate (under electrophoresis) according to their electrophoretic mobility (Fig. 1.2.1.a.ii). As analytes migrate, a brief period of zone crossover persists resulting in counteraction as a result of field strength difference (Fig. 1.2.1a(iii), (v) and b) of buffers. So, as the analyte zone approaches LE zone it immediately slows down because of the

low field/high pH environment and is pushed back into its zone. In similar manner, as the analyte crosses into TE zone it immediately speeds up because of the high field/low pH environment. This process causes dilution of zones and eventually a pseudo steady-state or dynamic equilibrium is reached leading to the formation of sharp discrete boundary between adjacent zones (Fig. 1.2.1a(v), and c). The counter-ions (common background ions) exit the column and are excluded during the equilibrium process. Notably in this state, all zones tend to migrate at the same velocity under condition of constant applied current.

A typical ITP isotacopherogram (Fig. 1.2.1b and c) shows ionic zones represented as stair case and the electric field is inversely proportional to ion mobility. At the interface between zones a sharp rise in field strength is seen. Essentially the height of the staircase is higher for lower mobility ion because of the high field strength. The plateau indicates the zone length. The zone length is relative to the difference in ion mobility.

For an anionic system (Fig. 1.2.1) the LE, TE and analyte ions are all negatively charged, and the background counter ions positively charged. Since LE is of higher mobility than analyte ions and TE (lowest mobility), zone formation or stacking will follow the order  $LE > Analyte > TE$ . However, for a cationic system the order would be reversed  $TE > Analyte > LE$ , and the counter ions would be negatively charged.

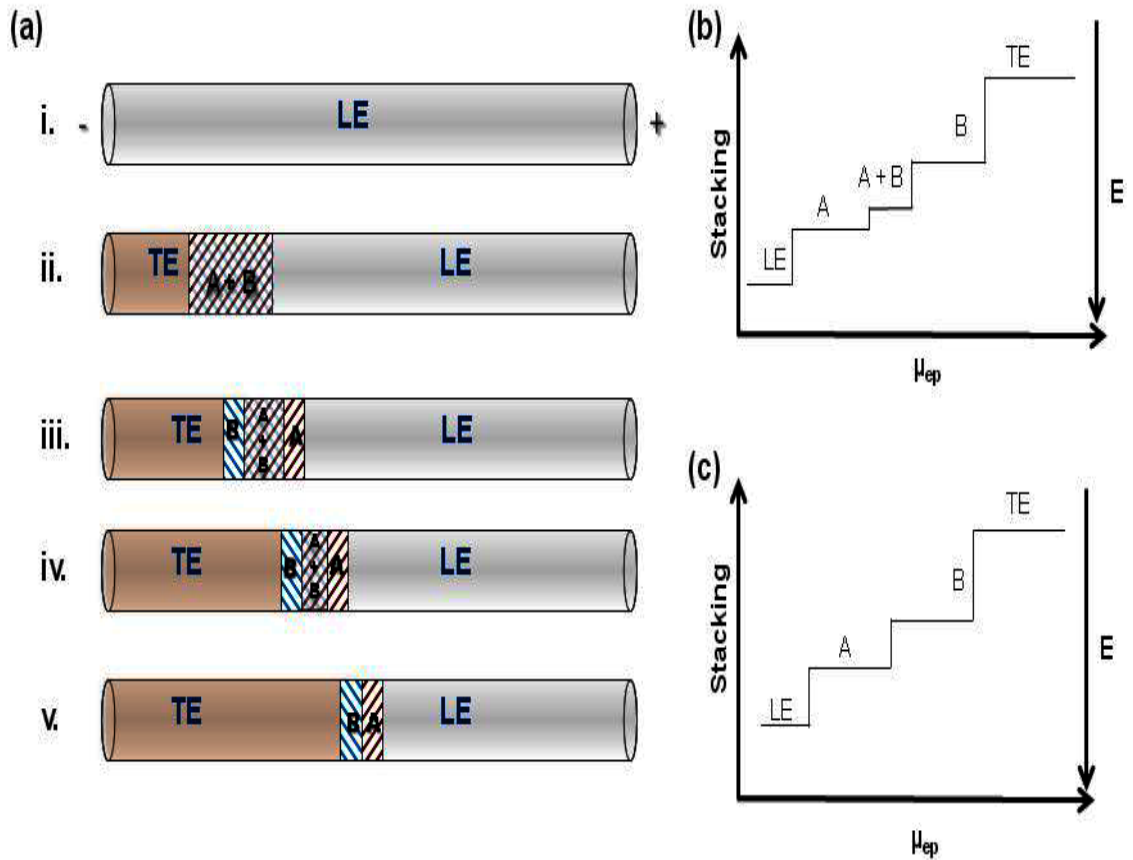


**Figure 1.2.1.** Schematic of Anionic Isotachopheresis (ITP) mode. (a) Typical stacking stages occurring in ITP are as follows: **i.** the capillary is filled with LE solution; **ii.** under a constant electric field a slug of undifferentiated analyte ions zone begin to migrate (by electrophoresis) with high mobility LE ions ahead of the slug; **iii.** ionic zones begin to form as migration proceeds and field strength changes as zone length overlaps; **iv.** same as **iii** but zone formation more defined; not shown is possible zone overlap between A and LE ions and B and TE ions (**iii-iv**); **v.** pseudo steady state results in discrete zones moving at same speed. (b) Non-steady state (analogous to (a) **iii** and **iv**); LE ions force slug to stack in direction towards high field. Stacking order of ions:  $LE > A > A+B$  (intermediate zone)  $> B > TE$ ; low mobility ions (TE) experience highest field strength. (c) analogous to (a)**v**; established pseudo-steady state profile of field strength as a function of electrophoretic velocity. Stacking order and field strength profiles same as (b) but no intermediate zones only discrete zones.

### 1.2.2.2. Kohlrausch Regulating Function in ITP

Today, initial work of Kohlrausch in 1897 originally developed for determining transfer number is instrumental in making theoretical description and explanation of the ITP process.<sup>34,35</sup> Other authors like Kendall, Innes and Longworth have derived a number of equations for evaluating compositions and interaction of the moving boundary of zones at steady-state based on Kohlrausch work. Kohlrausch derived the Kohlrausch Regulating Function (KRF) which can be used to quantitate the concentration at interface of tightly packed zones in a system undergoing electrophoresis and ITP that is at equilibrium.<sup>34,36-39</sup>

KRF is a time independent function relating the ratio of analyte concentration to that of the LE:

$$\frac{C_A}{C_{LE}} = \frac{\mu_A}{\mu_{LE} + \mu_R} \cdot \frac{\mu_{LE} + \mu_R}{\mu_{LE}} \cdot \frac{Z_A}{Z_{LE}} \quad (1)$$

where  $\mu_A$ ,  $\mu_{LE}$ ,  $\mu_R$ , are the respective electrophoretic mobilities of the analyte, LE, and counterion (or background ion) and the analyte and LE charge is denoted  $Z_A$ , and  $Z_{LE}$ , respectively.

It operates on the following assumptions:

- that time (t) and diffusion (slower than current) are negligible factors
- that temperature is directly proportional to field strength
- that the area of a zone (in ITP) is directly proportional to analyte concentration
- that concentration of LE is fixed, and ion mobility is constant

According to the KRF, concentration of zones in steady state can be established and determined as a result of regulating or balancing between LE of fixed concentration ( $C_{LE}$ ) with adjacent zones, and also common background ion (oppositely charge),  $C_R$ .

When the mobility of analyte is close to that of the LE, their concentrations will be almost equivalent. The LE ions concentration is used as a reference standard to determine concentration of adjacent zones because it has much lower resistance than TE ions.

Initially at the start of migration when current is applied, the starting concentration of ions is dilute, and present in large volume large. The analyte ions are sandwiched between buffer ions (LE and TE) of different buffering capacities and conductivity. The LE ion is of slightly higher ionic strength. Ions slowly move in the direction of lower field defining their boundary along the way. At steady state, the previously dilute analyte zones becomes highly concentrated and stack into discrete compacted zones resulting in high resolution of analyte ions at interface of preceding ions – zone sharpening effect.

#### *1.2.2.3. Resolution in ITP*

Although ITP is a preconcentration technique, a pseudo separation can be achieved between zones in direct contact. Usually ampholytes (non-absorbing species) which are made up of a combination of substances of different mobilities exhibiting a wide pH range (between pH 3-11) are used as spacer ions. Thus, to achieve resolution in ITP the ampholytes effectively creates a pH gradient between the adjacent zones causing them to stack at different point. If the sample ions are proteins or peptides, a gradient similar to IEF can create separation.<sup>40-44</sup> However, using large amount of ampholyte in ITP can reduce resolution.<sup>45</sup>

### 1.2.3. Instrumentation

Since the construction of the first ITP instrumentation in 1968 by Verheggen and Everaertes several modifications have been made to the instrument including size reduction and other instrumental accommodations. Today, a typical modern ITP instrument uses capillary or microfluidic device. An ITP instrument setup is similar to CE (discussed in 1.1.3.). Briefly, it contains high voltage power supply, pressure controller or vacuum, capillary, reservoirs, conducting electrodes, detector and computer. ITP is routinely carried out on a fused-silica capillary tube spanning the LE and sample reservoirs, each of which is equipped with a conducting electrode (preferably platinum wire). The electrodes are connected to the high voltage power supply design to deliver voltages up to 30 kV. The power supply also allows polarity adjustments to accommodate the analyte to be analyzed. That is, for anion the polarity is set to positive (+) and for cations it is switched to negative (-). Detection systems for ITP include the basic universal UV detector, conductivity and thermal detectors.

### 1.2.4. Counterflow in ITP

In ITP, counterflow employing pressure driven flow is useful for improving enrichment. Counterflow has the advantage of increasing the effective length of separation column by prolonging analyte's time spent on column; thus, alleviating the use of longer capillary. It can also be manipulated to combine preconcentration and separation in one step, which is an important advantage for trace compounds analysis.<sup>46-52</sup>

### 1.2.5. Modes of Operation

Recent research in ITP is directed to methods development for capillary, and microfluidic ITP as well as online coupling showing wide range of applications.<sup>21-25</sup> ITP has been successfully combined with other methods including capillary ITP (as in ITP/ITP), capillary zone electrophoresis (CZE), capillary gel electrophoresis (CGE), isoelectric focusing (IEF).<sup>10-18,32</sup> Transient ITP where analyte is allowed to stack for a brief period prior to being coupled to CZE is used to reduce dispersion between zones.<sup>27,29, 31,46</sup>

### 1.2.6. References Cited

1. Vesterberg, O. *Electrophoresis* **1993**, *14*, 1243-1249.
2. Vesterberg, O. *J. Chromatogr.* **1989**, *480*, 3-19.
3. Hjerten, S. *J. Chromatogr.* **1972**, *65*, 345-348.
4. Kartsova, L. A.; Bessonova, E. A. *J. Anal. Chem.* **2009**, *64*, 326-337.
5. Hahn, T.; O'Sullivan, C. K.; Drese, K. S. *Anal. Chem.* **2009**, *81*, 2904-2911.
6. Mala, Z.; Slampova, A.; Gebauer, P.; Bocek, P. *Electrophoresis* **2009**, *30*, 215-229.
7. Beckers, J. L.; Bocek, P. *Electrophoresis* **2000**, *21*, 2747-2767.
8. Meighan, M. M.; Staton, S. J. R.; Hayes, M. A. *Electrophoresis* **2009**, *30*, 852-65.
9. Kamande, M. W.; Ross, D.; Locascio, L. E.; Lowry, M.; Warner, I. M. *Anal. Chem.* **2007**, *79*, 1791-6.
10. Gebauer, P.; Bocek, P. *Electrophoresis* **2000**, *21*, 3898-3904.
11. Gebauer, P.; Bocek, P. *Electrophoresis* **2002**, *23*, 3858-3864.
12. Gebauer, P.; Mala, Z.; Bocek, P. *Electrophoresis* **2007**, *28*, 26-32.
13. Gebauer, P.; Mala, Z.; Bocek, P. *Electrophoresis* **2009**, *30*, 29-35.

14. Kasicka, V. *Electrophoresis* **2008**, *29*, 179-206.
15. Dolnik, V. *Electrophoresis* **2008**, *29*, 143-156.
16. Kasicka, V. *Electrophoresis* **2010**, *31*, 122-146.
17. Kohlheyer, D.; Eijkel, J. C. T.; van den Berg, A.; Schasfoort, R. B. M. *Electrophoresis* **2008**, *29*, 977-993.
18. Breadmore, M. C.; Thabano, J. R. E.; Dawod, M.; Kazarian, A. A.; Quirino, J. P.; Guijt, R. M. *Electrophoresis* **2009**, *30*, 230-248.
19. Kondratova, V. N.; Botezatu, I. V.; Shelepov, V. P.; Lichtenstein, A. V. *Anal. Biochem.* **2011**, *408*, 304-308.
20. Liu, D.; Ou, Z.; Xu, M.; Wang, L. *J. Chromatogr. A* **2008**, *1214*, 165-170.
21. Kaigala, G. V.; Bercovici, M.; Behnam, M.; Elliott, D.; Santiago, J. G.; Backhouse, C. J. *Lab. Chip* **2010**, *10*, 2242-2250.
22. Wang, J.; Zhang, Y.; Mohamadi, M. R.; Kaji, N.; Tokeshi, M.; Baba, Y. *Electrophoresis* **2009**, *30*, 3250-3256.
23. Chen, L.; Prest, J. E.; Fielden, P. R.; Goddard, N. J.; Manz, A.; Day, P. J. R. *Lab. Chip* **2006**, *6*, 474-487.
24. Prest, J. E.; Baldock, S. J.; Day, P. J. R.; Fielden, P. R.; Goddard, N. J.; Brown, B. J. T. *J. Chromatogr. A* **2007**, *1156*, 154-159.
25. Janasek, D.; Schilling, M.; Franzke, J.; Manz, A. *Anal. Chem.* **2006**, *78*, 3815-3819.
26. Jung, B.; Zhu, Y.; Santiago, J.G. *Anal. Chem.* **2007**, *79*, 345-349.
27. Krivankova, L.; Bocek, P. *J. Chromatogr. B* **1997**, *689*, 13-34.
28. Xu, Z. Q.; Hirokawa, T.; Nishine, T.; Arai, A. *J. Chromatogr. A* **2003**, *990*, 53-61.
29. Liu, D.; Chen, B.; Wang, L.; Zhou, X. *Electrophoresis* **2009**, *30*, 4300-4305.

30. Mohan, D.; Lee, C. S. *Electrophoresis* **2002**, *23*, 3160-3167.
31. Fang, X.; Wang, W.; Yang, L.; Chandrasekaran, K.; Kristian, T.; Balgley, B. M.; Lee, C. S. *Electrophoresis* **2008**, *29*, 2215-2223.
32. Reinhoud, N. J.; Tjaden, U. R.; van der Greef, J. *J Chromatogr. A* **1993**, *653*, 303-312.
33. Petr, J.; Maier, V.; Horakova, J.; Sevcik, J.; Stransky, Z. *J. Sep. Sci.* **2006**, *29*, 2705-2715.
34. Kohlrausch, F. *Ann. Phys. Chem.* **1897**, *62*, 209-239.
35. Lewis, G. N. *J. Am. Chem. Soc.* **1910**, *32*, 862-869.
36. Prochazkova, B.; Glovinova, E.; Pospichal, J. *Electrophoresis* **2007**, *28*, 2168-2173.
37. Zhang, W.; Jin, J.; Fan, L. Y.; Li, S.; Shao, J.; Cao, C. X. *J. Sep. Sci.* **2009**, *32*, 2123-2131.
38. Hruska, V.; Gas, B. *Electrophoresis* **2007**, *28*, 3-14.
39. Cao, C. X.; Zheng, Q. S.; Chen, W. K.; Zhu, J. H. *J. Chromatogr. A* **1999**, *863*, 219-26.
40. Kopwille, A.; Merriman, W. G.; Cuddeback, R. M.; Smolka, A. J.; Bier, M. J. *Chromatogr.* **1976**, *118*, 34-46.
41. Inano, K.; Tezuka, Sh.; Miida, T.; Okada, M. *Ann. Clin. Biochem.* **2000**, *37*, 708-716.
42. Acevedo, F. *J. Chromatogr. A* **1991**, *545*, 391-396.
43. Busnel, J. M.; Descroix, S.; Godfrin, D.; Hennion, M. C.; Kasicka, V.; Peltre, G. *Electrophoresis* **2006**, *27*, 3591-3598.
44. Bercovici, M.; Kaigala, G. V.; Santiago, J. G. *Anal. Chem.* **2010**, *82*, 2134-2138.
45. Mamunooru, M.; Jenkins, R. J.; Davis, N. I.; Shackman, J. G. *J. Chromatogr. A* **2008**, *1202*, 203-211.

46. Everaerts, F. M.; Vacik, J.; Verheggen, Th. P. E. M.; Zuska, J. *J. Chromatogr. A* **1971**, *60*, 397-405.
47. Ryslavy, Z.; Bocek, P.; Deml, M.; Janak, J. *J. Chromatogr. A* **1978**, *147*, 446-448.
48. Breadmore, M. C.; Quirino, J. P. *Anal. Chem.* **2008**, *80*, 6373-6381.
49. Vacik, J.; Zuska, J. *J. Chromatogr. A* **1974**, *91*, 795-808.
50. Bergmann, J.; Jaehde, U.; Schunack, W. *Electrophoresis* **1998**, *19*, 305-310.
51. Chen, S.; Lee, M. L. *Anal. Chem.* **1998**, *70*, 3777-3780.
52. Mazereeuw, M.; Spikmans, V.; Tjaden, U. R.; van der Greef, J. *J. Chromatogr. A* **2000**, *879*, 219-233.

### 1.3. COUNTERFLOW METHODS

#### 1.3.1. General overview

In the developing or modifying a technique, tradeoffs (like between resolution and sensitivity) are always inevitable and work as a situation of opportunity cost. An example is capillary electrophoresis, a simple and versatile method, that has rapidly expanded as popular technique, but suffers from low sensitivity when using UV detection.<sup>1</sup> Current efforts to improve CE sensitivity includes: using laser induced detection which may require derivatization or use of fluorogenic sample, configuration of detection window either to increase absorption pathlength or shorten it (to concentrate sample), and sample preconcentration prior to the CE step to increase the loadability and detected analyte amounts.<sup>2-7</sup>

Another example is IEF,<sup>8-12</sup> a widely used gradient focusing technique for the restrictive analysis of proteins and nucleotides. The fundamental basis of achieving focusing in IEF, can be exploited and transferred to development of other techniques in an effort to expand the class of analytes to be separated. Such developments have resulted in creating alternative field gradient focusing techniques: the first non-pH dependent technique counteracting chromatography electrophoresis (CACE)<sup>13</sup> developed in 1985 by O'Farrell, electric field gradient focusing (EFGF),<sup>14-17</sup> temperature gradient focusing (TGF),<sup>18-22</sup> and micellar affinity gradient focusing (MAGF).<sup>23,24</sup> Together all the focusing techniques found in literature are grouped as: displacement methods (as in ITP),<sup>25-29</sup> or equilibrium electrofocusing (as in gradient, conductivity and temperature-gradient).<sup>13,30-32</sup> Shackman et al<sup>4</sup> gave a detailed summary of these techniques and recently Vyas et al (as reviewed in ref. 33) restricted discussions to Gradient Elution

Moving boundary Electrophoresis (GEMBE),<sup>34-37</sup> GEITP,<sup>5-6</sup> and GEITP-CZE<sup>7</sup> in capillary and microfluidic format.

Counterflow is the phenomena used to describe opposing forces in a system undergoing transport; it is used to influence the focusing of analyte at a null point. The concept of counterflow was initially introduced by Preetz<sup>38</sup> using continuous flow in an ITP system to increase the ITP column length and marked another development that could be improved upon. When current is applied to an ITP system, crossing-over of zones is common under non-steady state effectively reducing peak area. Counterflow helps to establish discrete zones between analyte ions and the LE and TE ions. Counterflow<sup>39,40</sup> used with ITP, has the advantage of increasing the effective length of separation column by prolonging analyte's time spent on column; thus, alleviating the use of longer capillary. It can also be manipulated to combine concentration and separation in one step, a feature that can be investigated for studying trace level compounds. Applying these features to Mars robotics for future Mars missions could possibly improve limits of detection<sup>41</sup> of amino acids and other substances present in meteorites<sup>42,43</sup> on Mars.

In this thesis, the counterflow methods discussed will be restricted to the recently developed capillary based techniques: Gradient Elution Isotachophoresis (GEITP), GEITP coupled to Capillary Zonal Electrophoresis, (GEITP-CZE), Temperature Gradient Focusing (TGF), and Temperature Gradient Denaturing Focusing (TGDF). A summary of these techniques are presented in Table 1.3.1.

Table 1.3.1. Summary of counterflow techniques

<i>Method</i>	<i>Analyte</i>	<i>Detection</i>	<i>Enhancement (fold)</i>	<i>Analysis time (mins)</i>
GEITP -UV	Tyrosine, tryptophan	UV-Vis	860 - 1900	8
GEITP-CZE	Glutamate, aspartate, glycine, serine, valine, alanine	LIF	2,500 - 25000	11
TGF	Glutamate, aspartate, fluorecein, carboxyfluorescein	LIF	-	<5
TGDF	Synthetic 24mer basepair DNA with 5'-fluorecein probe complimentary strand – wildtype (WT), mutant (Mut) and GCWT	LIF	-	-

### 1.3.2. Basic theory

Counterflow techniques generally achieves focusing of analyte at a fixed point along column where a steady-state is created between electrophoresis and bulk flow (Fig. 1.3.1). The position of focusing and separation is different for analytes since they have different electrophoretic mobilities. This process lengthens separation velocity, and the focusing step concentrates analyte ions resulting in narrower peaks allowing for high resolution and sensitivity.

The counterflow concept can be understood in relation to mass transport (flux). According to Giddings' unified separation theory,<sup>44</sup> mass transport through a column, includes selective transport (when concentration gradient is established) and non-selective or bulk transport (in the absence of concentration gradient – pressure, EOF, or electrical field), both of which are governed by driving and dragging forces:

$$\text{Driving force } (F) = - \frac{d\mu}{dx} \quad (1)$$

$$\text{Dragging force } (F) = -f \frac{dx}{dt} \quad (2)$$

where chemical potential, separation length, flux time, and frictional coefficient, respectively, defines the following variables:  $d\mu$ ,  $dx$ ,  $dt$ ,  $f$  (where  $f = f'N$ ;  $f'$  is frictional coefficient of a particular molecule and  $N$  is Avogadro's number).

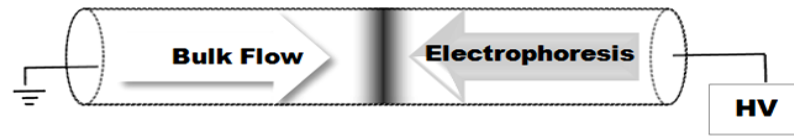


Figure 1.3.1. Counterflow schematic.

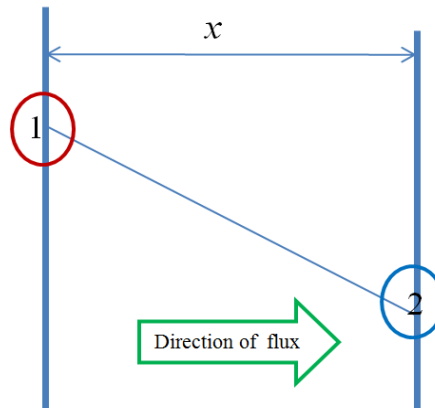


Figure 1.3.2. One dimensional diffusion.

Fick's law of diffusion describes a relationship for diffusion which depends on establishing a concentration gradient in a given time and distance. It ignores contributions from internal and external forces. The equation states:

$$J_i = -D_i \frac{\delta c_i}{\delta x} \quad (3)$$

where  $D$  is the diffusion or dispersion coefficient ( $D = RT/f$ , in  $m^2/s$ ),  $c_i$  is concentration gradient ( $mol/m^3$ ) in a particular direction ( $i$ ),  $x$  is the length of flow ( $m$ ), and  $J$  is flux density ( $mol/m^2s$ ) defined as the amount of flow through an area in a given time (in seconds). This  $D$ -term is the molecular transport which accounts for how spreading of the analyte band can affect the analyte's shape; it varies both in position ( $x$ ) along separation axis and concentration.

In a system subjected to flow a concentration gradient may be established as a result of diffusion. In a simple one dimensional case (Fig. 1.3.2), an analyte (A) will decrease in concentration down its concentration gradient, that is, from a high (1) to a low (2) concentration area creating flux density. For a two phase case, equilibrium would be reached over time.

In general, force ( $F$ ) due to motion is the product of mass,  $m$  and acceleration,  $a$ :

$$F = ma = m \frac{d^2x}{dt^2} \quad (4)$$

Assuming that the molar frictional drag for molecules is large (in the absence of vacuum condition), the acceleration term goes to zero. Thus, the sum of driving and dragging forces will equate to zero,

$$F = \frac{d\mu}{dx} - f \frac{dx}{dt} = N m \frac{d^2x}{dt^2} = 0 \quad (5)$$

Rearranging 5 gives an expression for velocity  $dx/dt$  ( $U$  or  $v$ ),

$$-\frac{1}{f} \frac{d\mu}{dx} = \frac{dx}{dt} \quad (6)$$

The “-” sign implies decrease in concentration in one direction is proportional to decrease in flux in that direction. The velocity can also be define in terms of flux,

$$\frac{J}{c} = \frac{dx}{dt} \quad (7)$$

Combining (6) and (7) gives an expression for the flux density (J),

$$J = -\frac{c}{f} \frac{d\mu}{dx} \quad (8)$$

Usually in an analytical separation system dilute solution is used (non-ideal case); thus,

$$\mu_i = \mu_i^o + RT \ln c_i \quad (10)$$

where the variables  $\mu_i^o$ ,  $R$ ,  $T$ ,  $c_i$  (for a two-phase system  $c_i = c_i^\beta / c_i^\alpha$ ) are the reference chemical potential, universal gas constant, temperature, and concentration (in moles or g/L), respectively. For a system with phases changes, the total chemical potential,  $\Delta\mu_i$ , includes all contributions from internal sources (solution pH, conductivity, etc.) and external sources (induces gradient: voltage, temperature, pressure, etc.),

$$\Delta\mu_i = \Delta\mu^o + \Delta\mu^{int} + \Delta\mu^{ext} \quad (11)$$

Therefore, the total flux in a separation system can be derived by taking the derivative of equation 10 and substituting into 8,

$$J = -\frac{c}{f} \left[ \frac{d\mu^o}{dx} + \frac{d\mu^{ext}}{dx} + RT \ln C \right] \quad (12)$$

Also written as,

$$J = -\frac{c}{f} \left[ \frac{d\mu^o}{dx} + \frac{d\mu^{ext}}{dx} \right] + -\frac{RT}{f} \frac{dc}{dx} \quad (13)$$

or,

$$J = (U + v)c - D \frac{dc}{dx} \quad (14a)$$

Thus, the analyte flux along a separation axis is influenced by combining both driving and dragging forces giving the unified separation equation:

$$J_i = c_i(U_x + \mu_i E_x) - D_i \frac{\delta c_i}{\delta x} \quad (14b)$$

where  $U_x$  is total convective velocity (or displacement velocity caused as a result of external sources), flow velocity is expressed as  $v = \mu E$ , and  $E_x$  is electric field strength along the x-axis; all other variables were described elsewhere.

Counterflow focusing is realized when  $J_i$  is equal to zero, which can occur by varying the other parameters (velocity, charge, mobility, current, or conductivity) so that a dynamic equilibrium exists. Separation results by having different discrete parameter values or by employing a gradient so long as the analytes to be separated have differing properties, such as mobility. The newly developed methods presented here generate counterflow from electrophoresis and bulk flow; balancing of these forces along the separation column result in focusing.

### 1.3.3. References Cited

1. Breadmore, M. C. *Electrophoresis* **2007**, *28*, 254-281.
2. Hawkins, K.R.; Yager, P. *Lab Chip* **2003**, *3*, 248-252.
3. Breadmore, M. C.; Thabano, J. R. E.; Dawod, M.; Kazarian, A. A.; Quirino, J. P.; Guijt, R. M. *Electrophoresis* **2009**, *30*, 230-248.
4. Simpson, L. S.; Quirino, J. P.; Terabe, S. *J. Chromatogr. A* **2008**, *1184*, 504-541.
5. Shackman, J. G.; Ross, D. *Electrophoresis* **2007**, *28*, 556-571.
6. Shackman, J. G.; Ross, D. *Anal. Chem.* **2007**, *79*, 6641-6649.
7. Mamunooru, M.; Jenkins, R. J.; Davis, N. I.; Shackman, J. G. *J. Chromatogr. A* **2008**, *1202*, 203-211.
8. Vesterberg, O. *Methods Enzymol.* **1971**, *22*, 389-412.
9. Righetti, P. G.; Bossi, A. *Elsevier Biomedical Press.* **1983**.
10. Righetti, P. G.; Bossi, A. *Anal. Chim. Acta.* **1998**, *372*, 1-19.
11. Rodriguez-Diaz, R.; Wehr, T.; Zhu, M. D. *Electrophoresis* **1997**, *18*, 2134-2144.
12. Kilar, F. *Electrophoresis* **2003**, *24*, 3908-3916.
13. O'farrell, P. H. *Science* **1985**, *227*, 1586-1589.
14. Shimura, K. *Electrophoresis* **2002**, *23*, 3847-3857.
15. Huang, Z.; Ivory, C. F. *Anal. Chem.* **1999**, *71*, 1628-1632.
16. Koegler, W. S.; Ivory, C. F. *J. Chromatogr. A* **1996**, *726*, 229-236.
17. Petsev, D. N.; Lopez, G. P.; Ivory, C. F.; Sibbett, S. S. *Lab. Chip* **2005**, *5*, 587-597.
18. Humble, P. H.; Kelly, R. T.; Woolley, A. T.; Tolley, H. D.; Lee, M. L. *Anal. Chem.* **2004**, *76*, 5641-5648.
19. Ross, D.; Locascio, L. E. *Anal. Chem.* **2002**, *74*, 2556-2564.

20. Balss, K. M.; Vreeland, W.N.; Phinney, K. W.; Ross, D. *Anal. Chem.* **2004**, *76*, 7243-7249.
21. Hoebel, S. J.; Balss, K. M.; Jones, B. J.; Malliaris, C. D.; Munson, M. S.; Vreeland, W. N.; Ross, D. *Anal. Chem.* **2006**, *78*, 7186-7190.
22. Shackman, J. G.; Munson, M. S.; Ross, D. *Anal. Bioanal. Chem.* **2007**, *387*, 155-158.
23. Balss, K. M.; Vreeland, W. N.; Howell, P. B.; Henry, A. C.; Ross, D. *J. Am. Chem. Soc.* **2004**, *126*, 1936-1937.
24. Kamande, M. W.; Ross, D.; Locascio, L. E.; Warner, I. M. *Anal. Chem.* **2007**, *79*, 1791-1796.
25. Davis, N. I.; Mamunooru, M.; Vyas, C. A.; Shackman, J. G. *Anal. Chem.* **2009**, *81*, 5452-5459.
26. Ren, L.; Masliyah, J.; Li., D. *J. Colloid Interface Sci.*, **2003**, *257*, 85-92.
27. Lin, C. H.; Kaneta, T. *Electrophoresis* **2004**, *25*, 4058-4073.
28. Quirino, J. P.; Terabe, S. *J. Chromatogr. A* **2000**, *902*, 119-135.
29. Osbourn, D. M.; Weiss, D. J.; Lunte, C. E. *Electrophoresis* **2000**, *21*, 2768-2779.
30. Meighan, M.; Stanton, S. J. R.; Hayes, M. A. *Electrophoresis* **2009**, *30*, 852-865.
31. Ivory, C. F. *Electrophoresis* **2007**, *28*, 15-28.
32. Ivory, C. F. *Sep. Sci. Technol.* **2000**, *35*, 1777-1793.
33. Vyas, C. A.; Flanigan, P. M.; Shackman, J. G. *Bioanalysis* **2010**, *2*, 815-827.
34. Shackman, J. G.; Munson, M. S.; Ross, D. *Anal. Chem.* **2007**, *79*, 565-571.
35. Ross, D.; Romantseva, E. F. *Anal. Chem.* **2009**, *81*, 7326-7335.
36. Ross, D.; Kralj, J. *Anal. Chem.* **2008**, *80*, 9467-9474.

37. Flanigan, P. M.; Ross, D., Shackman, J. G. *Electrophoresis* **2010**, *31*, 3466-3474.
38. Preetz, W. *Talanta* **1966**, *13*, 1649-1660.
39. Giddings, J. C.; Dahlgren, K. *Sep. Sci. Technol.* **1971**, *6*, 345-356.
40. Everaerts, F. M.; Vacik, J.; Verheggen, T. P. E. M.; Zuska, J. *J. Chromatogr. A* **1970**, *49*, 262-268.
41. Everaerts, F. M.; Verheggen, T. P. E. M.; Van De Venne, J. L. M. *J. Chromatogr. A* **1976**, *123*, 139-148.
42. Glavin, D. P.; Schubert, M.; Botta, O.; Kminek, G.; Bada, J. L. *Earth and Planetary Science Letters* **2001**, *185*, 1-5.
43. Mcdonald, G.D.; Storrie-Lombardi, M. C. *Astrobiology* **2006**, *6*, 17-33.
44. Giddings, J.C. *Unified Separation Science*, Wiley, New York, **1991**.

## **CHAPTER 2**

### **GRADIENT ELUTION ISOTACHOPHORESIS**

#### **2.1. Gradient Elution Isotachophoresis with Direct Ultraviolet Absorption Detection for Sensitive Amino Acid Analysis**

##### **2.1.1. Abstract**

This work demonstrates coupling of GEITP to a low-cost, conventional ultraviolet absorbance detector to realize sensitive measurements with a universal detector, eliminating the need for fluorescent analytes or derivatization. The effects of various parameters on enrichment were studied, including current density varied by LE concentration, current density varied by applied electric field, and counter-flow acceleration across varying capillary inner diameters. Optimized parameters were applied to the enrichment and separation of the amino acids tryptophan (Trp) and tyrosine (Tyr). Limits of detection for Trp and Tyr were 51 nM and 215 nM, respectively, reflecting sensitivity enhancements of 860- and 1900-fold. Analysis times were less than 6 min, and peak height RSD were less than 4%. A demonstration of enrichment and separation of these amino acids from artificial cerebrospinal fluid is additionally shown as a first step to realizing biochemical monitoring by GEITP.

### 2.1.2. Introduction

CE is gaining much attention and admiration as a separation technique in a myriad of fields, including chemistry, biology, and the pharmaceutical sciences; CE has truly matured from mainly a research technique to a routine method due to the ability to perform high resolution separations with small sample requirements. However, in order to perform sensitive analyses, frequently CE requires the use of laser induced fluorescence (LIF), necessitating either natively fluorescent analytes or derivatization techniques. Universal detectors, such as UV absorption or refractive index, suffer from low concentration limits of detection (LODs).<sup>1,2</sup> The detection problem has been exacerbated when translated to microfluidic devices, which can employ channel widths down to the nanometer regime, thick substrates, and substrates with high autofluorescence or UV absorption characteristics.<sup>3</sup> As an alternative to improved detection schemes, pre- or on-line concentration methods can be utilized to enrich analytes above the detection limits of the common detectors used with CE instruments.

Many methods have been developed for sample enrichment in CE (as reviewed in References 4-6), including: isotachopheresis (ITP); field amplified sample stacking or injection (FASS and FASI); sweeping; pH junction methods; gradient electrofocusing; and solid phase extraction (SPE). Electrophoretically based preconcentration, which achieves enrichment through differences in electrophoretic velocities of analytes during separation, can be loosely grouped into two categories. The first, equilibrium electrofocusing, relies on creating a point within the separation region where analytes experience zero net velocity. Velocity gradients can be achieved through pH, as in isoelectric focusing (IEF), electric fields, as in electric field gradient focusing (EFGF), or

conductivity, as in conductivity or temperature gradient focusing (CGF and TGF).<sup>5,7</sup> While IEF is the most popular of the methods, it is typically limited to proteins and peptides, which have accessible isoelectric points, while the other gradient methods have proven to be more universal, with concentration improvements on the order of 10-10000-fold.

The second category, dynamic enrichment methods, also utilize velocity gradients but without a null velocity point, and include FASS, FASI, and sweeping methods. Enrichments typically on the order of 10-5000-fold have been noted. While ITP with a counter-flow could be considered an equilibrium method, it is more frequently employed in CE as a transient preconcentration step and has been demonstrated in both single and coupled-column formats, obtaining 100-500,000-fold concentration enhancements.<sup>4,8</sup>

Gradient elution moving boundary electrophoresis (GEMBE) is a recently described separation technique which combines continuous sample injection with a hydrodynamically controlled variable bulk counter-flow in a capillary or microchannel.<sup>9</sup> As the counter-flow is reduced from high to low, ionic analytes are sequentially eluted onto the column and detected as boundary interfaces. GEMBE exhibits the advantages of using short separation lengths (typically 1 cm or less) and the elimination of the need to form an injection plug, making it highly amenable to high-throughput and high-density microdevices. GEMBE was further improved by combining an ITP enrichment step with gradient elution (GEITP). In GEITP, leading electrolyte (LE) is introduced into the counter-flow buffer and terminating electrolyte (TE) into the sample matrix.<sup>10</sup> Enrichment can begin outside the capillary at a counter-flow rate great enough to push LE into the sample reservoir, which forms an ionic interface near the capillary inlet.

Analytes form ITP-enriched zones at the discontinuous buffer interface. As the counter-flow is reduced, the enriched analytes are introduced onto the column for detection. Analyte resolution can be achieved through the use of non-detectable spacing ions (Fig. 2.1.1).<sup>11,12</sup>

GEITP achieves both short length separations (a 30 micrometer separation has been demonstrated) without defining a discrete injection and rapid enrichment (up to 100,000-fold in 8 min) for trace analyses. Additionally, as compared to other ITP methods, GEITP does not necessitate any buffer or polarity switching, yielding a more reliable and automatable system. The initial description of GEITP studied various parameters' affects on sensitivity enhancement using fluorescence microscopy, including initial counter-flow velocity, counter-flow acceleration, electric field strength, and LE concentration. In this work, we have coupled a low-cost single wavelength UV detector to GEITP to demonstrate the applicability of the method with universal detection. Further systematic studies were performed to optimize the enrichment process. Specifically, the affect of current density varied by LE concentration, current density varied by electric field, and counter-flow acceleration were compared across varying capillary inner diameters. Two significant deviations from the previous work's methodology were undertaken. First, the parametric study was constrained to maintaining a constant enrichment time; the prior study did not normalize enrichment to equivalent enrichment times, yielding ambiguous results. Second, lower mobility analytes, tryptophan (Trp;  $\mu_{ep} = -25.4 \times 10^{-9} \text{ m}^2/(\text{Vs})$ ) and tyrosine (Tyr;  $\mu_{ep} = -40.0 \times 10^{-9} \text{ m}^2/(\text{Vs})$ )<sup>13</sup> were utilized, as compared to the high mobility, doubly charged

carboxyfluorescein anion; use of slower analytes allowed for more realistic limits of the method, as compared to the use of ideal, highly mobile analytes.

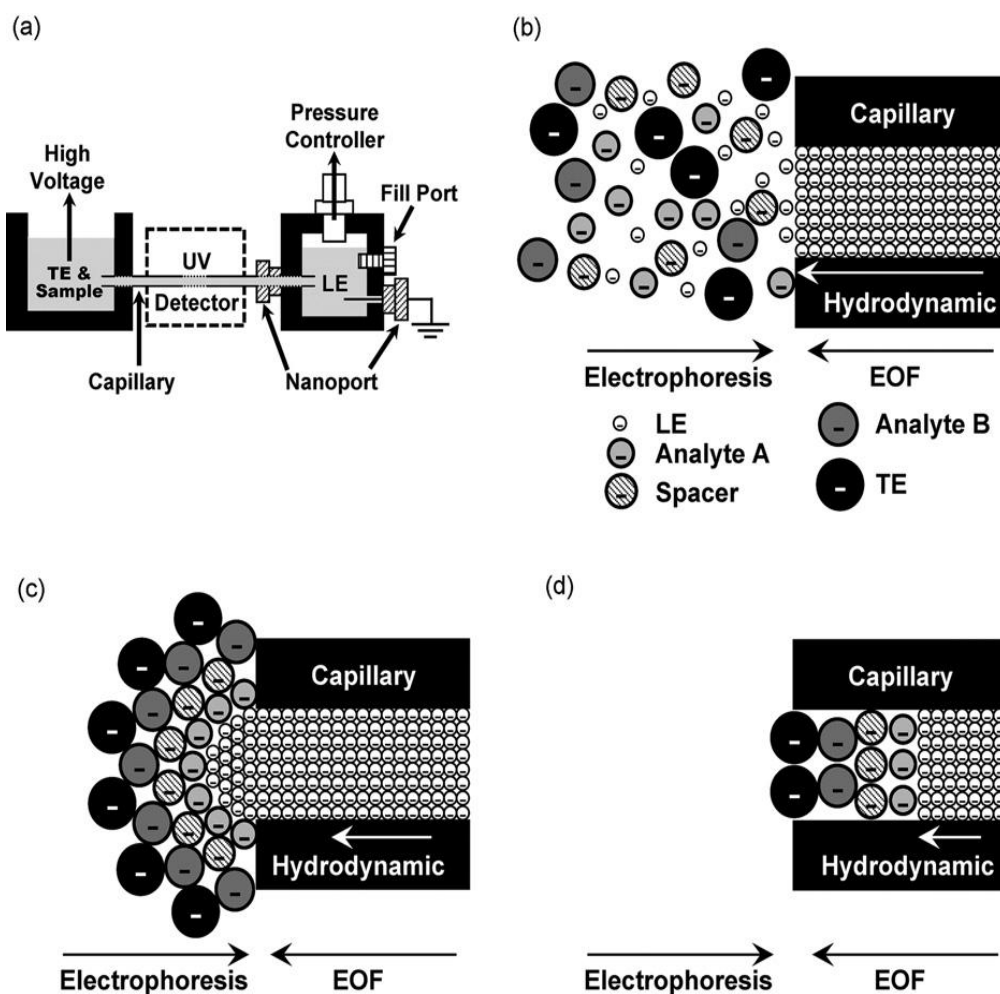


**Figure 2.1.1.** Instrumentation and concept of GEITP. (a) Schematic of instrument used for performing GEITP with UV detection. A 15 cm capillary connected a pressure controlled and grounded reservoir containing 750  $\mu\text{L}$  of leading electrolyte (LE) solution to a 100  $\mu\text{L}$  sample reservoir maintained at high voltage. Detection was performed 6 cm from sample inlet. (b) In GEITP the initial bulk flow (hydrodynamic and electroosmotic, EOF) is high enough that LE is pushed into the sample reservoir. (c) It is hypothesized that the LE creates an ionic interface upon which analytes and trailing electrolyte (TE) are enriched as the counter-flow is reduced. (d) As the hydrodynamic flow is further reduced, the interface and analyte zones are pulled into the capillary forming enriched zones based on order of electrophoretic mobility where they will be detected on-capillary. Zone resolution can be achieved using non-detectable spacer ions.

Trp, an essential amino acid, and Tyr, a non-essential amino acid, have been extensively studied due to their prevalence in biological fluids, such as cerebral spinal fluid and serum, and in common food and beverages. Current methods to measure Trp and Tyr by CE based separations include: LIF with fluorescence derivatization, with Trp LOD = 33 nM;<sup>14</sup> direct LIF, Trp LOD = 0.15 nM and Tyr LOD = 50 nM;<sup>15</sup> contactless conductivity, 3 to 50  $\mu$ M LOD;<sup>16,17</sup> and electrochemical methods, 55 nM to 250 nM LOD.<sup>18,19</sup> Dankova *et al.* described an ITP-CE method for Trp enantiomer measurements at 220 nm by UV;<sup>20</sup> while noting a 10 nM LOD, the method required an hour of analysis time to load a large sample volume. Recently, Qu *et al.* developed an amino acid enrichment technique using the interaction of zwitterions with etched fused-silica capillary surfaces; analysis times were on the order of 10 min with 1 min of sample injection.<sup>21</sup> The method achieved 40 nM LOD for Trp but required multiple buffer and voltage switching steps to load and separate mixtures and exhibited relatively poor peak height RSD, such as 13% for Trp. A simple, sensitive, and rapid analytical method, such as GEITP-UV, would greatly facilitate measurements of these and other biological molecules. Table 2.1.1 summarizes these methods and their relevant figures of merit.

Previous work utilizing solely ITP (as opposed to transient ITP or ITP-CE) to assay biomolecules from CSF typically emphasized protein analytes.<sup>22-24</sup> Hiraoka *et al.* developed an ITP method for determining glutamine from CSF as a biomarker for neurological disorders.<sup>25</sup> The method required 10  $\mu$ L of CSF injected into a *ca.* 125  $\mu$ L PTFE ITP tube. Typical measurement values were in the mid-micromolar range with 40 min of analysis time. Oefner *et al.* identified 11 small organic molecules in CSF by ITP, also making a 10  $\mu$ L injection into the instrument.<sup>26</sup> In this work, we demonstrate the

rapid enrichment and separation of Trp and Tyr from artificial CSF (aCSF) by GEITP as a step towards performing amino acid monitoring from microdialysis samples without derivatization.

**Table 2.1.1.** Selected CE-based methods for Trp and Tyr measurements

Reference	Detection Method	Analysis time (min)	Trp LOD (nm)	Tyr LOD (nm)	RSD (%) <sup>a</sup>	Comments
[14]	LIF	25	33	-	4-6	MEKC <sup>b</sup> method, fluorescently labeled Trp
[15]	LIF	10	0.15	50	3-6	Direct LIF with UV pulsed laser
[16]	Contactless conductivity	50	3,000	3500	-	Acetonitrile stacked injection
[17]	Contactless conductivity	3	50,000	-	-	Microfabricated device
[18]	Electrochemical	6	610	-	3	Amperometric
[19]	Electrochemical	10	150	210	3	MEKC, amperometric
[20]	UV Absorbance	40-60	10	-	-	ITP coupled to CE
[21]	UV Absorbance	10	40	-	13	Electrostatic enrichment injection
This work	UV Absorbance	2-6	51	215	4	GEITP

<sup>a</sup> As reported by the authors for peak height measurements.

<sup>b</sup> Micellar electrokinetic chromatography.

### 2.1.3. Experimental

#### 2.1.3.1. Chemicals and Reagents

Reagent grade L-tryptophan (Trp), L-tyrosine (Tyr), ethanolamine (ETA), and high resolution ampholyte mixture (pH 3.0–10.0) were obtained from Sigma-Aldrich (St. Louis, MO). All other chemicals were obtained from Fisher and were of the highest purity available. All solutions were made from Milli-Q (Millipore, Bedford, ME)  $\geq 18$  M $\Omega$  cm deionized water. Amino acid stock solutions were 10 mM Trp and 1 mM Tyr in 0.1 M sodium hydroxide with 0.2% (v/v) ampholyte. LE was acetate at various concentrations (as described in the text), pH adjusted to 9.5 with ETA. TE was either 0.1 M NaOH with 0.2% ampholyte or 25 mM NaOH with 0.1% ampholyte, as noted in the text. aCSF consisted of (in mM) 145 NaCl, 2.68 KCl, 1.01 MgSO<sub>4</sub>, and 1.22 CaCl<sub>2</sub>.

#### 2.1.3.2. Instrumentation

Experiments were carried out on an apparatus similar to the original instrument described for GEITP (Fig. 2.1.1a).<sup>10</sup> Briefly, 15 cm of fused silica capillary (either 30, 50, or 75  $\mu$ m I.D., as described in the text; 360  $\mu$ m O.D.; Polymicro Technologies, LLC, Phoenix, AZ) were prepared with a 2 mm wide optical window (Microsolv Window Maker; Eatontown, NJ) centered 6 cm from the sample inlet end. The sample inlet end of the capillary was inserted through a Teflon-backed silicon septum (Fisher) into a 400  $\mu$ m diameter hole drilled into a machined 100  $\mu$ L Delrin sample reservoir (McMaster-Carr; Robbinsville, NJ) maintained at high voltage (Spellman CZE1000R; Hauppauge, NY) by platinum electrode. The optical window was centered through a Lambda 1010 single wavelength UV detector equipped with a CE flow cell set to 280 nm (Groton Biosystems;

Boxborough, MA). The capillary outlet was coupled to a 750  $\mu\text{L}$  polymethyl methacrylate machined buffer reservoir (McMaster-Carr) *via* an Upchurch Nanoport (N-124S; Oak Harbor, WA); a grounding platinum electrode was also coupled to this reservoir *via* a Nanoport. Buffer exchange was through a Nylon screw secured fill port. The buffer reservoir was connected to a  $\pm 69$  kPa (10 psi) precision pressure controller (Series 600, Mensor, San Marcos, TX) for counter-flow regulation. All instrument control and data acquisition was performed using LabVIEW software (National Instruments, Austin, TX) written in-house. The software program allowed for changing the applied pressure in defined time increments (Pa/s) to the buffer reservoir via the pressure controller. Digitization of the UV output utilized a USB-6221 module (National Instruments) recording at 100 Hz. Data analysis was performed using Cutter software<sup>27</sup> with 1 Hz low-pass filtering of raw UV data. Plate number (N) was measured at width at half height,  $w_h$ . Peak identification of mixtures was accomplished through individual analyte runs and spiking of analytes.

#### **2.1.4. Results and discussion**

##### *2.1.4.1. Effect of Capillary I.D. on Enrichment*

GEITP is a modification of previous ITP methods and can be thought of as a combination of counter-flow ITP and volume-coupled ITP. Counter-flow has traditionally been utilized in ITP to effectively lengthen the separation column by prolonging analyte's residence time within the column.<sup>28,29</sup> Rather than a static counter-flow, GEITP relies upon a constantly changing counterflow. The counter-flow is a combination of electroosmotic flow (EOF) and hydrodynamic flow, with the latter being

modified during the course of an experiment by changing the applied pressure at the outlet buffer reservoir. Initially in GEITP, the counter-flow velocity can be great enough to disperse the LE rapidly into the sample reservoir (Fig. 2.1.1b). As the applied pressure and counterflow are lowered, the dispersion of LE is reduced until a discrete ionic interface is formed in the sample reservoir near the capillary inlet; enrichment of analytes occurs at this discontinuous boundary (Fig. 2.1.1c). Enrichment continues as the concentrated analyte bands are sequentially introduced onto the capillary for detection (Fig. 2.1.1d). This process was visualized in the initial description of GEITP<sup>10</sup> and is similar to the effect seen in field-amplified continuous sample injection TGF (FACSI-TGF),<sup>30</sup> as well as noted as a side effect by Breadmore and Quirino in stationary ITP (sITP).<sup>31</sup> The starting applied pressure to initiate enrichment of the highest mobility analyte must generate a counter-flow great enough to extend the LE interface into the sample well. An excessively large initial counter-flow only prolongs the analysis time while insufficient counter-flow dramatically reduces enrichment, as shown previously;<sup>10</sup> the optimal counter-flow must be empirically determined for any new analyte or buffer system by noting enrichment *versus* starting pressure.

Volume-coupling in ITP increases the injected sample amount by using a large volume sample capillary for loading and smaller capillary for detection.<sup>32-34</sup> In GEITP the sample reservoir serves as the “large volume” sample capillary. The influence of capillary geometry is hence a critical question in GEITP. Verheggen *et al.* compared PTFE tubes of 0.4, 0.2, and 0.1 mm I.D. in a standard ITP arrangement with thermometric, conductivity, and UV detection.<sup>33</sup> An improvement in resolution and detection sensitivity was noted as the I.D. was reduced, although a quantitative analysis

of enrichment was not presented. This work demonstrates the effect on GEITP enrichment using capillaries of 75, 50, and 30  $\mu\text{m}$  I.D. and Trp as a model analyte. To compare relative enrichment values, standard concentrations were simply flowed through (FT) the capillary by switching the counter-flow from positive to negative in the absence of an applied field (Fig. 2.1.2a). The calibration curve slope (sensitivity) generated was compared with standards measured under enriching conditions (i.e., voltage applied and linear decrease in counter-flow velocity). All calibration curves throughout have a correlation coefficient  $R^2 \geq 0.99$ . All measurements at a given concentration had <6% RSD in peak heights. Example GEITP electropherograms for Trp is shown in Fig. 2.1.2b.

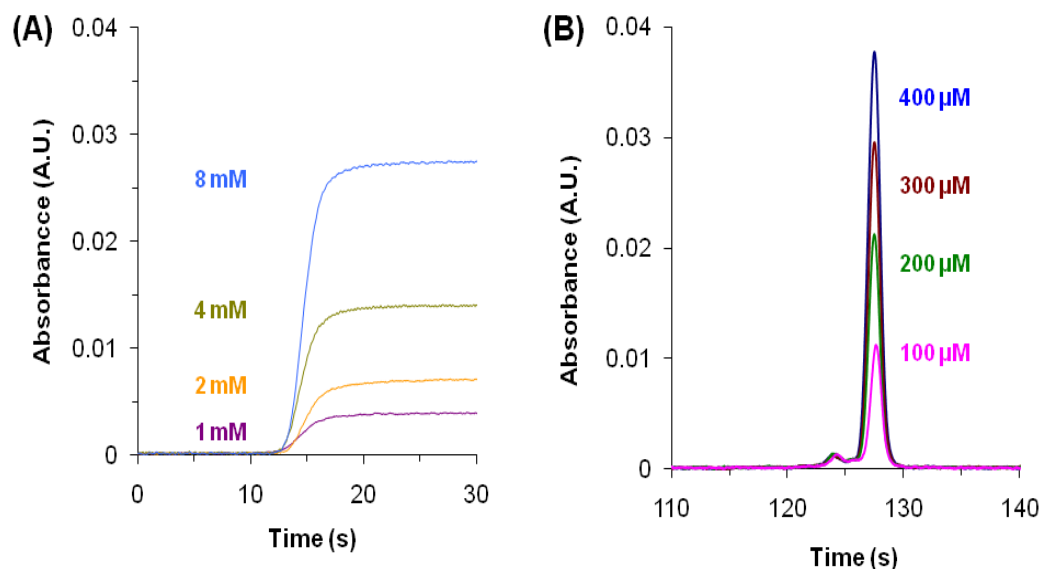


**Figure 2.1.2.** Examples of flow-through (FT) and GEITP-UV detection. (A) FT in a 30  $\mu\text{m}$  I.D. capillary of 1, 2, 4, and 8 mM Trp obtained by step-changing the applied pressure from 7000 Pa to -7000 Pa at the start of data collection. (B) GEITP-UV of 100, 200, 300, and 400  $\mu\text{M}$  Trp. 15 cm capillary (30  $\mu\text{m}$  I.D.); 6 cm separation length; -400 V/cm; -58.6 Pa/s acceleration; LE: 50 mM acetate balanced to pH 9.5 with ETA; TE, 0.1 M NaOH with 0.2% (v/v) ampholyte.

**Table 2.1.2** Experimental parameters to assess affect of capillary I.D. on enrichment

I.D. ( $\mu\text{m}$ )	[LE] mM <sup>a</sup>	$i$ ( $\mu\text{A}$ )	$E$ (V/cm)	$\Delta P$ (Pa/s)	$t_m$ (s)	LOD ( $\mu\text{M}$ )	Slope (AU/M)	N
75	50	90	-400	-1.5	$124.1 \pm 3.9$	0.922	419	1215
50	50	34	-400	-1.5	$122.5 \pm 2.3$	0.405	286	2078
50	50	34	-400	-7.6	$121.4 \pm 1.4$	0.728	229	11436
50	128	90	-400	-1.5	$130.0 \pm 3.5$	0.516	748	5704
50	128	90	-400	-7.6	$126.0 \pm 1.1$	0.437	586	19122
30	50	9	-400	-1.5	$123.3 \pm 8.6$	2.688	108	2754
30	50	9	-400	-58.6	$126.9 \pm 0.5$	2.109	97	71912
30	535	90	-400	-1.5	$130.0 \pm 2.5$	0.373	681	14240
30	535	90	-400	-58.6	$130.0 \pm 3.4$	0.458	627	109209

<sup>a</sup> TE was 0.1 M NaOH with 0.2% (v/v) ampholyte in all cases.

Initially, GEITP was performed on a 75- $\mu\text{m}$  I.D. capillary using 50 mM acetate (balanced to pH 9.5 with ETA) as LE and 0.1M NaOH with 0.2% ampholyte as TE (Fig. 2.1.3a). The strongly alkaline TE (pH *ca.* 13) allowed the amino acids to retain a net negative charge, with hydroxide acting as the terminating ion.<sup>35</sup> An electric field strength of  $-400$  V/cm was applied at the sample reservoir, yielding an initial current of  $90$   $\mu\text{A}$  and current density of  $20,000\text{A}/\text{m}^2$ . The change in counter-flow velocity due to a pressure step ( $\Delta P$ ) of  $-1.5$  Pa/s gave a migration time ( $t_m$ ) for Trp of  $124.1 \pm 3.9$  s. A LOD of  $922$  nM was observed under GEITP conditions, as compared with  $11.5$   $\mu\text{M}$  by FT. Comparison of sensitivities showed a modest 17-fold improvement under GEITP conditions. The reduced enrichment as compared with the original GEITP demonstration<sup>10</sup> could be attributed to the increased capillary I.D. ( $75$   $\mu\text{m}$  vs.  $30$   $\mu\text{m}$ ). Alternatively, the poorer performance could have been due to the much reduced mobility of the zwitterion Trp relative to the multiply charged carboxyfluorescein or due to the longer capillary inlet to detector length required of the UV detector ( $6$  cm vs.  $1$ cm used previously), although in both cases the enrichment was *ca.* 2 min.

Next, the experimental conditions of LE, TE, electric field, current, and  $\Delta P$  were held constant as the capillary I.D. was reduced. The starting pressure was adjusted until  $t_m$  was between  $120$  and  $130$  s. In this manner, the total enrichment time would be approximately equivalent across all conditions. Simply reducing the capillary I.D. to  $50$  and  $30$   $\mu\text{m}$  improved sensitivity enhancement to 25- and 31-fold, respectively (Fig. 2.1.3b and c).

The counter-flow velocity at the start of the analysis has a significant role in the enrichment rate of the analyte. If the flow rate was too low, it would lead to limited enrichment since the ionic interface cannot exit the capillary, and, if the rate were too high, analysis time would simply increase with minimal enrichment improvement. To maintain equivalent  $t_m$  and a constant starting counter-flow fluid flux ( $Q$ ) and a constant fluid acceleration,  $\Delta P$  must be increased in a fourth power manner as the capillary radius ( $r_c$ ) is reduced to conform to the Hagen-Poiseuille equation:<sup>36</sup>

$$Q = \frac{\pi \Delta P r_c^4}{8L\eta} \quad (1)$$

where solution viscosity ( $\eta$ ) and capillary length ( $L$ ) remain constant. Adjustment of  $\Delta P$  to -7.6 and -58.6 Pa/s for 50 and 30  $\mu\text{m}$  I.D. capillaries, respectively, had a slight degradation affect on enrichment enhancement (20-fold for 50  $\mu\text{m}$  and 28-fold for 30  $\mu\text{m}$  I.D. capillaries), suggesting that the initial counter-flow was adequate but the increased hydrodynamic flow rate caused slight detrimental dispersion (Fig. 2.1.3b and c).

As opposed to using the same LE concentration as the 75  $\mu\text{m}$  I.D. capillary, with an assumed equivalent current density as I.D. is reduced, the affect of initial absolute current was studied. LE acetate concentration was increased until an initial current of 90  $\mu\text{A}$  was observed in the smaller capillaries. The increased current's affect on enrichment was studied at both the same  $\Delta P$  and same acceleration (by increasing the magnitude of  $\Delta P$  *via* Eq. (1)) as the 75  $\mu\text{m}$  I.D. capillary. A marked improvement in enrichment was shown at higher currents, with the 50  $\mu\text{m}$  I.D. capillary having 65- and 51-fold enhancement for equivalent  $\Delta P$  and acceleration, respectively; the 30  $\mu\text{m}$  I.D. capillary had 197- and 181-fold improvement for equivalent  $\Delta P$  and acceleration, respectively.

The same degradation in enrichment as the magnitude of  $\Delta P$  was increased to achieve equivalent accelerations was observed with the increased ionic strength conditions (Fig. 2.1.3b and c).

Table 2.1.2 and Figs. 2.1.3d and 2.1.3e summarize the trends of enrichment and  $N$  across the three capillaries. Although  $N$  is not an ideal predictor of potential resolving power in focusing-based separations,<sup>5</sup> as all peaks had equivalent  $t_m$  it was a useful measure of zone broadening. In all cases, reduction of capillary I.D. improved both enrichment and peak efficiency. While decreasing the magnitude of  $\Delta P$  had a slight improvement in enrichment, it had a dramatically deleterious effect on  $N$ ; hence, a larger acceleration appeared to be the preferred mode of operation. In general it would appear that I.D. reduction was favorable for enrichment; however, when utilizing UV detection, the reduction in optical pathlength concomitantly degrades sensitivity. Hence, similar best LOD of approximately 400 nM for Trp were observed during the parametric study for the 50 and 30  $\mu\text{m}$  I.D. capillaries. This disadvantage would not be problematic using detectors without pathlength dependence.

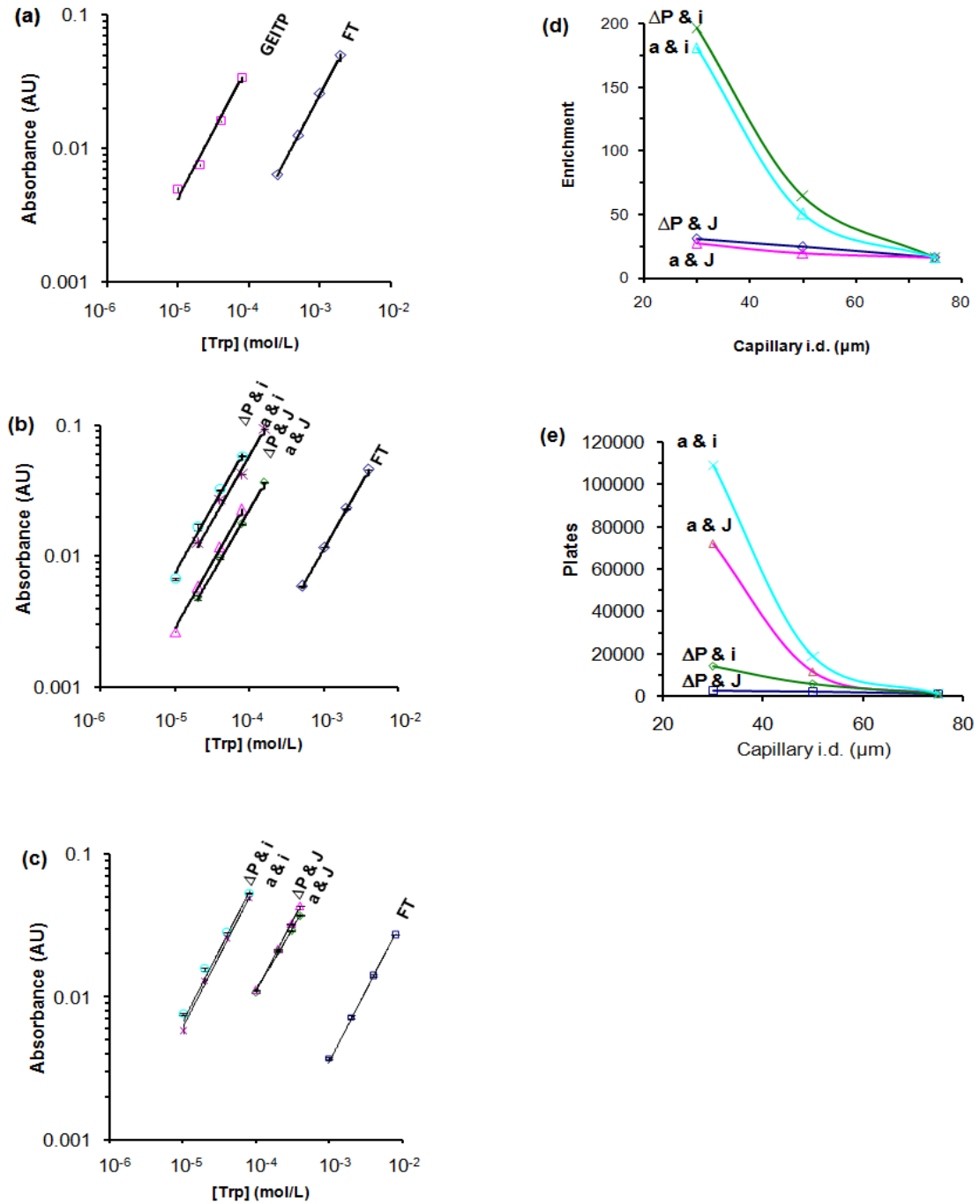


**Figure 2.1.3.** Effect of capillary I.D. on GEITP enrichment. See Table 2.1.2 for individual separation conditions. (a) FT and GEITP calibration curves using 75  $\mu\text{m}$  I.D. capillary. (b) 50  $\mu\text{m}$  I.D. capillary calibration curves with the same acceleration and current density ( $a$  and  $J$ ), pressure step and current density ( $\Delta P$  and  $J$ ), acceleration and current ( $a$  and  $i$ ), and pressure step and current ( $\Delta P$  and  $i$ ) as used for the 75  $\mu\text{m}$  I.D. capillary in (a). (c) Same as (b) using 30  $\mu\text{m}$  I.D. capillary. (d) Comparison of sensitivity enrichment over FT versus capillary I.D. (e) Comparison of  $N$  vs. capillary I.D. All error bars are 1 SD ( $n = 3$ ).

#### 2.1.4.2. Comparison of LE versus electric field adjustment of current

Both driving current and current density could be modified either through LE concentration or through electric field strength. While the prior work<sup>10</sup> noted a logarithmic increase in enrichment as LE concentration was increased and a linear improvement as the field was increased within a given capillary, this work was performed without maintaining equivalent enrichment times, although the acceleration and starting pressure were held constant. Using a 30  $\mu\text{m}$  I.D. capillary, -400 V/cm, -58.6 Pa/s, and 0.1 M NaOH with 0.2% ampholyte TE, enrichment of Trp was evaluated using 50, 100, and 150 mM acetate LE. These results were compared to a series of analyses using 50 mM acetate LE as the field was increased to match the initial current of the 100 and 150 mM acetate LE experiments (Table 2.1.3 and Fig. 2.1.4). All analyses were conducted with  $t_m$  between 120 and 130 s. While both methods improved enrichment in a linear manner for the ranges studied, clearly increasing LE was the preferred method to achieve sensitivity enhancement.

**Table 2.1.3.** Experimental parameters to compare current adjustment by LE or electric field

I.D. ( $\mu\text{m}$ )	[LE] mM <sup>a</sup>	$i$ ( $\mu\text{A}$ )	$E$ (V/cm)	$\Delta P$ (Pa/s)	$t_m$ (s)	LOD ( $\mu\text{M}$ )	Slope (AU/M)	N
30	50	9	-400	-58.6	$126.9 \pm 0.5$	2.109	97	71912
30	100	18	-400	-58.6	$122.2 \pm 0.6$	1.299	201	92874
30	150	26	-400	-58.6	$122.7 \pm 0.8$	0.857	274	115021
30	50	18	-682	-58.6	$128.6 \pm 1.0$	1.989	138	15983
30	50	26	-780	-58.6	$123.2 \pm 1.6$	1.186	178	10461

<sup>a</sup> TE was 0.1 M NaOH with 0.2% (v/v) ampholyte in all cases.

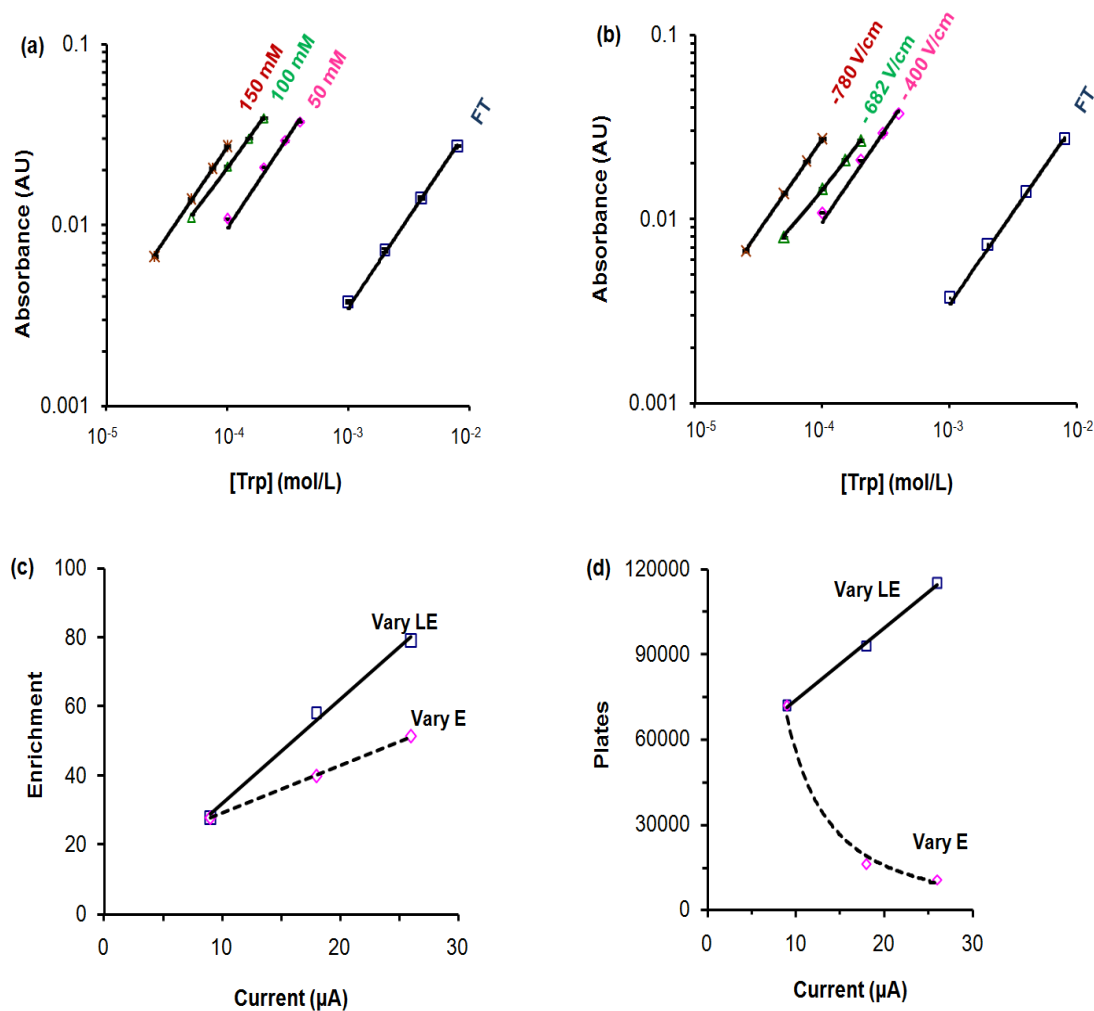


**Figure 2.1.4.** Comparison of LE vs. electric field strength ( $E$ ) adjustment of current. See Table 2.1.3 for individual separation conditions. (a) Calibration curves of GEITP enrichment using various concentrations of acetate as LE (all balanced to pH 9.5 with ETA). (b) Calibration curves of GEITP enrichment using fields of -400, -682, and -780 V/cm to generate equivalent initial currents as generated using 50, 100, and 150 mM acetate LE at -400 V/cm. (c) Comparison of sensitivity enrichments when current was adjusted by either LE or field strength. (d) Comparison of plate number when current was adjusted by either LE or field strength. All error bars are 1 SD ( $n = 3$ ).

The difference may be due to the affect each method had on  $N$  (Fig. 2.1.4b). While increasing LE concentration led to a linear improvement in peak efficiency, increasing the field strength had a deleterious effect (best fit to a power function of  $N=4.08 \times 10^6 \times i^{-1.86}$ , where  $i$  was current). The decrease in  $N$  may have been due to increased Joule heating. Increasing LE ionic strength would lead to increased heating in the LE zone, while the local heating of the sample and TE zones would remain relatively unaffected; increasing the field would increase heating across all ITP zones. Ohm's law plots relating current *versus* voltage are commonly used to detect Joule heating in CE.<sup>37</sup> However, Ohm's law plots determined when the capillary is filled only with LE (Fig. 2.1.5a) cannot adequately describe the dynamic process of GEITP, where the fluid composition within the capillary is constantly changing. Alternatively, monitoring the current throughout the course of the counter-flow change would give a better description of the potential for Joule heating; Fig. 2.1.5b shows examples of the current passed under various operating conditions. These examples were recorded with a higher starting pressure than used for the Trp analyses to assess enrichment and efficiency in order to better record the initial state when only LE was present in the capillary; additionally, the total analysis time was increased until full flow reversal was noted, as indicated by a sharp rise in current due to only NaOH being present in the capillary. At equivalent LE concentrations *versus* elevated field strength (50 mM LE at  $-400$  and  $-780$  V/cm), a higher overall current was seen throughout the entire gradient with increased applied voltage. Comparison of 50 mM LE at  $-780$  V/cm and 150 mM LE at  $-400$  V/cm showed initially equivalent currents when only LE was present in the capillary. However, the higher LE at lower field strength had a lower overall current throughout the gradient than

the lower LE at higher field strength, which would suggest a reduced potential for Joule heating.

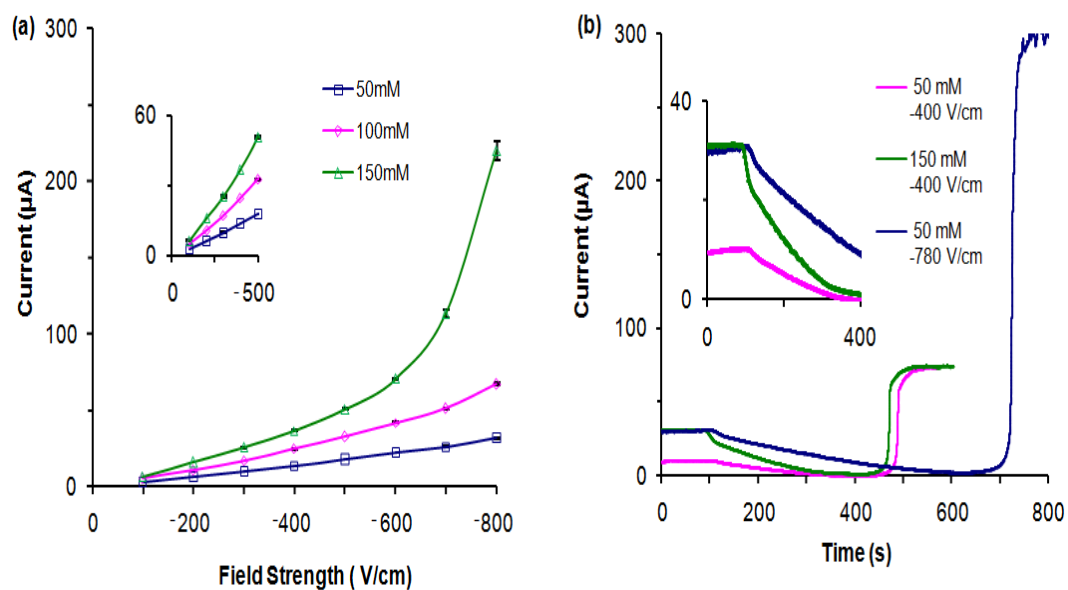


**Figure 2.1.5.** Monitoring current in GEITP. (a) Ohm's law plots of 50, 100, and 150mM acetate balanced to pH 9.5 with ETA present in both the sample and pressure controlled reservoirs. No pressure was applied during the current measurement. All error bars are 1 SD ( $n = 3$ ). (b) Examples of current changes during the course of GEITP using 50mM acetate LE at  $-400$  V/cm, 150mM LE at  $-400$  V/cm, and 50mM LE at  $-720$  V/cm. TE, 0.1M NaOH with 0.2% (v/v) ampholyte. The power supply had a maximal output of  $300 \mu\text{A}$ .

### 2.1.4.3. Application to Amino Acid Analyses

The above optimization of parameters was applied to the sensitive determination of Trp and Tyr (Fig. 2.1.6a). Conditions used were 30  $\mu\text{m}$  I.D. capillary, -400 V/cm, 250 mM acetate LE, and -58.6 Pa/s. The parametric study suggested that an optimal arrangement when considering both sensitivity and efficiency includes use of smaller bore capillaries with high concentrations of LE. It was found that further reduction of capillary I.D. from 30  $\mu\text{m}$  was limited by the pressure range of the counter-flow controller. At field strengths of -300 V/cm and below, enrichment was severely degraded, similar to observations made in the previous work.<sup>10</sup> At a field strength of -400 V/cm, there was only slight degradation in enrichment when reducing the LE concentration from 535 to 250 mM acetate; however, the system was less prone to bubble generation and more stable. Additionally, it was noted that reduction in TE NaOH concentration to 25 mM with 0.1% ampholyte (v/v) improved sensitivity enhancement. Further reduction in TE concentration reduced enrichment, presumably due to the ampholyte becoming a major buffering constituent and reducing the TE pH. 0.1% ampholyte, which was the source of spacing ions, was determined to be the minimal concentration necessary to adequately resolve the analytes. The small range of concentrations for the FT Tyr calibration was due to poor solubility. An example of the optimized separation of a mixture of Trp and Tyr, using the ampholyte mixture as a universal spacer, is shown in Fig. 2.1.6b. The minor peaks were systemic and believed to be due to absorbing species in the ampholyte mixture. Individual LODs for Trp and Tyr were 51 and 215 nM, respectively, reflecting sensitivity enhancements of 860- and 1900-fold. These enrichment values are within the range expected for GEITP of low mobility

analytes, comparable to the 300-fold enrichment seen for proteins,<sup>10</sup> with the higher mobility Tyr exhibiting improved enrichment as compared with Trp. Additionally, each concentration had less than 4% RSD in peak heights.

As a first step to demonstrating GEITP-UV's applicability to biochemical monitoring, a sample consisting of 2  $\mu\text{M}$  Tyr and 500 nM Trp in a solution of 5  $\mu\text{L}$  aCSF and 95  $\mu\text{L}$  TE (25 mM NaOH with 0.1% ampholyte) was analyzed. The 20-fold dilution of the aCSF was similar to that used in previous ITP and CE work.<sup>14,15,25,26</sup> Comparison of electropherograms without (Fig. 2.1.6b) and with (Fig. 2.1.6c) aCSF were remarkably similar with respect to the Tyr and Trp peaks, a surprising finding considering that the sample contained over 7 mM NaCl in only 25 mM NaOH. The minimal effect due to chloride ( $\mu_{\text{ep}} = -79.1 \times 10^{-9} \text{ m}^2/(\text{Vs})$ ) could be due to the choice of the lower mobility acetate LE ( $\mu_{\text{ep}} = -53 \times 10^{-9} \text{ m}^2/(\text{Vs})$ ),<sup>35</sup> so that chloride would actually pass ahead of the ITP enrichment boundary. A greater effect was exhibited in the systemic ampholyte peaks preceding the target amino acids, which were more fully resolved from each other and Tyr, possibly due to the other aCSF components acting as spacing ions. The peak at 282 s was an impurity in the aCSF solution itself. As both human and rodent models have shown Tyr and Trp levels between 1 and 20  $\mu\text{M}$  in CSF.<sup>15,38,39</sup> GEITP-UV is a potential analytical tool for studying these amino acids directly from microdialysate without derivatization.

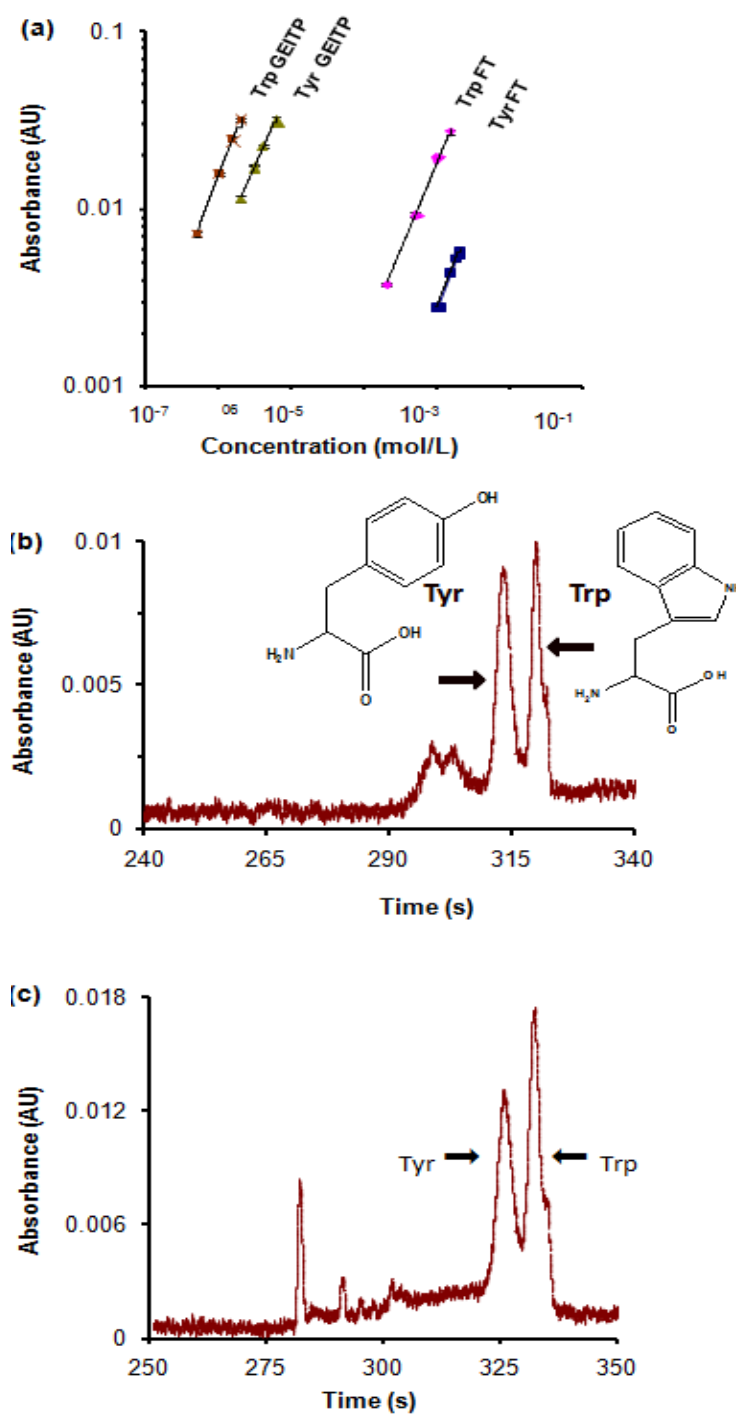


**Figure 2.1.6.** Optimized amino acid analyses by GEITP. (a) FT and GEITP calibration curves for Trp and Tyr. 15 cm capillary (30  $\mu$ m I.D.); 6 cm separation length; -400 V/cm; -58.6 Pa/s acceleration; LE: 250 mM acetate balanced to pH 9.5 with ETA; TE: 0.1 M NaOH with 0.2% (v/v) ampholyte. Error bars are 1 SD ( $n = 3$ ). Example electropherograms showing the separation of 2  $\mu$ M Tyr and 500 nM Trp samples (b) in only TE and (c) in 1:20 aCSF:TE.

### 2.1.5. Conclusion

This work demonstrates the first successful coupling of GEITP to a low-cost conventional UV detector for sensitive amino acid measurements. Mid-nanomolar LODs for Trp and Tyr were observed, with analysis times of a few minutes. These LODs are similar to those obtained using an etched capillary surface interaction enrichment method with direct UV detection;<sup>21</sup> however, GEITP-UV does not require multiple buffer or voltage switches and exhibits better peak height reproducibility (<4% vs. 13% RSD). A first demonstration of amino acid measurements from aCSF additionally shows the applicability of the method to assays from biological matrices.

Further experimental evidence provides a better understanding of the mechanism and improved optimization of the GEITP technique. It was found that reduced capillary I.D. leads to increased enrichment and efficiency; however, the full advantage in detection sensitivity cannot be realized using pathlength dependent detectors, such as absorbance. Small geometries for trace measurement applications would best be realized by coupling GEITP to sensitive, pathlength independent techniques, such as LIF or electrochemical detection. Fluorescence would also allow for a wider selection of spacing ions, many of which absorb in the UV, for resolution of analyte zones. GEITP-UV does provide utility in applications where analytes do not natively fluoresce, require unconventional excitation sources (e.g., UV lasers), have poor fluorescent derivatization efficiencies, or no available fluorescent labeling chemistries. Additionally, it was found that enrichment improvements realized by increasing the LE conductivity was dramatically advantageous over simply increasing the electric field strength when

considering separation efficiency. Dynamic current monitoring indicated that larger Joule heating across the total capillary at elevated potentials leads to the degradation in efficiency.

In addition to rapid enrichment, the other primary advantages of the method are the short separation lengths utilized and the elimination of defining an injection plug. Furthermore, the counter-flow can be utilized to remove potentially capillary fouling components, such as large proteins, as demonstrated in a related technique, counter-flow rejection TGF.<sup>40</sup> These features make GEITP-UV an attractive possibility for conducting sensitive amino acid assays from a variety of matrices, such as biological fluids. Analyte zone discrimination is difficult in GEITP-UV, similar to traditional ITP with UV detection, due to the necessity of non-detectable spacers. Alternative detection schemes, such as conductivity or multiple wavelengths UV, would facilitate measurements of multi-component mixtures. A potential use of GEITP would be in a 'sensor mode' for small numbers of analytes. Judicious choice of the LE and TE or use of discrete spacing ions can be exploited to isolate specific analytes from mixtures.<sup>10</sup> As an alternative implementation, GEITP could be coupled to traditional CE, as has been done in ITP methods, to allow for high-resolution separations without the need for inclusion of spacing ions.

### 2.1.6. References Cited

1. Weinberger, R. *Practical Capillary Electrophoresis*, Academic Press, New York, 1993.
2. Goetz, S.; Karst, U. *Anal. Bioanal. Chem.* **2007**, *387*, 183-192.
3. Hawkins, K. R.; Yager, P. *Lab Chip* **2003**, *3*, 248-252.
4. Breadmore, M. C. *Electrophoresis* **2007**, *28*, 254-281.
5. Shackman, J. G.; Ross, D. *Electrophoresis* **2007**, *28*, 556-571.
6. Lin, C. H.; Kaneta, T. *Electrophoresis* **2004**, *25*, 4058-4073.
7. Ivory, C. F. *Electrophoresis* **2004**, *28*, 15-25.
8. Osburn, D. M.; Weiss, D. J.; Lunte, C. E. *Electrophoresis* **2000**, *21*, 2768-2779.
9. Shackman, J. G.; Munson, M. S.; Ross, D. *Anal. Chem.* **2007**, *79*, 565-571.
10. Shackman, J. G.; Ross, D. *Anal. Chem.* **2007**, *79*, 6641-6649.
11. Inano, K.; Tezuka, S.; Miida, T.; Okada, M. *Ann. Clin. Biochem.* **2000**, *37*, 708-716.
12. Chartogne, A.; Reeuwijk, B.; Hofte, B.; van der Heijden, R.; Tjaden, U.R.; van der Greef, J. *J. Chromatogr. A* **2002**, *959*, 289-298.
13. Pospichal, J.; Gebauer, P.; Bocek, P. *Chem. Rev.* **1989**, *89*, 419-430.
14. Zhao, S.; Liu, Y. *Electrophoresis* **2001**, *22*, 2769-2774.
15. Bayle, C.; Siri, N.; Poinot, V.; Treilhou, M.; Causse, E.; Couderc, F. *J. Chromatogr. A* **2003**, *1013*, 123-130.
16. Tuma, P.; Samcova, E.; Andelova, K. *J. Chromatogr. B* **2006**, *839*, 12-18.

17. Tanyanyiwa, J.; Abad-Villar, E. M.; Fernandez-Abedul, M. T. ; Costa-Garcia, A.; Hoffmann, W.; Guber, A. E.; Herrmann, D.; Gerlach, A.; Gottschlich, N.; Hauser, P. C. *Analyst* **2003**, *128*, 1019-1022.
18. Chu, Q.; Guan, Y.; Geng, C.; Ye, J. *Anal. Lett.* **2006**, *39*, 729-749.
19. Wang, Q.; Yu, H.; Li, H.; Ding, F.; He, P.; Fang, Y. *Food Chem.* **2003**, *83*, 311-317.
20. Dankova, M.; Kaniansky, D.; Fanali, S.; Ivanyi, F. *J. Chromatogr. A* **1999**, *838*, 31-43.
21. Qu, Q.; Liu, Y.; Tang, X.; Wang, C.; Yuang, G.; Hu, X.; Yan, C. *Electrophoresis* **2006**, *27*, 4500-4507.
22. Smuts, H. E.; Russell, B. W.; Moodie, J. W. *J. Neurol. Sci.* **1982**, *56*, 283-292.
23. Kjellin, K. G.; Hallander, L. *J. Neurol.* **1979**, *221*, 235-244.
24. Kopwillem, A.; Merriman, W. G.; Cuddeback, R. M.; Smolka, A. J.; Bier, M. *J. Chromatogr.* **1976**, *118*, 34-46.
25. Hiraoka, A.; Miura, I.; Tominaga, I.; Hattori, M. *Clin. Biochem.* **1989**, *22*, 293-296.
26. Oefner, P.; Hafele, R.; Bartsch, G. *J. Chromatogr.* **1990**, *516*, 251-262.
27. Shackman, J. G.; Watson, C. J.; Kennedy, R. T. *J. Chromatogr. A* **2004**, *1040*, 273-282.
28. Everaerts, F. M.; Vacik, J.; Verheggen, T. P. E. M.; Zuska, J. *J. Chromatogr. A* **1970**, *49*, 262-268.
29. Everaerts, F. M.; Verheggen, T. P. E. M.; van de Venne, J. L. M. *J. Chromatogr. A* **1976**, *123*, 139-148.
30. Munson, M. S.; Danger, G.; Shackman, J. G. ; Ross, D. *Anal. Chem.* **2007**, *79*, 6201-6207.

31. Breadmore, M.C.; Quirino, J. *Anal. Chem.* **2008**, *80*, 6373-6381.
32. Mazereeuw, M.; Tjaden, U. R.; van der Greef, J. *J. Chromatogr. A* **1994**, *677*, 151-157.
33. Verheggen, Th. P. E. M.; Mikkers, F. E. P.; Everaerts, F. M. *J. Chromatogr.* **1977**, *132*, 205-215.
34. Chen, S.; Lee, M. L. *Anal. Chem.* **1998**, *70*, 3777-3780.
35. Bocek, P.; Deml, M.; Gebauer, P.; Dolnik, V. *Analytical Isotachophoresis*, VCH, New York, **1988**.
36. Giddings, J. C. *Unified Separation Science*, Wiley, New York, **1991**.
37. Landers, J. P. *Handbook of Capillary Electrophoresis*, 2<sup>nd</sup> ed., CRC Press, Boca Raton, FL, **1997**.
38. Comai, S.; Longatti, P.; Perin, A.; Bertazzo, A.; Ragazzi, E.; Costa, C.V. ; Allegri, G. *J. Neurosci. Res.* **2006**, *84*, 683-91.
39. Molfino, A.; Muscaritoli, M.; Cascino, A.; Fanfarillo, F.; Fava, A.; Bertini, G.; Citro, G.; Fanelli, F. R.; Laviano, A. *Pharmacol. Biochem. Behav.* **2008**, *89*, 31-35.
40. Munson, M. S.; Meacham, J. M.; Locascio, L. E.; Ross, D. *Anal. Chem.* **2008**, *80*, 172-178.

## **2.2. Gradient Elution Isotachopheresis Coupled to Capillary Zonal Electrophoresis for Sensitive Amino Acid Analyses**

### **2.2.1. Abstract**

In this work, gradient elution isotachopheresis was combined with capillary zone electrophoresis (GEITP-CZE) in a single microcolumn. The multi-stage approach addresses the issues of analyte resolution difficulties in GEITP, as well as poor concentration sensitivity in CZE. GEITP employs rapid electrophoretic focusing at a discontinuous ionic interface within a sample well generated through combined electroosmotic and hydrodynamic flows. The interface and enriched analytes are then pulled into a capillary or microchannel as the counter-flow is reduced for on-column detection. To transform GEITP-focused samples to CZE-based separation, the sample solution is replaced with CZE buffer solution while maintaining hydrodynamic flow to ensure migration towards the detector. The single solution switch and lack of polarity inversion allows for reproducible separations (typically <6% relative standard deviation in peak heights and <0.5% in migration times). Low-pressure hydrodynamic flow during CZE allowed for flexible resolution adjustment, with a linear increase *versus* the square root of migration time, without altering the separation column, field strength, or electrolyte system. As a first demonstration of the applicability of GEITP-CZE, a series of amino acids to be assayed for in future Mars exploration missions as indicators of biological life were studied. Separation of six amino acids, with limits of detection as low as 200 fM, were achieved using a capillary format with a total analysis time of 11 min.

### 2.2.2. Introduction

In recent years numerous advances in capillary electrophoresis (CE) techniques have been made due to the attractiveness of low volume requirements and rapid analyses. Improvements in CE sensitivity continue to be of great interest, especially as methods are translated to microfluidic devices.<sup>1,2</sup> As an alternative to detector improvements, much work has been devoted to preconcentration or enrichment methods to increase the loaded and detected analyte amounts (as reviewed in References 3-5). Electrophoretic enrichment methods include field amplified sample stacking (FASS), field amplified sample injection (FASI), pH junctions, isotachopheresis (ITP), and focusing methods such as isoelectric, electric field gradient, and temperature gradient techniques.

ITP for capillary or microfluidic separations has been implemented as a stand-alone method, coupled to CZE (ITP-CZE), or as a transient stage prior to CZE (tITP).<sup>6-8</sup> Impressive preconcentration has been achieved using ITP, such as recent work by Santiago's group achieving 500,000-fold sensitivity improvements and attomolar detection of small fluorescent dyes by microfluidic tITP.<sup>9,10</sup> ITP requires a two-electrolyte system, with the choice of background ions critical to defining the enrichment and separation window. Generally, the sample is introduced between a high-mobility leading electrolyte (LE) and a low-mobility trailing electrolyte (TE), with the desired analytes being of intermediate mobilities. When voltage is applied, sample zones are compressed between the LE and TE in order of their respective mobilities, forming tightly focused zones once a steady state is reached. The purified, adjacent sample zones can be interrogated directly (*e.g.*, by conductivity), isolated using non-detectable spacing ions, or transferred to a second CZE stage.

A recently developed electrophoretic technique, gradient elution ITP (GEITP),<sup>11</sup> combines continuous electrokinetic sample injection with variable hydrodynamic flow to form a discontinuous ionic interface within the sample reservoir. To perform GEITP, LE is incorporated into a bulk counter-flow (a combination of hydrodynamic and electroosmotic, EOF, flows) of fluid through the microcolumn and TE is present in the sample matrix. The bulk flow, initially great enough to force LE into the sample reservoir, is reduced during the analysis, creating a LE-sample-TE ITP region outside of the separation column. The sample ions are focused and separated into adjacent regions based on their respective mobilities. As counter-flow is further reduced, enriched zones are loaded on-capillary for detection. Previous GEITP work employed non-detectable spacing ions to provide spatial resolution between analytes such as small dyes, amino acids, DNA, and proteins using either absorbance and fluorescence detection.<sup>11-14</sup>

Reinhoud *et al.*<sup>15-17</sup> developed a method for coupling ITP to CZE on a single capillary for analysis of either cations or anions using static hydrodynamic flow. When using LE as the background electrolyte for anionic CZE, the capillary (initially filled with LE) was hydrodynamically loaded with a large volume of sample. The sample vial was replaced with TE and positive voltage was applied to the outlet. A static counter-flow was used to balance analyte migration and EOF in order to prevent sample from exiting the capillary. After focusing was complete (5-20 min), the hydrodynamic flow was stopped and the inlet vial replaced with LE, flushing sample and TE towards the inlet by EOF. Once the majority of TE was removed (but without allowing the sample to exit) the potential was inverted for transition into CZE. Precise timing was crucial for voltage switching, as overly long flushing would result in sample migrating out of capillary; early

switching left large amounts of TE in the capillary, consequently disrupting the CZE process due to a large degree of field strength inhomogeneity.

We have built upon this early work for a new method to couple GEITP with CZE for anionic analyses with simplified operation. As enrichment primarily occurred off-column, the end of focusing situated the enriched zones just inside the separation column inlet, eliminating the need for TE flushing. The major advantage of off-column preconcentration was sensitivity improvement was not limited to capillary volume but could easily be tuned by increasing the GEITP duration. Once focusing was complete, the sample solution was replaced with LE. For anionic CZE, a static hydrodynamic flow was utilized to balance EOF, negating the need for polarity inversion or capillary coatings to suppress EOF and allowing for the use of native capillaries and microchannels. Resolution on short microcolumns could also be easily adjusted through the bulk flow, similar to work by Jorgenson and Culbertson<sup>18</sup> who used switched hydrodynamic flow to increase sample zone residence time on-column. The combination of these features results in a method that offers the advantages of simplicity, rapid analysis, high separation efficiency, and flexibility through the effective use of variable bulk flow.

As a first demonstration of GEITP-CZE, the technique was applied to amino acid analyses in a single microcolumn. The specific amino acids chosen for the present work have been found at low levels in carbonaceous Martian meteorites and are expected to be found in Martian soil.<sup>19</sup> *In situ* analyses of these biomolecules will require a robust, sensitive, portable, and flexible method. CE-based microfluidics, such as the Mars Organic Analyzer (MOA),<sup>20-23</sup> have demonstrated many of these features, with the exception of adjustable sensitivity and resolution. The ability to tune both parameters

“on-the-fly”, as demonstrated in this work, would be a key advantage for extra-terrestrial missions. Using fluorescamine-labeled amino acid standards, MOA demonstrated a 13 nM LOD;<sup>22</sup> more recently, using Pacific Blue-labeled standards, a 75 pM LOD has been achieved.<sup>23</sup> GEITP using spacers has demonstrated enrichment and resolution of the target amino acids at low nanomolar levels, but required lengthy (~ 1 hr) analysis times to achieve separation.<sup>12</sup> The adaptation of GEITP coupled to CZE, as compared to the previous standalone GEITP amino acid method, achieves a 10-fold reduction in analysis time and a 1000-fold improvement in sensitivity.

### **2.2.3. Experimental**

#### *2.2.3.1. Chemicals and Reagents*

Reagent grade L-amino acids (alanine, Ala; aspartic acid, Asp; glutamic acid, Glu; glycine, Gly; serine, Ser; and valine, Val. Abbreviations refer to the fluorescently-labeled species) and fluorescent grade tris(hydroxymethyl) aminomethane (tris), citric acid, and boric acid were obtained from Sigma (St. Louis, MO). 5-carboxyfluorescein, succinimidyl ester (FAM, SE) single isomer was purchased from Invitrogen (Carlsbad, CA). All other reagents were obtained from Fisher Scientific (Pittsburgh, PA). All solutions were made using Milli-Q (Millipore, Bedford, MA)  $\geq 18 \text{ M}\Omega \text{ cm}$  deionized (DI) water. LE was various concentrations of citrate (as noted in the text) balanced to pH 8.5 with tris. TE was 0.25 M tris/borate (pH 8.5).

Stock solutions of amino acids were 1 mM in 15 mM sodium borate buffer (pH 9.2). FAM, SE was 0.1 M in dimethyl sulfoxide. For labeling, 2.5  $\mu\text{L}$  of FAM, SE stock was added to 247.5  $\mu\text{L}$  amino acid stock. The resulting mixture solution was vortexed to mix and incubated in the dark for 12 h at room temperature before being stored at 4 °C.

For analysis, dilutions of labeled amino acids were made in TE without removal of free dye. Each amino acid was labeled separately to allow for peak identification. The degree of labeling was not characterized.

### 2.2.3.2. Instrumentation

Capillary experiments were carried out on an apparatus similar to one previously described for GEITP<sup>11,12</sup> and shown in Figure 2.1A. Briefly, 11 cm of fused-silica capillary (25  $\mu\text{m}$  i.d.; 360  $\mu\text{m}$  o.d.; Polymicro Technologies, Phoenix, AZ) with a 2-mm optical window (Microsolv Window Maker, Eatontown, NJ) located 6 cm from the inlet was inserted into a machined 100- $\mu\text{L}$  Derlin sample reservoir (McMaster-Carr, Robbinsville, NJ) with a 400- $\mu\text{m}$  diameter hole sealed with a Teflon-backed silicon septum (Sigma). High voltage (CZE 3000, Spellman High Voltage Electronics, Hauppauge, NY) was applied to the sample reservoir by platinum electrode. Solution switching was accomplished by micropipette. For GEITP-CZE, the sample solution was removed, the reservoir washed sequentially with DI water and LE, followed by replacement with LE; the complete cycle was completed in 60 s. The capillary outlet was connected to a 750- $\mu\text{L}$  polymethyl methacrylate machined buffer reservoir (McMaster-Carr) *via* an Upchurch Nanoport (N-124S; Oak Harbor, WA); a grounding platinum electrode was also coupled to this reservoir *via* a Nanoport. The buffer reservoir was connected to a  $\pm$  69 kPa (10 psi) precision pressure controller (Series 600, Mensor, San Marcos, TX) for hydrodynamic flow regulation through a removable Nylon Swagelok union (Penn Fluidic System Technologies, Huntingdon Valley, PA), which also was the access for fluid exchange.

Detection for capillary experiments was performed using an in-house modified Axio Observer A1 upright fluorescence microscope (Carl Zeiss, Thornwood, NY). The arc-lamp optical train was removed and the output of a 30-mW diode-pumped solid state 488-nm laser (Melles Griot, Carlsbad, CA) was directed onto a fluorescein-specific optical block containing a 500-nm longpass dichroic and 510- to 560-nm emission bandpass filter (QMAX Green series, Omega Optical, Battleboro, VT). Laser excitation was focused through a 20× objective (0.4 numerical aperture (NA), Carl Zeiss) into the capillary. Fluorescence emission was collected through the same objective and detected through a 3-mm spatial filter with a Hamamatsu (Bridgewater, NJ) H5784 photosensor module and C7169 power supply.

All instrument control and data acquisition was performed using LabVIEW software (National Instruments, Austin, TX) written in-house. Digitization of the PMT output utilized a USB-6221 module (National Instruments) recording at 100 Hz. Data analysis was performed using Cutter software<sup>24</sup> with 1 Hz low-pass filtering of raw data. Peak identification of mixtures was accomplished through individual analyte runs and spiking of analytes. Unreacted and side products of FAM, SE conjugation (labeled as Dye on electropherograms) were identified by performing the labeling reaction described above without amino acids. All electropherogram time scales include GEITP enrichment and solution switching times.

## 2.2.4. Results and Discussion

### 2.2.4.1. GEITP-CZE Operation

Figure 2.2.1C schematically describes the series of steps to perform GEITP-CZE. During the initial stage (i), sample and TE are present at the microcolumn inlet at a negative potential (for anionic analyses). LE is dispersed into the sample reservoir by a relatively high bulk counter-flow, which is a combination of EOF and hydrodynamic flow. As counter-flow is reduced, GEITP is initiated outside of the microcolumn (ii), characterized by the formation of an ionic interface that focuses analytes between LE and TE. GEITP enrichment continues during further reduction in bulk flow until enriched zones are introduced onto the separation column (iii). Once the enriched zones are on-column, applied potential and pressure are terminated (iv), and the inlet solution is replaced with LE. The electric field is reinitiated, as well as a static hydrodynamic flow to ensure analyte migration towards the detector (v). Note that these conditions are equivalent to tITP and polarity inversion is not required. It is believed that re-focusing during tITP reduces diffusional band-broadening during the solution switch stage. Once the inlet LE breaches the ITP stack, separation proceeds under CZE until zones migrate past the detector (vi).

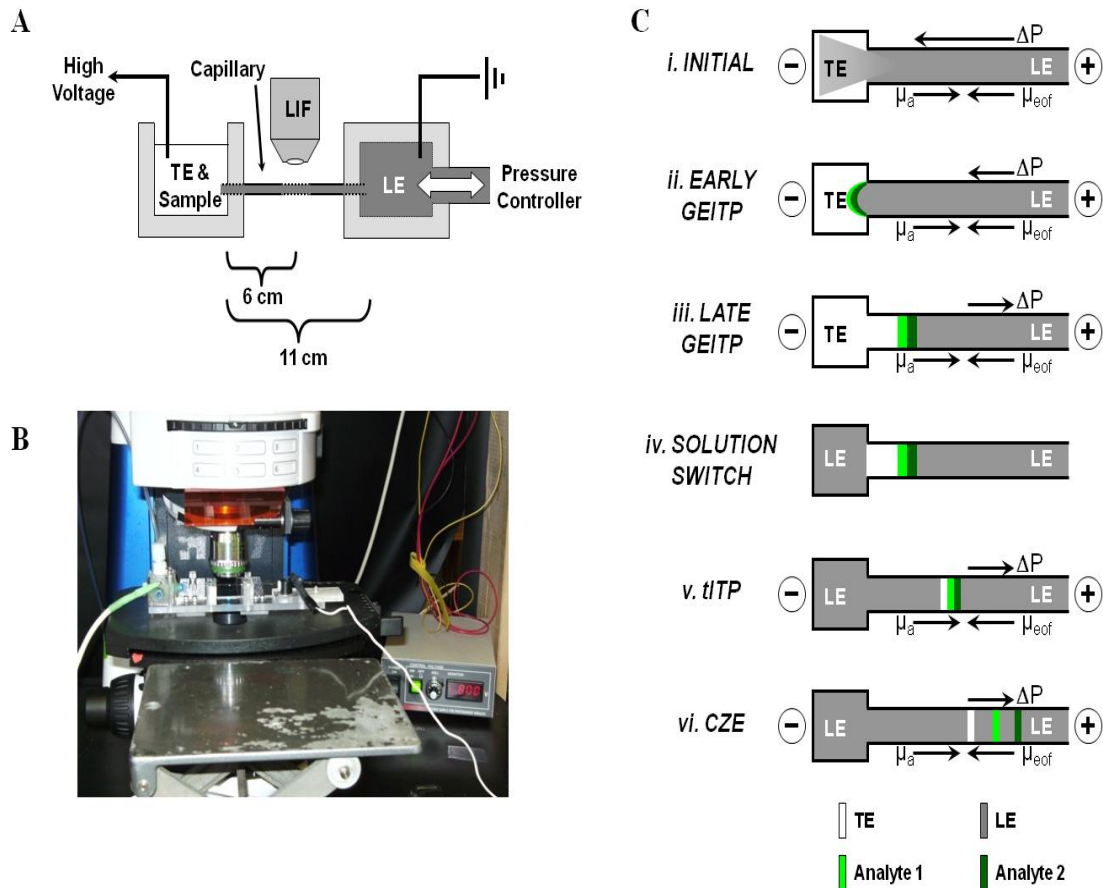


**Figure 2.2.1.** Instrumentation for and concept of GEITP-CZE. (A) The capillary format utilized 11 cm of capillary connecting a pressure controlled and grounded 750  $\mu\text{L}$  reservoir containing leading electrolyte (LE) to a 100  $\mu\text{L}$  open-atmosphere reservoir containing sample and trailing electrolyte (TE). Detection was performed by laser-induced fluorescence (LIF) microscopy 6 cm from the sample inlet. (B) In-house instrumental set-up. (C) The stages to perform GEITP-CZE are as follows: (i) Initially, LE is dispersed into sample reservoir by relatively high bulk flow, a combination of hydrodynamic ( $\Delta P$ ) and EOF ( $\mu_{\text{EOF}}$ ) flows. Anionic analyte mobility ( $\mu_a$ ) is toward the microcolumn outlet. (ii) As pressure is reduced, analytes form ITP zones at the ionic interface and are enriched between LE and TE. (iii) Pressure is further reduced, and enriched zones are introduced onto the microcolumn. (iv) Applied pressure and voltage are discontinued. LE replaces the TE and sample solution. (v) Voltage and static hydrodynamic flow toward the outlet are applied. Because of the presence of TE, a short stage of tITP occurs. (vi) Once LE enters the TE zone, CZE conditions are present and analytes separate based on their respective electrophoretic mobilities.

#### 2.2.4.2. Hydrodynamic Flow Effects During CZE

Hydrodynamic flow in CE can be used to suppress or reverse electrophoretic migration in order to improve resolution by increasing the time on-column.<sup>18,25-27</sup> In contrast to flow counterbalanced CE,<sup>18</sup> which utilized short, periodic counter-flow bursts to push analyte zones back to the capillary inlet, a low, sustained hydrodynamic flow was used during the CZE stage of the present method. The choice was due to the additional band-broadening from pressure-induced parabolic flow being directly proportional to time but having a squared dependence on applied pressure. Despite being limited to a 6-cm effective capillary length, a dramatic improvement in resolution could be obtained simply by modifying the applied pressure during CZE. Using 500 pM each of Gly and Ala as a model mixture, resolution was measured at various applied pressures after a short (12 s) GEITP stage (Fig. 2.2.2A). Similar to previous pressure-induced flow work in CZE,<sup>18</sup> a linear increase in resolution *versus* the square root of migration time was observed (Fig. 2.2.2B). Note that all pressures used were relatively small, with the maximum pressure studied being -5000 Pa (less than 1 psi) and baseline resolution obtained at -2500 Pa (less than 0.5 psi). Additionally, the system was highly reproducible, with less than 4% average relative standard deviation (RSD) in resolution ( $n = 3$ ). The important feature is that resolution in the presence of hydrodynamic flow becomes an adjustable parameter, without altering the separation column, field strength, or electrolyte system.

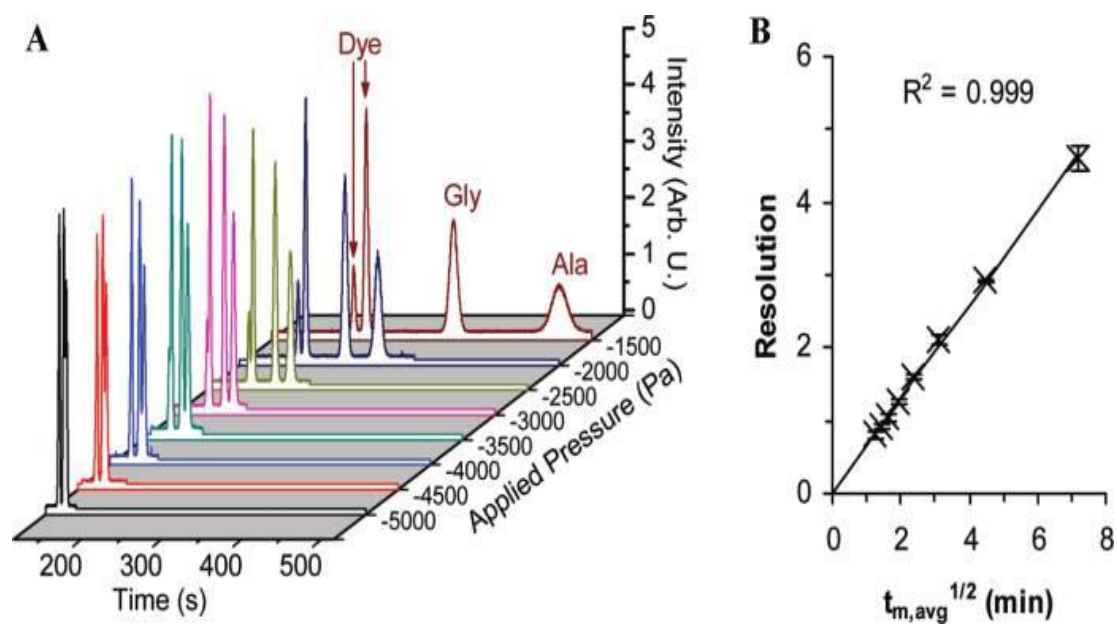


**Figure 2.2.2.** Effect of hydrodynamic flow on CZE resolution. (A) Example electropherograms of 500 pM Gly/Ala mixtures introduced by GEITP and separated by CZE at various pressures. Peaks marked Dye were due to unreacted conjugate and side reaction products. LE, 50 mM citrate balanced with tris (pH 8.5); TE, 250 mM tris-borate (pH 8.5); -600 V/cm; GEITP initial, 2000 Pa; GEITP final, -4000 Pa; gradient, -500 Pa/s. (B) Plot of resolution versus square root of average migration times ( $t_{m,avg}$ ). Error bars are 1 standard deviation ( $n = 3$ ).

### 2.2.4.3. LE Effects on Enrichment

Earlier ITP and GEITP work has demonstrated that preconcentration can be improved by increasing LE concentration.<sup>11,13,28</sup> Sensitivity enhancement was previously calculated based on comparison of purified analyte (either fluorescent dyes by fluorescence or unlabeled amino acids by absorbance) being constantly infused through a field-free capillary relative to GEITP results. Due to unreacted FAM, SE, as well as side reaction products, pure, labeled amino acids could not be used in a similar manner. Unreacted dye was not used due to likely changes in quantum yield after reaction.<sup>29</sup> Solely hydrodynamic loading (*i.e.*, GEITP operated in the absence of applied voltage) followed by CZE was also discarded as a comparison method due to the difference in amount of sample volume loaded. The bulk flow during loading was the sum of EOF and hydrodynamic flow; equivalent pressure profiles with and without an applied field would have significantly different total volumes introduced on capillary. For these reasons, enrichment trends of Gly at elevated LE concentrations were compared against a baseline GEITP system using 50 mM LE and short GEITP (-250 Pa/s for 24 s). The applied pressure during the CZE stage was adjusted during trial analyses using the various LE solutions until the migration time of Gly was  $150 \pm 10$  s for all LE concentrations. Due to the different LE conductivities and, hence, different analyte electrophoretic velocities at each concentration, the CZE applied pressure was necessarily different in order to normalize the time on-column. All other parameters (field strength, starting pressure, gradient steepness, *etc.*) were equivalent. The Gly peak height was then compared against the 50 mM LE Gly calibration (10-150 pM).

Increasing LE to 175 mM followed previously noted trends, with a roughly linear increase in enrichment. However, amounts of LE above this level actually resulted in a decrease in sensitivity (Fig. 2.2.3A). The loss in enrichment can be explained by the current during the GEITP-CZE process using the various LE solutions (Fig. 2.2.3B). An initial current (time zero) during the GEITP stage matching the final CZE current was indicative of the presence of only LE in capillary. During bulk flow reduction, the capillary began to fill with TE, resulting in a current decrease. The middle, zero-current region corresponded to replacing sample with LE. The removal of TE after reapplication of voltage was evident from the increase in current as LE entered the capillary. As CZE proceeded, the current returned to fully-filled LE levels. Presumably, the higher LE concentrations had reduced EOF velocities and lower initial bulk flow.<sup>30</sup> As EOF was reduced, higher applied pressures would have been needed to produce counter-flow sufficient to generate the GEITP interface outside of the capillary. With a constant pressure profile, the lower bulk velocities due to conductivity increases led to a larger volume of sample being loaded onto the capillary during the GEITP stage. These results suggest that initiation of enrichment outside of the capillary by GEITP was superior to large on-capillary loadings followed by tITP (stage (v) of Fig. 2.2.1C).

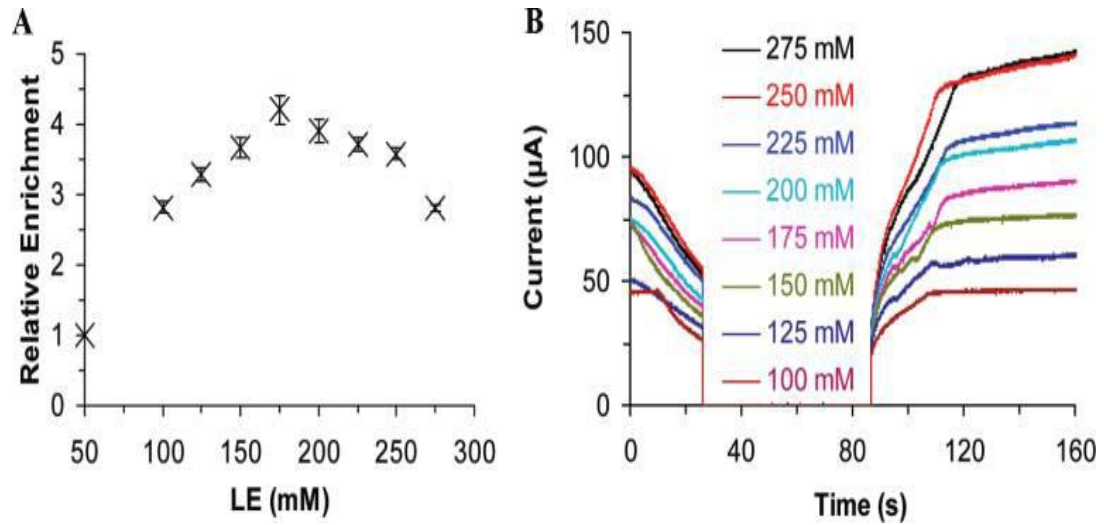


**Figure 2.2.3.** Effect of LE on enrichment with constant GEITP parameters: (A) Gly enrichment (relative to 50 mM LE, as described in the text) as LE concentration increased. Error bars are 1 standard deviation ( $n = 3$ ). LE, citrate balanced with tris (pH 8.5); TE, 250 mM tris-borate (pH 8.5); -600 V/cm; GEITP initial: 2000 Pa; GEITP final: -4000 Pa; gradient, -250 Pa/s; CZE pressure, normalized to  $t_m = 150 \pm 10$  s. (B) Example currents observed at the LE concentrations used in part A. The middle, zero-current region was the point of solution exchange.

#### 2.2.4.4. *Initial Pressure Effects on Enrichment*

To further confirm that GEITP initiated outside the capillary was more effective than tITP, the initial pressure was varied for GEITP focusing with a constant pressure differential (the difference between the initial GEITP pressure and the pressure at the end of GEITP) of 3000 Pa and -250 Pa/s gradient (Fig. 2.2.4). The constant differential and gradient with variable initial pressures essentially scanned the window of GEITP focusing. Again, CZE migration time was normalized to  $150 \pm 10$  s for each pressure differential by performing trial analyses at various CZE applied pressures; all other parameters were held constant. Electropherograms in Fig. 2.2.4A show the effect of moving the pressure window on enrichment of 50 pM Gly using 200 mM LE, which was the first LE concentration to deviate from linear increases in enrichment at an initial pressure of 2000 Pa. The range of start pressures spanned from the point where sample was not introduced into the capillary (10000 Pa) to the point where the sample passed the detector prior to the end of GEITP (just below -6000 Pa). While larger volumes of sample could be loaded on-capillary with lower initial pressures, as noted by the increase in peak area in Fig. 2.2.4B, the broadening resulted in a significant decrease in efficiency (Fig. 2.2.4C) which follows the peak height trend. Optimal signal was found between 2000 and 4000 Pa (Fig. 2.2.4B), which corresponds to the point on the current plots (Fig. 2.2.4D) with a short initial plateau at maximal current, indicative of enrichment beginning outside the capillary. Note that the initial pressure requirement for optimal enrichment as measured by peak height was above 2000 Pa, the starting pressure used for studying the effects of LE concentration. At and below 2000 Pa, despite even larger volumes of sample being loaded for tITP, peak heights decreased, possibly due to the

larger hydrodynamic pressures (and associated band broadening) necessary to maintain equivalent migration times. With the exclusion of the -6000 Pa condition (the point where the sample was loaded extremely close to the detector), peak heights were <5% average RSD ( $n = 3$ ). This further demonstrates that use of pressure to modify bulk flow, rather than EOF modifiers, can be quite reproducible.

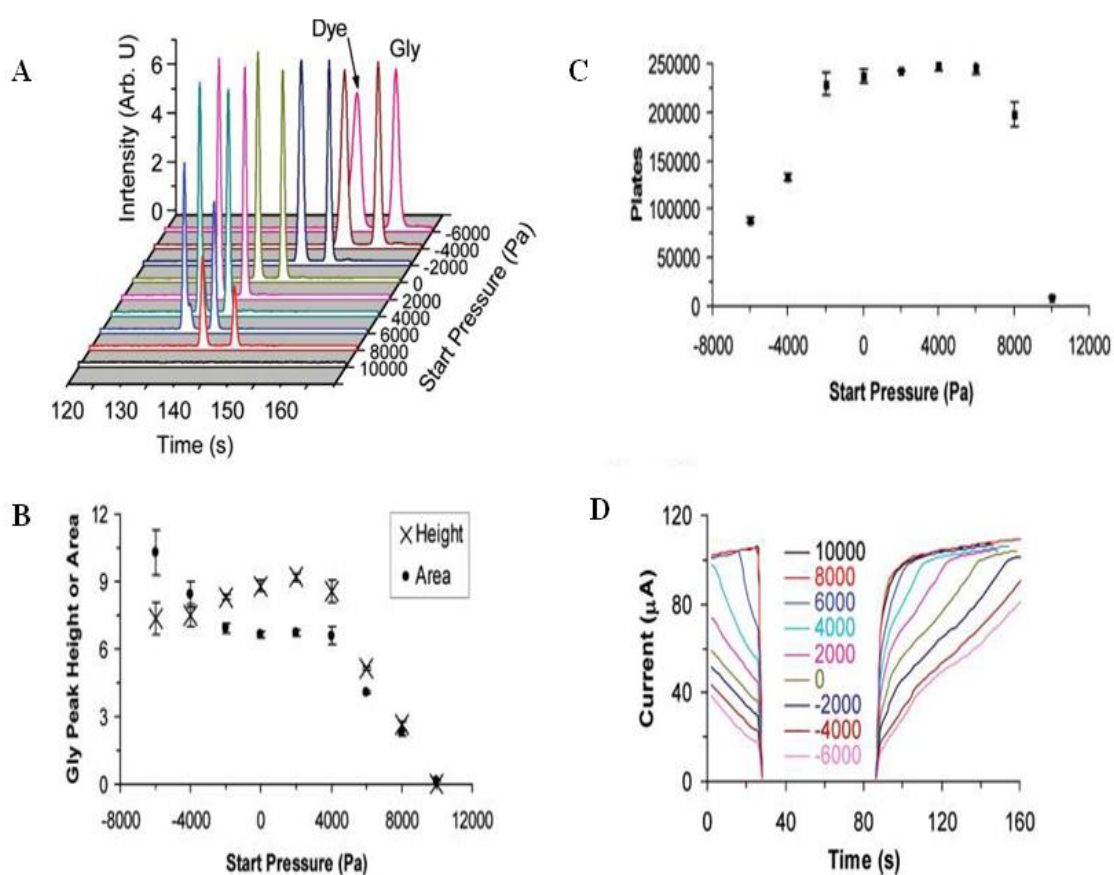


**Figure 2.2.4.** Effect of initial GEITP pressure on enrichment. (A) Example electropherograms of 50 pM Gly introduced by GEITP with varying start pressures but constant gradients and pressure differentials (initial minus final pressure). Peaks marked Dye were due to unreacted conjugate and side reaction products. LE, 200 mM citrate balanced with tris (pH 8.5); TE, 250 mM tris-borate (pH 8.5); -600 V/cm; GEITP pressure differential, 6000 Pa; gradient, -250 Pa/s; CZE pressure, normalized to  $t_m = 150 \pm 10$  s. (B) Measured Gly peak heights and areas as the start pressure varied. (C) Measured Gly peak plates as the start pressure varied. Error bars for parts B and C are 1 standard deviation ( $n = 3$ ). (D) Example currents observed as the start pressure varied. The middle, zero-current region was the point of solution exchange.

#### 2.2.4.5. GEITP Duration Effects

While LE concentrations were one means to adjust sensitivity, a simpler and more flexible approach, without requiring electrolyte changes, was to increase the length of the GEITP enrichment process. Once an optimal starting pressure and differential were determined for a given system, GEITP could be performed for longer focusing times by decreasing the bulk flow acceleration, which was proportional to the incremental pressure change (measured as Pa/s). By adjusting only the gradient steepness, the CZE stage was unaffected such that the enriched analytes began at the same point within the capillary, as the pressure differential and field strength remained the same.

Gly was measured with a constant pressure change from 2000 to -1000 Pa as the gradient was reduced from -500 to -2.5 Pa/s (yielding GEITP durations of 12 s to 40 min). Figure 2.2.5 shows the enrichment improvements relative to the fastest gradient (-500 Pa/s). Applied pressure during the CZE stage was held constant for all gradients at -2500 Pa. Variability of peak migration times for all gradients were <0.5% RSD and peak heights were <7% average RSD ( $n = 3$ ). Thus, with a single, non-chemical adjustment, enrichment was easily tuned. Additionally, although the higher LE seemed favorable for improved enrichment under GEITP, the higher current was detrimental for efficient CZE analysis. Lower LE concentrations could still yield impressive enrichment results and serve as more suitable CZE electrolytes. Decoupling of GEITP LE and CZE background electrolytes would be beneficial and could be realized in either a coupled-capillary format or a multi-channel microdevice.

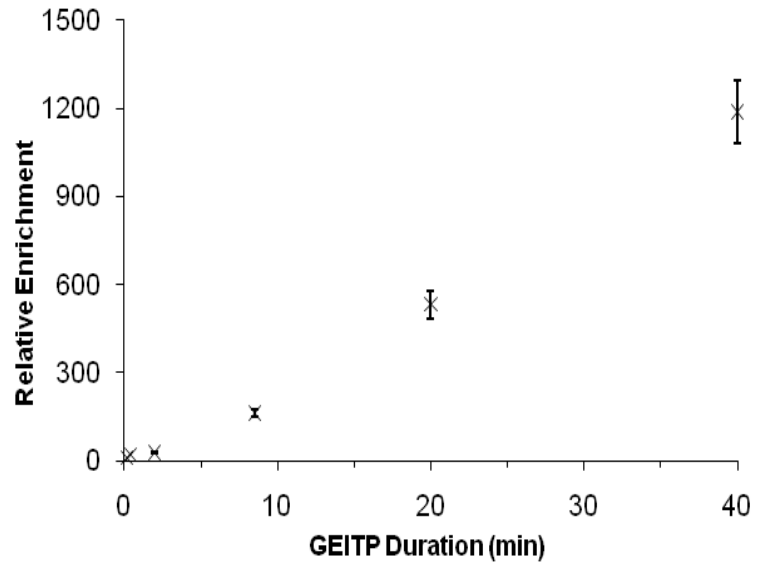


**Figure 2.2.5.** Effect of GEITP duration on enrichment. With a constant initial and final pressure for GEITP, the gradient steepness was reduced to increase the enrichment time. Plot shows increasing Gly enrichment (relative to the shortest time, 12 s, as described in the text) as GEITP duration increased. Error bars are 1 standard deviation ( $n = 3$ ). LE, 50 mM citrate balanced with tris (pH 8.5); TE, 250 mM tris-borate (pH 8.5); -600 V/cm; GEITP initial, 2000 Pa; GEITP final, -4000 Pa; CZE pressure, -2500 Pa.

### 2.1.3.6. Application to Amino Acid Mixtures

GEITP-CZE was then applied to a mixture of the six proteinogenic amino acids to be assayed for in future extra-terrestrial missions. An example electropherogram is shown in Fig. 2.2.6. Adjacent amino acid peaks (and Glu from Dye associated peaks) had greater than unit resolution with the exception of Ala and Ser, with a resolution of 0.9. However, these results were obtained in 6 cm with a static CZE counter-flow and without additional buffer additives to improve separation (*e.g.*, cyclodextran or sodium dodecyl sulfate). A peak capacity of 40 was calculated using the baseline widths of four amino acids (Ala and Ser were excluded as the widths were not easily measurable).<sup>31</sup> The entire analysis was completed in 11 min, yielding femtomolar detection limits (Table 2.2.1) with only 200 s of GEITP and without costly or exotic detection equipment such as high magnification/N.A. objectives, confocal optics, sheath-flow cuvettes, or avalanche photodiodes.<sup>32</sup> As enrichment was related to electrophoretic mobility, higher mobility analytes showed greater sensitivity than lower mobility species. This effect can be seen from Table 2.2.1, listing the amino acid detection limits (calculated at 3 times the standard deviation of the noise), with the acidic amino acids having an order of magnitude better detectability than the electrophoretically slower Val.

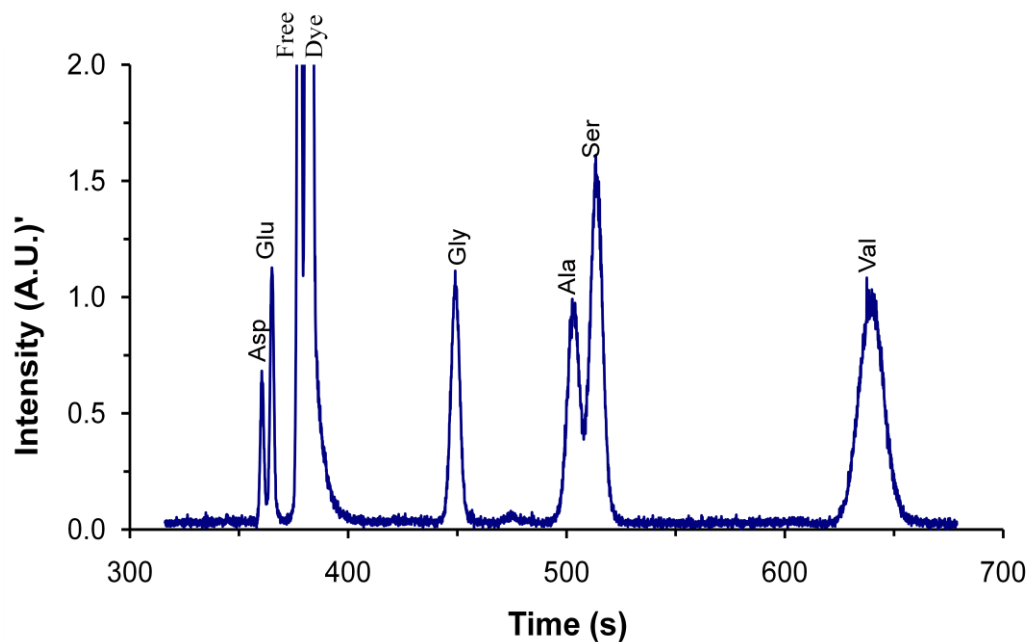


**Figure 2.2.6.** Capillary GEITP-CZE analysis of six carboxyfluorescein-labeled amino acids. The sample consisted of (in picomolar): 6.25 Asp, 6.25 Glu, 12.5 Gly, 25 Ala, 25 Ser, and 62.5 Val. Peaks marked Dye were due to unreacted conjugate and side reaction products. LE, 50 mM citrate balanced with tris (pH 8.5); TE, 250 mM tris-borate (pH 8.5); -600 V/cm; GEITP initial, 1000 Pa; GEITP final, -1000 Pa; gradient, -10 Pa/s; CZE pressure, -600 Pa.

**Table 2.2.1.** Amino Acid Detection Limits<sup>a</sup>

<i>Analyte</i>	<i>LOD (pM)</i>
Asp	0.3
Glu	0.2
Gly	0.4
Ala	0.9
Ser	0.6
Val	2.0

<sup>a</sup> Conditions as described in Figure 2.2.6. Limits of detection (LOD) calculated by the peak height at 3 times the standard deviation of the noise.

### 2.2.5. Conclusion

GEITP coupled with CZE was shown to achieve femtomolar detection limits of amino acids, accomplishing separations in short length microcolumns without the need for spacing ions. One major difference between the present method and other electrophoretic preconcentration techniques was that enrichment was not limited to the capillary volume; GEITP focusing initiated outside of the separation column was more effective than loading large volumes on-column followed by tITP. The elimination of EOF control through surface modification or additives, as well as the elimination of a TE flushing step, resulted in highly reproducible separations in native capillaries. Additionally, no field polarity inversion was required and, subsequently, there was no analyte migration order reversal. The purified, adjacent zones produced from GEITP continued to separate in the same migration order during CZE under static hydrodynamic flow conditions. The novel use of variable hydrodynamic flow in both enrichment and separation stages yielded a technique with the ability to adjust both sensitivity and resolution by simply changing the pressure profiles during the assay, a highly desirable feature for remote analyses where unknown analyte concentrations and interferents may be encountered.

From this initial work, several areas of development could be explored. An autosampler unit could be incorporated to eliminate the manual solution switching steps and reduce the total analysis time. The use of surfactants and/or chiral selectors could improve the separation power; alternatively, the CZE stage could also use dynamic flow programming (*versus* static) to maximize the separation space, as previously shown with standalone GEITP.<sup>11</sup> Multi-channel microfluidics offer the ability to couple isolated

GEITP and CZE buffer systems without detrimental dilution at the transfer junction, as is encountered with capillary unions. Optimal electrolyte systems could then be individually selected for each stage of analysis. While this work emphasized trace analysis of amino acids to be assayed for on Mars, the advantages could be widely applicable to CE-based separations where sensitivity is an issue.

### 2.2.6. References Cited

1. Breadmore, M. C. *Electrophoresis* **2007**, *28*, 254-281.
2. Sueyoshi, K.; Kitagawa, F.; Otsuka, K. *J. Sep. Sci.* **2008**, *31*, 2650-2666.
3. Breadmore, M. C.; Thabano, J. R. E.; Dawod, M.; Kazarian, A. A.; Quirino, J. P.; Guijt, R. M. *Electrophoresis* **2009**, *30*, 230-248.
4. Simpson, L. S.; Quirino, J. P.; Terabe, S. *J. Chromatogr. A* **2008**, *1184*, 504-541.
5. Shackman, J. G.; Ross, D. *Electrophoresis* **2007**, *28*, 556-571.
6. Chen, L.; Prest, J. E.; Fielden, P. R.; Goddard, N. J.; Manz, A.; Day, P. J. R. *Lab Chip* **2006**, *6*, 474-487.
7. Gebauer, P.; Mala, Z.; Bocek, P. *Electrophoresis* **2007**, *28*, 26-32.
8. Gebauer, P.; Mala, Z.; Bocek, P. *Electrophoresis* **2009**, *30*, 29-35.
9. Jung, B.; Bharadwaj, R.; Santiago, J. G. *Anal. Chem.* **2006**, *78*, 2319-2327.
10. Jung, B.; Zhu, Y.; Santiago, J. G. *Anal. Chem.* **2007**, *79*, 345-349.
11. Shackman, J. G.; Ross, D. *Anal. Chem.* **2007**, *79*, 6641-6649.
12. Danger, G.; Ross, D. *Electrophoresis* **2008**, *29*, 4036-44.
13. Mamunooru, M.; Jenkins, R. J.; Davis, N. I.; Shackman, J. G. *J. Chromatogr. A* **2008**, *1202*, 203-211.

14. Vyas, C. A.; Mamunooru, M.; Shackman, J. G. *Chromatographia* **2009**, *70*, 151–156.
15. Reinhoud, N. J.; Tjaden, U. R.; van der Greef, J. J. *J. Chromatogr. A* **1993**, *641*, 155-162.
16. Reinhoud, N. J.; Tjaden, U. R.; van der Greef, J. J. *J. Chromatogr. A* **1993**, *653*, 303-312.
17. Mazereeuw, M.; Tjaden, U. R.; Reinhoud, N. J. *J. Chromatogr. Sci.* **1995**, *33*, 686-697.
18. Culbertson, C. T.; Jorgenson, J. W. *Anal. Chem.* **1994**, *66*, 955-962.
19. Poinot, V.; Rodat, A.; Gavard, P.; Feurer, B.; Couderc, F. *Electrophoresis* **2008**, *29*, 207-223.
20. Bada, J. L.; Glavin, D. P.; McDonald, G. D.; Becker, L. *Science* **1998**, *279*, 362-365.
21. Hutt, L. D.; Glavin, D. P.; Bada, J. L.; Mathies, R. A. *Anal. Chem.* **1999**, *71*, 4000-4006.
22. Skelley, A. M.; Scherer, J. R.; Aubrey, A. D.; Grover, W. H.; Ivester, R. H. C.; Ehrenfreund, P.; Grunthaner, F. J.; Bada, J. L.; Mathies, R. A. *PNAS* **2005**, *102*, 1041-1046.
23. Chiesl, T. N.; Chu, W. K.; Stockton, A. M.; Amashukeli, X.; Grunthaner, F.; Mathies, R. A. *Anal. Chem.* *81*, 2537-2544.
24. Shackman, J. G.; Watson, C. J.; Kennedy, R. T. *J. Chromatogr. A* **2004**, *1040*, 273-282.
25. Kok, W. T. *Anal. Chem.* **1993**, *65*, 1853-1860.

26. Iwata, T.; Kurosu, Y. *Anal. Sci.* **1995**, *11*, 131-133.
27. Kar, S.; Dasgupta, P. K. *J. Microchem.* **1999**, *62*, 128-137.
28. Khurana, T. K.; Santiago, J. G. *Anal. Chem.* **2008**, *80*, 6300-6307.
29. Sjoback, R.; Nygren, J.; Kubista, M. *Biopolymers* **1998**, *46*, 445-453.
30. Weinberger, R. *Practical Capillary Electrophoresis*; Academic Press, Inc.: San Diego, **1993**.
31. Neue, U. D. *J. Chromatogr. A* **2005**, *1079*, 153-161.
32. Johnson, M. E; Landers, J. P. *Electrophoresis* **2004**, *25*, 3513-3527.

## CHAPTER 3

### TEMPERATURE GRADIENT FOCUSING

#### 3.1. Abstract

TGF is an attractive method for biochemical monitoring and trace analyses. It is capable of achieving analytes focusing in high saline matrix without the formation of discrete zones, making it especially useful for analyzing neurotransmitters present in microdialysate samples. This work demonstrates proof of concept of TGF focusing on an 8 cm capillary short length microcolumn with temperature a gradient of 15 °C/mm (spanning a range between 80-20°C) applied across a 2-mm optical window. Detection was achieved using laser induced fluorescence (LIF). Unoptimized parameters were applied to the enrichment and separation of the fluorescent dye molecules (carboxyfluorescein, fluorescein) and neurotransmitters (aspartate, glutamate). Analysis time was less than 5 minutes for all analytes except fluorescein, and peak height RSD were less than 3%.

### 3.2. Introduction

Analyzing biological samples usually present in low volume and concentration remains a challenge and an area of interest. Most focusing techniques generally require that sample concentrates at a fix or null point along a separation channel in order to achieve sensitive detection as a result of a dynamic equilibrium process. The classic isoelectric electric focusing (IEF) technique establishes gradient using two pH dependent buffer systems (usually between pH 3-11)<sup>1-7</sup> along the separation column to achieve focusing at the analyte's isoelectric point (pI), where the net charge equals zero. Though currently the most extensively used focusing technique, it is limited to the restrictive analysis of proteins and nucleotides. Other techniques unique to this class of field gradient<sup>11</sup> techniques include isotachopheresis,<sup>8-10</sup> electric field gradient focusing,<sup>12-15</sup> and more recently micellar affinity gradient focusing,<sup>16,17</sup> GEITP,<sup>18-20</sup> and TGF.<sup>21-38</sup> These techniques generally combines sample preconcentration significant for enrichment and separation in one step, a promising feature for improving detection sensitivity.

In 2002, Ross and Locascio<sup>21</sup> introduced the TGF method using a microfluid chip to demonstrate that different types of analyte can achieved focusing from temperature gradient produced by buffer ionic strength and variable joule heating along the microchannel. The temperature gradient focusing technique, a type of field gradient method, uses counterflow electrofocusing to concentrate and focus analytes along a thermal column. The focusing of analyte ion is achieved from the balancing effect between counterflows: analyte ions migrating by electrophoresis and bulk flow on a column with different temperature profiles. The balancing process forcing the focusing/preconcentration at well defined spatial position along the column will not be

the same for all analytes due to their difference in electrophoretic velocity and ionic properties. The bulk flow is predominantly EOF driven, the pressure controls help balance forces of EOF and electrophoresis so that analyte(s) speed up (in hot region) and slow down (in cool region) until a dynamic equilibrium is reached. Similar to GEITP,<sup>18-20</sup> a high negative pressure (direction of flow: from anode to cathode) pushes the bulk solution toward the sample reservoir. However, no LE and TE effect is used in TGF. TGF like CE operates on one buffer system. This one step process sets the stage for both electrophoresis and TGF focusing to operate simultaneously. The pressure is empirically defined; high pressure prevents loading on column, and optimal pressure help define the spatial focusing position. To separate ions, the ion with the higher electrophoretic mobility gets loaded on column first and is allowed to focus as the result of a zero total velocity of both of analyte and bulk flow, then next the slower ions. The temperature gradient is established from heating and cooling systems imposed on the separation column. Alternatively, temperature gradient in TGF can be facilitated, in the absence of external heating source, through joule heating<sup>21,24,35,37</sup> where the applied electric field strength is sufficient to generate temperature increase in the buffer resulting in non-uniform temperature profiles along the column.

Currently only a few applications using TGF are found in literature (between 2002-present) which shows applicability to the study of proteins, DNA, small dye molecules, and amino acids, both in capillary and microfluidic formats.<sup>17, 21-38</sup> TGF as a stand-alone method has shown high-resolution separations with over 10,000-fold concentration enrichment. In some cases the scanning<sup>22,26</sup> TGF mode and joule heating were employed to improve resolution and separation. With further improvements, TGF is

expected to show comparable analysis to and/or be used as an alternative to CE. Common advantages and disadvantages associated with the technique are summarized in Tables 3.1. The validation presented sets the stage for exploring modifications to the TGF technique.

Table 3.1. List of advantages and disadvantages of TGF

<i>Advantages</i>	<i>Disadvantages</i>
Applicable to a wide variety of analyte types	High energy consumption – heating & cooling equipment, HV power supplies, pressure controller etc.
Parallelization-TGF can be independently operated making it suitable for two-dimensional studies (eg. TGF-CZE)	Limited portability due to heating, cooling and other external sources
Can be operated in saline matrix (buffer concentration is independent of salt)	Long focusing time (between 5-30 mins)
Short column length (2-3 cm) make it suitable for miniaturized	Due to limited peak capacity not ideal for high throughput analysis
Focusing results from different spatial position	Requires temperature dependent buffer
Simple, straight forward technique	
Not diffusion limited as there is no need for a defined injection plug	
Both concentration and separation achievable in one step	
Adjustable sensitivity with changing bulk scan rate	

### 3.3. Theory of TGF

The TGF theory is discussed at length in literature.<sup>19,33-37</sup> TGF focusing results from gradient established along the column, similar to IEF and EFGF methods. Unlike IEF and EFGF, the velocity gradient causing focusing in TGF is produced by temperature difference along the column.

In capillaries or microchannels, the three forces involved are electroosmotic flow (EOF), hydrodynamic flow, and total ion mobility, with the first two forces comprising a non-selective bulk flow. The bulk flow generated balances ion velocity (which varies along the separation axis) resulting in a null-velocity point that is unique for a given analyte (Figure 3.1 C-E). In TGF, the velocity gradient is generated by the temperature difference along the column which subsequently induces gradient in both  $v_{ep}$  and  $v_{Bulk}$ . Hence, the net focusing point ( $v_T$ ), the point of zero velocity, results from balancing of electrophoretic velocity of analyte ( $v_{ep}$ ) against electrophoretic velocity of solution ( $v_{Bulk}$ ),

$$v_T = v_{ep} + v_{Bulk} \quad (1)$$

The analyte's electrophoretic velocity (already discussed in chapter 1) is defined by the product of electric field and electrophoretic velocity,

$$v_{ep} = \frac{q}{f} E \approx v_{ep} = E \mu_{ep} \quad (2)$$

Selection of TGF buffer is critical to separation and focusing. A TGF buffer should have a temperature dependent ionic strength and the buffer pH should be equal to or near the pKa of atleast one of the buffer components. In general, temperature dependence in buffer conductivity and electric field gradient is produced as a result of

temperature dependence in the buffer salts. The  $f(T)$  plot developed by the founders of TGF is used as a yardstick to select temperature dependent buffer.<sup>20</sup>  $F(T)$ <sup>21</sup> is a function that accounts for temperature dependent factors of buffer ionic strength not related to viscosity changes; it is measured at a reference temperature and conductivity (usually water at 20 °C). Temperature dependence in TGF results from factors including: electrophoretic mobility, conductivity, field strength, voltage and viscosity. Equation 3 gives a non-dimensional relationship for the  $f(T)$  function:

$$f(T) = \frac{\sigma_{20} \eta_{20}}{\sigma_T \eta_T} \equiv \frac{f(T)_{non-viscosity}}{f(T)_{viscosity}} \equiv \frac{f(20)}{f_{ep}(T)} \quad (3)$$

where  $f(T)$  or  $f(20)$  is a function which describes temperature dependence resulting from ionic strength,  $\sigma_{20}$  and  $\sigma_T$  are conductivities of water and buffer, and  $\eta_{20}$  and  $\eta_T$  are viscosities of water and buffer; 20 °C is the reference temperature.

TGF utilizes a single microcolumn filled with a temperature-dependent buffer, and a spatial temperature gradient is applied. A typical aqueous solution will exhibit viscosity changes along the gradient yielding a temperature dependent conductivity function ( $\sigma(T)$ ). In TGF, the difference in temperature gradient can only result in a velocity gradient when: either  $f(20) \neq f_{ep}(T)$ , or  $f(20)$  is non-constant and  $f_{ep}(T)$  is constant. This means that they do not the same temperature dependence temperature dependence and a gradient would be created both in E and v resulting in temperature gradient; hence, focusing would occur. Conversely, for  $f(20) = f_{ep}(T) = 1$ , or where  $f(20)$  and  $f_{ep}(T)$  are constant or have equivalent temperature dependence, gradient would only be generated in E and not  $v_{ep}$ . So  $v_{ep}$  is not temperature dependent, and focusing will not be possible. In other words, as long as temperature dependent conductivity changes not due to viscosity effects (*e.g.*, ionic strength) are different from viscosity-based changes, a

gradient in electrophoretic mobility will occur. As the ionic strength is raised, ion mobility decreases (due to a local drop in electric field strength). These relationships can be written as:<sup>21</sup>

$$\mu_{analyte} = E^0 \nu_{analyte}^0 \left( \frac{f(T)_{non-viscosity}}{f(T)_{viscosity}} \right) \quad (4)$$

where  $E^0$  and  $\mu^0$  reflect the field strength and mobility at a constant temperature of 20 °C normalize to  $f(20)_{non-viscosity} = 1$ . Most buffer systems and analytes have equivalent temperature functions,  $f(T)_{viscosity} = f(T)_{non-viscosity}$ . However, several electrolytes have highly temperature dependent  $pK_a$ 's, such as many Goods buffers,<sup>25</sup> yielding non-equivalent temperature functions and focusing of analytes.

### 3.4. Experimental

#### 3.4.1. Chemicals and reagents

Reagent grade L-glutamate (Glu), L-Aspartate (Asp), fluorescent grade tris(hydroxymethyl) aminomethane (tris), and boric acid were obtained from Sigma-Aldrich (St. Louis, MO). Carboxyfluorescein (FAM) and fluorescein were purchased from Fluka (Milwaukee, WI) while 5-carboxyfluorescein, succinimidyl ester (FAM, SE) single isomer was purchased from Invitrogen (Carlsbad, CA). All solutions were made using Milli-Q (Millipore, Bedford, MA)  $\geq 18 \text{ M}\Omega \text{ cm}$  deionized (DI) water.

Amino acid stock solutions were 1 mM in 15 mM sodium borate buffer (pH 9.2). FAM, SE was 0.1 M in dimethyl sulfoxide. For labeling, 2.5  $\mu\text{L}$  of FAM, SE stock was added to 247.5  $\mu\text{L}$  amino acid stock. The resulting mixture solution was vortexed to mix and incubated in the dark for 12 h at room temperature before being stored at 4 °C. For analysis, dilutions of labeled amino acids were made in TE without removal of free dye.

Each amino acid was labeled separately to allow for peak identification. The degree of labeling was not characterized. Background buffer was 0.5 M Tris-borate balanced to pH of approximately 8.3.

### 3.4.2. Instrumentation

Experiments were carried out on an apparatus similar to the original instrument described for TGF.<sup>20</sup> The TGF apparatus (Fig 3.1A and B) consists of two copper blocks anchored to polymethyl methacrylate (PMMA) base. The cold copper block maintained 20 °C temperature of circulating water bath. The temperature at the hot copper block equipped with thermistor, and thermoelectric module generated heated regulated *via* a proportional-integrative-derivative controller. Briefly, 8.0 cm of fused silica capillary (25  $\mu\text{m}$  I.D.; 360  $\mu\text{m}$  O.D.; Polymicro Technologies, LLC, Phoenix, AZ) long was prepared with a 2 mm wide optical window (Microsolv Window Maker; Eatontown, NJ) centered 1.9 cm from the sample inlet end. The capillary spanned the two copper blocks at a 4 mm gap (distance between blocks). The sample inlet end of the capillary, positioned next to the cold copper block, was inserted through a Teflon-backed silicon septum (Fisher) into a 400  $\mu\text{m}$  diameter hole drilled into a machined 100  $\mu\text{L}$  Delrin sample reservoir (McMaster-Carr; Robbinsville, NJ). The sample reservoir was held in place with a copper holder containing adjustable clamp to keep capillary in place. The capillary outlet was connected to a 750  $\mu\text{L}$  PMMA buffer reservoir (McMaster-Carr) *via* an Upchurch Nanoport (N-124S; Oak Harbor, WA); a grounding platinum electrode was also coupled to this reservoir *via* a Nanoport. High voltage (CZE 3000, Spellman High Voltage Electronics, Hauppauge, NY) was applied to the sample reservoir through platinum

electrode. The buffer reservoir was connected to a  $\pm 69$  kPa (10 psi) precision pressure controller (Series 600, Mensor, San Marcos, TX) for hydrodynamic flow regulation through a removable Nylon Swagelok union (Penn Fluidic System Technologies, Huntingdon Valley, PA), which also was the access for fluid exchange.

Detection for capillary experiments was performed using an in-house modified Axio Observer A1 upright fluorescence microscope (Carl Zeiss, Thornwood, NY). The arc-lamp optical train was removed and the output of a 30-mW diode-pumped solid state 488-nm laser (Melles Griot, Carlsbad, CA) was directed onto a fluorescein-specific optical block containing a 500-nm longpass dichroic and 510- to 560-nm emission bandpass filter (QMAX Green series, Omega Optical, Battleboro, VT). Laser excitation was focused through a 20 $\times$  objective (0.4 numerical aperture, N.A., Carl Zeiss) into the capillary. Fluorescence emission was collected through the same objective and detected through a 3-mm spatial filter with a Hamamatsu (Bridgewater, NJ, USA) H5784 photosensor module and C7169 power supply.

All instrument control and data acquisition was performed using LabVIEW software (National Instruments, Austin, TX) written in-house. Digitization of the UV output utilized a USB-6221 module (National Instruments) recording at 100 Hz. Data analysis was performed using Cutter software<sup>39</sup> with 1 Hz low-pass filtering of raw UV data. Plate number (N) was measured at width at half height,  $w_h$ . Peak identification of mixtures was accomplished through individual analyte runs and spiking of analytes.

### 3.5. Results and Discussion

#### 3.5.1. TGF Concept and Operation

Separation and focusing in TGF does not follow stacking and forming zonal boundaries which suffer from band broadening leading to poor resolution. The balancing between counterflows (bulk and  $\mu_{EP}$ ) on the column facilitates the concentration of analyte to a unique equilibrium position resulting in narrower focused peaks.

Sample from the sample reservoir is continuously loaded onto the microcolumn by applying a constant voltage. Once on column analytes move by electrophoretic velocity which is opposed by the EOF in the capillary, the applied pressure serves as referee between these counter exchanges until focusing is achieved at a steady state unique to the each analyte. Both EOF and  $\Delta P$  move toward the sample reservoir (left to right) while  $\mu_{EP}$  of the anionic species is directed toward the  $\Delta P$  block (right to left). In other words,  $\mu_{BULK}$  controls the flow rate in the column. The copper blocks ensure temperature regulation is maintained between 20 °C (cold) and 80 °C (hot). Together the temperature gradient between the blocks and the temperature-dependent background electrolyte create a gradient in field strength and electrophoretic velocity. The temperature drop across the capillary spanning these blocks is defined by distance (gap) between the blocks. Previous research using the technique recommends that the gap be as small as possible (usually 2-5 mm)<sup>21,22</sup> to minimize the temperature drop per cross-sectional area of the capillary, and that steeper gradient be used to improve resolution. As seen in figure 3.1D, at the low temperature end (from capillary inlet) the conductivity is low and the field strength is high so that electrophoretic velocity is greater compared to that of EOF on the high temperature end (from capillary outlet). This is a similar analogy to LE and TE effect in

GEITP to achieve conductivity gradient on column. Analyte(s) speed up (in hot region, as in TE) and slow down (in cool region, as in LE) until a dynamic equilibrium is reached. Thus, spatial focusing occurs at an equilibrium point where both counterflow velocities ( $\mu_{\text{BULK}} + \mu_{\text{EP}}$ ) are zero (Fig 3.1E). Analytes separate as a result of the difference in their electrophoretic mobility under column conditions which can be regulated by the amount of applied pressure. LIF is used for sensitive detection of separate species.

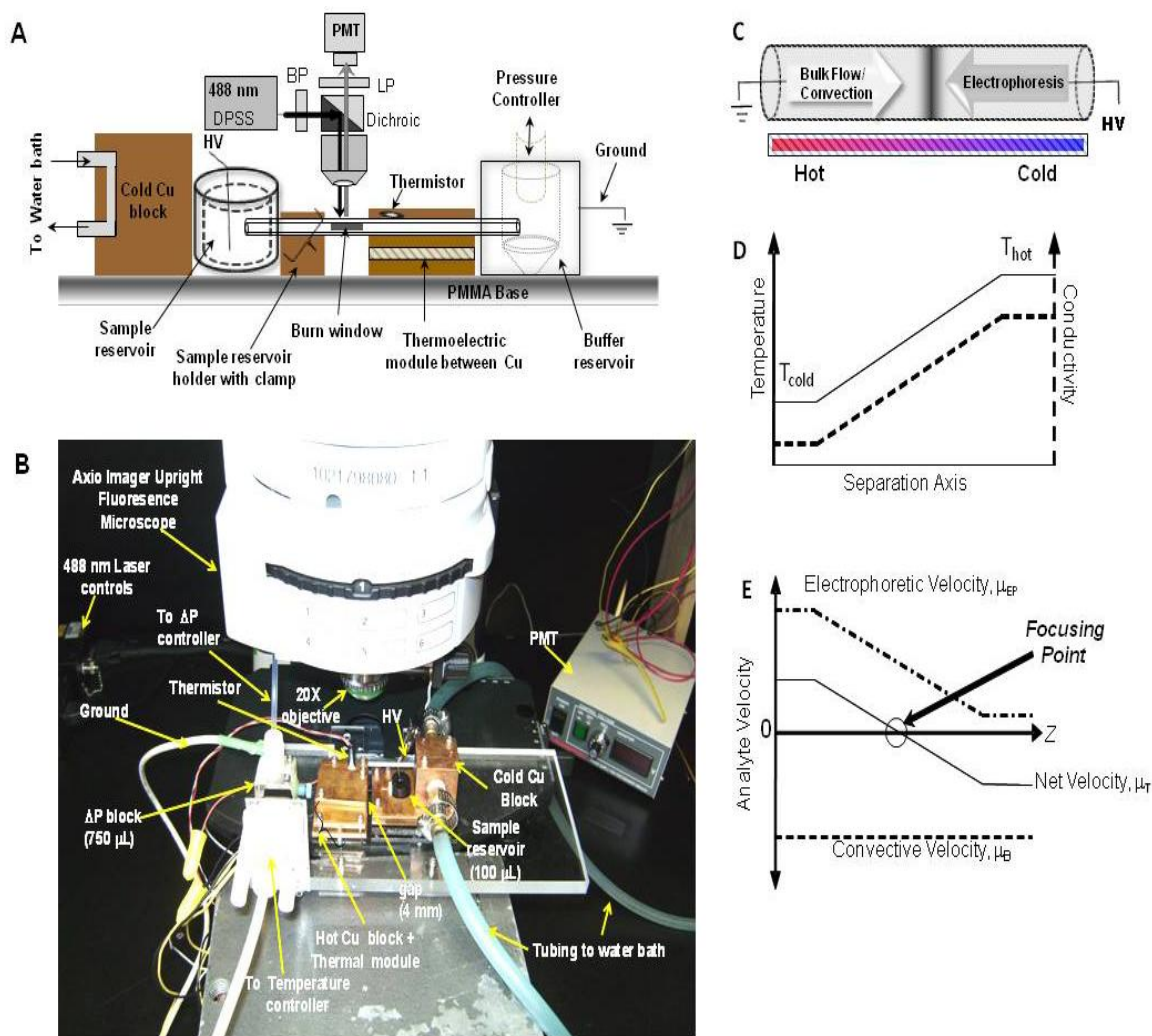


**Figure 3.1.** TGF instrumentation and concept. **A.** Assembly of the capillary format of TGF. 8.0 cm of capillary (1.9 cm from the sample inlet) connecting a pressure controlled and grounded 750  $\mu\text{L}$  reservoir containing background buffer to a 100  $\mu\text{L}$  open-air reservoir containing sample and background electrolyte matrix. Detection was performed by laser-induced fluorescence (LIF) microscopy. **B.** Photograph of the in-house instrument set-up. **C.** Schematic of TGF in a microcolumn. **D.** Establishment of conductivity due to temperature change across a microcolumn. For a given electrolyte, the relationship may be as shown or reversed. **E.** Illustration of the three major forces involved in focusing.<sup>20,28</sup> The convective or bulk velocity incorporates both hydrodynamic and EOF velocities. Focusing occurs at the equilibrium point where electrophoretic and convective velocities balance.

### 3.5.2. TGF separation of carboxyfluorescein and fluorescein

A demonstration of TGF focusing and separation of two fluorescent dye molecules, carboxyfluorescein (FAM), and fluorescein is shown (Figs. 3.2C). Initially, standard concentrations of FAM were simply flowed through (FT) on 8.0 cm fused silica capillary (25  $\mu\text{m}$  I.D.) with 1.9 cm effective separation length to estimate enrichment enhancement and check detector response (Fig. 3.2A). In the absence of applied field, counterflow was applied at the start of data collection using step-change in the applied pressure from positive to negative at an acceleration rate of -10 Pa/s. An example electropherogram (Fig. 3.2C) is shown for separation and focusing of two fluorescent dye molecules, carboxyfluorescein and fluorescein under similar TGF experimental conditions: applied field of -1000V/cm, -10 Pa/s acceleration rate, spanning a temperature gradient between 80 °C (hot) and 20 °C (cold) with maximum gradient of 5 °C/mm, and 0.5 M Tris borate (pH 8.29) running buffer. The average migration times were  $219 \pm 0.74$  s for FAM, and  $450 \pm 1.83$  s for fluorescein (showed the longest migration time under these unoptimized conditions).

The limit of detection (LOD) for FT analysis was calculated as three times the standard deviation of the noise (or blank) to be 152 pM. The calibration curve (Fig. 3.2B) generated a linear response giving a correlation coefficient,  $R^2 = 0.9997$  and less than 3% average relative standard deviation (RSD) in peak heights ( $n=3$ ). As a routine, capillary was simultaneously conditioned with 0.1 M NaOH, deionized water and buffer (5 minutes each) prior to first use and between runs as needed to facilitate suitable EOF.

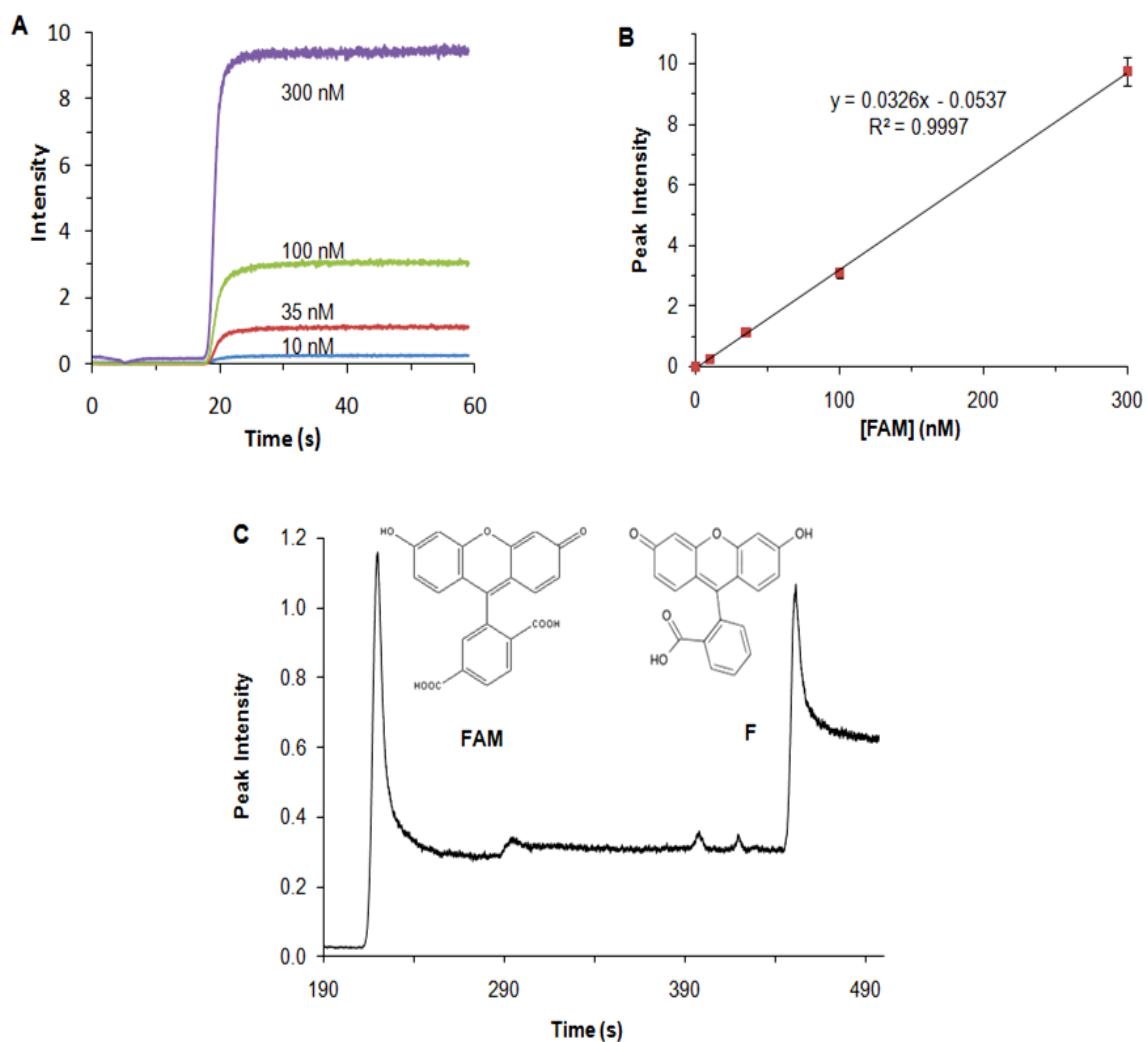


**Figure 3.2.** Example of flow-through (FT) of carboxyfluorescein (FAM). **A.** FT in a 25  $\mu\text{m}$  I.D. capillary of 10, 35, 100, and 300 nM FAM obtained by step-changing the applied pressure from 10,000 Pa to -10000 Pa at the start of data collection. **B.** TGF calibration curve of 10, 35, 100, and 300 nM FAM. 8.0 cm capillary (25  $\mu\text{m}$  I.D.); -1000 V/cm; -10 Pa/s acceleration; buffer: 0.5 M Tris-Borate balanced to pH 8.29. **C.** Example electropherogram showing separation of carboxyfluorescein (FAM) and fluorescein. TGF separation of 10 nM F and FAM in 8.0 cm capillary (25  $\mu\text{m}$  I.D.); -1000 V/cm; -10 Pa/s acceleration; buffer: 0.5 M Tris-Borate balanced to pH 8.29.

### 3.5.3. TGF separation of amino acids

As noted in other studies, smaller bore capillary is a key factor in improving sensitivity and efficiency.<sup>19,20</sup> Asp and Glu separation (Fig. 3.3C) followed the same experimental conditions for FAM and F. The average migration time for Asp and Glu were  $231 \pm 0.63$  s, and  $239 \pm 0.56$  s, respectively; both analytes migrated in less than five minutes. The limit of detection (LOD) was 537.8 pM for Asp and 454.6 pM for Glu. The calibration curve (Fig. 3.2B) generated a better linear response for all analytes. Overall, the system was highly reproducible for all measurements ( $n=3$ ); however, based on the correlation residual squared values there is probably instrumental error associated with the data.

## 3.6. Conclusion

The results presented here is a validation that TGF separation and focusing can be achieved on newly built TGF instrument. A demonstration of TGF in common TGF buffer showed high resolution separation and focusing (based on counterflow) for anionic analytes; however, the experimental conditions were not optimized. TGF focusing and separation of dyes - carboxyfluorescein (FAM), fluorescein (F), and amino acids – aspartate, glutamate, was less than five minutes (except for fluorescein).

Since known applications of TGF have separated a wide range of analytes, future studies can focus on parallelization and multiplexing the technique in microdevices.

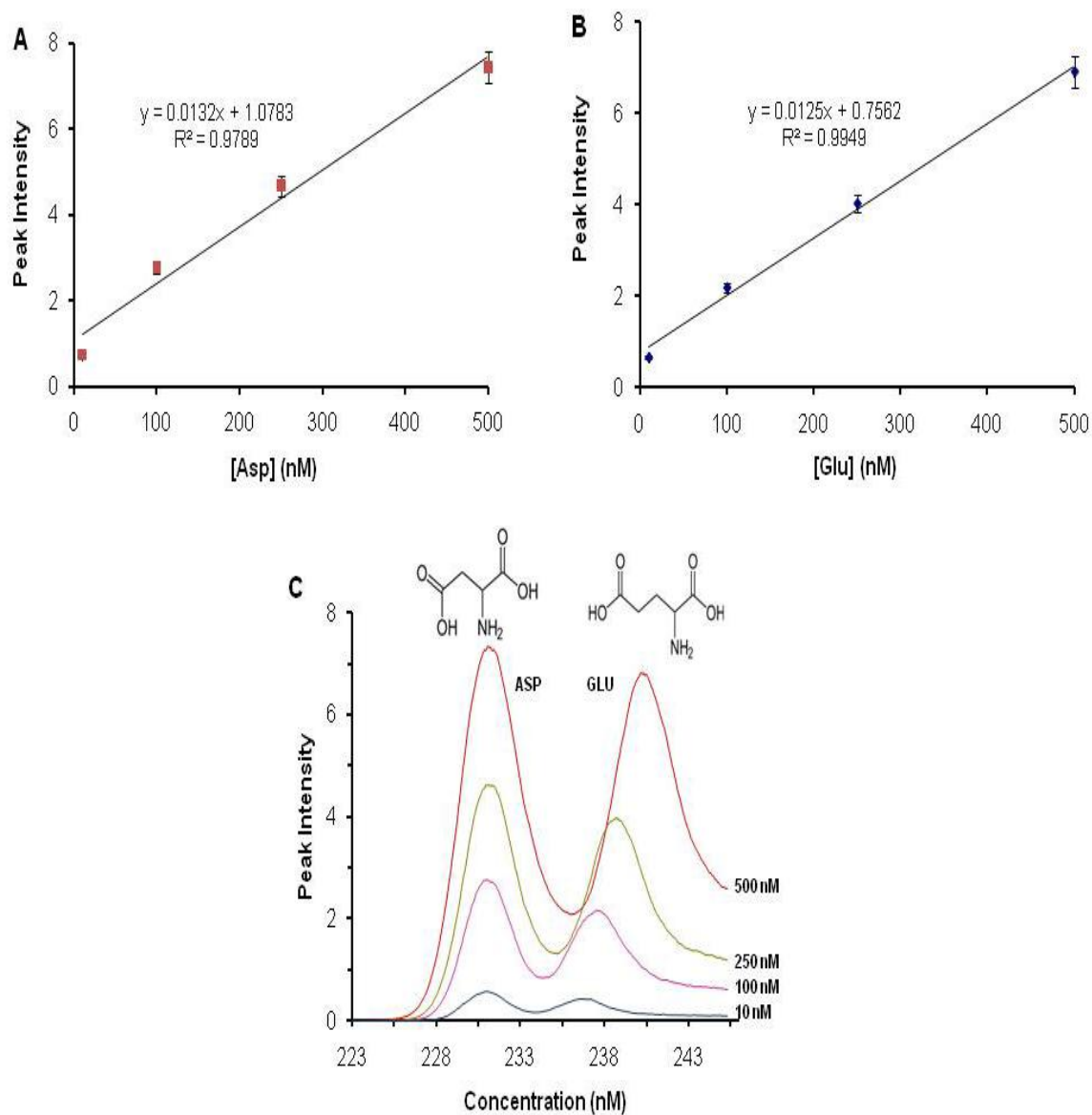


**Figure 3.3.** Separation of aspartate (Asp) and glutamate (Glu). Calibration curves for 10, 100, 250, and 500 nM Asp (**A**) and Glu (**B**) in 8.0 cm capillary (25  $\mu\text{m}$  I.D.); -1000 V/cm; -10 Pa/s acceleration; buffer: 0.5 M Tris-Borate balanced to pH 8.29. **C.** Example electropherogram of TGF separation and focusing of Asp and Glu.

### 3.8. References Cited

1. Kolin, A. *J. Chem. Phys.* **1954**, *22*, 1628–1629.
2. Hjertén, S.; Zhu, M. D. *J. Chromatogr. A* **1985**, *346*, 265–270.
3. Tulp, A.; Verwoerd, D.; Hart, A. A. *Electrophoresis* **1997**, *18*, 767-773.
4. Rodriguez-Diaz, R.; Wehr, T.; Zhu, M. D. *Electrophoresis* **1997**, *18*, 2134-2144.
5. Righetti, P. G.; Bossi, A. *Anal. Chim. Acta* **1998**, *372*, 1-19.
6. Kilar, F. *Electrophoresis* **2003**, *24*, 3908-3916.
7. Shimura, K. *Electrophoresis* **2002**, *23*, 3847-3857.
8. Lin, C. H.; Kaneta, T. *Electrophoresis* **2004**, *25*, 4058-4073.
9. Quirino, J. P.; Terabe, S. *J. Chromatogr. A* **2000**, *902*, 119-135.
10. Osbourn, D. M.; Weiss, D. J.; Lunte, C. E. *Electrophoresis* **2000**, *21*, 2768-2779.
11. Giddings, J. C.; Dahlgren, K. *Sep. Sci. Technol.* **1971**, *6*, 345-356.
12. Huang, Z.; Ivory, C. F. *Anal. Chem.* **1999**, *71*, 1628-1632.
13. Koegler, W. S.; Ivory, C. F. *J. Chromatogr. A* **1996**, *726*, 229-236.
14. Petsev, D. N.; Lopez, G. P.; Ivory, C. F.; Sibbett, S. S. *Lab. Chip* **2005**, *5*, 587-597.
15. Humble, P. H.; Kelly, R. T.; Woolley, A. T.; Tolley, H. D.; Lee, M. L. *Anal. Chem.* **2004**, *76*, 5641-5648.
16. Balss, K. M.; Vreeland, W. N.; Howell, P. B.; Henry, A. C.; Ross, D. *J. Am. Chem. Soc.* **2004**, *126*, 1936-1937.
17. Kamande, M. W.; Ross, D.; Locascio, L. E.; Lowry, M.; Warner, I. M. *Anal. Chem.* **2007**, *79*, 1791-1796.
18. Shackman, J. G.; Ross, D. *Anal. Chem.* **2007**, *79*, 6641-6649.

19. Mamunooru, M.; Jenkins, R. J.; Davis, N. I.; Shackman, J. G. *J. Chromatogr. A* **2008**, *1202*, 203-211.
20. Davis, N. I.; Mamunooru, M.; Vyas, C. A.; Shackman, J. G. *Anal. Chem.* **2009**, *81*, 5452-5459.
21. Ross, D.; Locascio, L. E. *Anal. Chem.* **2002**, *74*, 2556-2564.
22. Balss, K. M.; Ross, D.; Begley, H. C.; Olsen, K. G.; Tarlov, M. J. *J. Am. Chem. Soc.* **2004**, *126*, 13474-13479.
23. Balss, K. M.; Vreeland, W. N.; Phinney, K. W.; Ross, D. *Anal. Chem.* **2004**, *76*, 7243-7249.
24. Kim, S. M.; Sommer, G. J.; Burns, M. A.; Hasselbrink, E. F. *Anal. Chem.* **2006**, *78*, 8028-8035.
25. Shackman, J. G.; Munson, M. S.; Kan, C. W.; Ross, D. *Electrophoresis* **2006**, *27*, 3420-3427.
26. Hoebel, S. J.; Balss, K. M.; Jones, B. J.; Malliaris, C. D.; Munson, M. S.; Vreeland, W. N.; Ross, D. *Anal. Chem.* **2006**, *78*, 7186-7190.
27. Matsui, T.; Franzke, J.; Manz, A.; Janasek, D. *Electrophoresis* **2007**, *28*, 4606-4611.
28. Munson, M. S.; Danger, G.; Shackman, J. G.; Ross, D. *Anal. Chem.* **2007**, *79*, 6201-6207.
29. Shackman, J. G.; Munson, M. S.; Ross, D. *Anal. Bioanal. Chem.* **2007**, *387*, 155-158.
30. Danger, G.; Ross, D. *Electrophoresis* **2008**, *29*, 3107-3114.

31. Munson, M. S.; Meacham, J. M.; Ross, D.; Locascio, L. E. *Electrophoresis* **2008**, *29*, 3456-3465.
32. Munson, M. S.; Meacham, J. M.; Locascio, L. E.; Ross, D. *Anal. Chem.* **2008**, *80*, 172-178.
33. Becker, M.; Mansouri, A.; Beilein, C.; Janasek, D. *Electrophoresis* **2009**, *30*, 4206-4212.
34. Huber, D. E.; Santiago, J. G. *Electrophoresis* **2007**, *28*, 2333-2344.
35. Sommer, G. J.; Kim, S. M.; Littrell, R. J.; Hasselbrink, E. F. *Lab. Chip* **2007**, *7*, 898-907.
36. Lin, H.; Shackman, J. G.; Ross, D. *Lab. Chip* **2008**, *8*, 969-978.
37. Tang, G.; Yang, C. *Electrophoresis* **2008**, *29*, 1006-1012.
38. Huber, D. E.; Santiago, J. G. *Proc. R. Soc. A* **2008**, *464*, 595-612.
39. Shackman, J. G.; Watson, C. J.; Kennedy, R. T. *J. Chromatogr. A* **2004**, *1040*, 273-282.

## **CHAPTER 4**

### **TEMPERATURE GRADIENT DENATURING FOCUSING**

#### **4.1. Abstract**

A novel technique, temperature gradient denaturing focusing (TGDF) with LIF detection is described for detection of synthetic DNA on a single microcolumn. TGDF eliminates the need for gel matrices, and presents a platform for DNA mutation detection. The rapid electrophoretic focusing is based on conformational change using continuous injection and counterflow along thermal gradient microcolumn. A demonstration of rapid enrichment of synthetic oligonucleotides (24mers base pairs) evaluated in a variety of matrices is shown using TGDF.

## 4.2. Introduction

The completion of the human genome project (HGP) has provided a large library of DNA sequences that holds the key to understanding the many diseases<sup>1-4</sup> and phenotypic changes prevalent to our species. Notably, a larger percentile of the human genome comprises of repetitive sequences (which include transposons, duplications, and repeats) and the remaining are non-repetitive sequences. The activities of some of these sequences are responsible for gene mutation (due to insertion, deletion, substitution, rearrangement) and results in variations in gene frequency. The most abundant gene frequency is single nucleotide polymorphisms (SNPs) affect over 3 million people<sup>5-8</sup> totaling approximately 1% in the population. SNPs are found in coding as well as non-coding regions (more frequently)<sup>9,10</sup> and usually results from base pair (bp) substitutions, although infrequently may be due to bp insertions and deletions.<sup>11</sup>

Of the almost 4,000 kilobases (kb) of genes in the human genome, only a small portion (~ 1%) of genes, the exons, code for functional protein while the function (s) of the rest (introns) are not entirely understood. For other model organisms chromosome mapping have revealed characteristic traits present on each chromosome making it possible to detect mutations and make other predictions.

Gene mutations not only affect the whole population, but can persist into a hereditary inheritance. Some known diseases caused by SNP include sickle cell anemia,<sup>12,13</sup> cystic fibrosis,<sup>14,15</sup> hereditary hemochromatosis,<sup>16,17</sup> and Tay-Sachs disease.<sup>18,19</sup> Although a mutation may be dominant or recessive in phenotypic expression, the overall gene function maybe altered. Detection of mutations in a single base pair of

DNA, or single nucleotide polymorphisms (SNPs), is a critical step in diagnosing and understanding the causes of a variety of genetic disorders.

Currently available mutation detection techniques typically exhibit trade-offs between sensitivity, selectivity, and throughput, with the most sensitive methods being the most difficult to automate or perform in parallel. The DNA microarrays and PCR-based methods<sup>9,20</sup> are used to pre-screen genomic regions and to isolate target sequences for full sequencing. A disadvantage of these methods is that they require a skilled operator and prior knowledge of the sequence to be screened. Also, the PCR method is susceptible to contamination and error prone additional mutation in each cycle.<sup>21,22</sup>

More commonly, electrophoresis based methods either on a gel slab, capillary or microfluidic device is used to obtain molecular weight information and to observe conformational changes inherent from gene mutation which results in changes in electrophoretic mobility. DNA sequencing on slab gels has been recognized as the “gold standard” for detecting mutations. Although the slab gel formats offer the ability to run parallel analyses, as well as two-dimensional separations, conducting experiments on slab gel is costly, labor intensive and time consuming, all of which collectively hinders its use in routine screening of mutations.<sup>23,24</sup> The microcolumn formats (capillary and microfluidic) allow much smaller injection volumes, application of higher field strengths resulting in rapid analyses (minutes compared to hours) and higher efficiency separations. Capillary arrays and multiplexed microfabricated devices allow for higher throughput applications. Notably, the replacement of slab gel DNA sequencing with capillary arrays was a key factor in completing the HGP ahead of schedule.<sup>25,26</sup>

Methods like the single strand conformation polymorphism (SSCP)<sup>27-29</sup> and heteroduplex analysis (HA)<sup>30,31</sup> both rely on creating conformational changes after fully melting double stranded DNA (dsDNA) prior to analysis. SSCP snap-freezes the single stranded DNA (ssDNA), which fold onto themselves into different conformers based on sequence and ideally produce variations in mobility. In HA the melted DNA containing both wildtype (WT) and mutant (mut) strains are slowly cooled then reannealed forming both homo- and heteroduplexes. The mismatched bases in the heteroduplexes can lead to species separable by electrophoresis (although the homoduplexes are often unresolved from each other). SSCP has shown better sensitivity to SNP detection than HA but often requires empirical method development for each new sequence to be studied, as ssDNA conformations after snap-freezing are difficult to predict.<sup>32</sup>

Other known methods achieve mutation detection from establishing temperature gradient. The denaturing/temperature gradient gel electrophoresis (DGGE/TGGE)<sup>33-36</sup> are related techniques which achieve separation as a result of difference in mobility shift of tandem strands. DGGE uses a denaturing agent (such as high concentrations of urea) to create a chemical gradient to facilitate melting along the separation axis. TGGE (also known as temperature gradient denaturing electrophoresis, TGDE, to incorporate non-gel conditions)<sup>37-52</sup> achieves the same effect through imposing a temperature gradient, which is easier to implement than a chemical gradient and is better understood due to the breadth of research into DNA melting. Unlike HA and SSCP, both DGGE and TGGE have demonstrated the same or better sensitivity to mutation detection even showing the ability to handle longer DNA fragments with high accuracy in detection.<sup>33</sup> Current

research efforts are gear towards transferring either temporal or spatial gradients in capillary TGDE applications to microfluidic devices.<sup>53-55</sup>

With the wealth of information made possible from HGP, the major challenge lie in developing methods for transferring the information into accessible and accurate information for possible detection, diagnosis and early treatment of diseases.<sup>1-4</sup> This work will focus on the development of a novel approach to combining thermal denaturing gradients with electrofocusing for high-throughput DNA mutation detection. A first step in the process would focus on development of a single microcolumn assay based on mobility shift assay for detecting mutations. A combination of both counterflow electrofocusing and temperature gradient (similar to TGF) would be employed for online focusing and separation of DNA duplexes. It is expected that joining the simultaneous enrichment and electrophoretic separation power of microcolumn counterflow electrofocusing with the simplicity and selectivity of temperature denaturing gradients will result in assays with both exceptional sensitivity and selectivity.

### 4.3. Theory of TGDF

The theory of TGDF follows principles of electrophoresis and TGF already discussed. TGDF is a first demonstration of focusing based solely on conformational changes. The method combines aspects from TGGE and TGF. It utilizes either a TGF or non-TGF background buffer, a thermal microcolumn to facilitate conformational changes and melting, and counteraction from bulk flow and electrophoresis to achieve focusing and separation of DNA at a null point. It is expected that single and double stranded DNA/complexes would be separated simultaneously because of their chain length and complexity; single strands would migrate faster and be detected ahead of the double stranded DNA.

To summarize, electrophoretic mobility can be used to describe DNA conformational changes resulting from changes in mutations, chain length or base components of DNA sequence. For example, analysis carried out on a capillary, microcolumn or gel media, the velocity of analyte is directly proportional to the analyte's electrophoretic mobility,  $\mu$ , and the electric field strength  $E$ . The mobility is proportional to the analyte charge,  $z$ , and inversely related to a frictional force constant. The frictional force increases as the analyte's effective hydrodynamic radius,  $r$ , increases:<sup>56,57</sup> The relationship is described as follows:

$$v_{analyte} = \mu_{analyte} E \quad (1a)$$

$$v_{analyte} = \frac{z}{6\pi r \eta} E \quad (1b)$$

where  $\eta$  is the solvent viscosity. In conventional electrophoresis, the analyte size does not change throughout the separation, and single bp mutations do not significantly change

the mobility of DNA (and are not separated from one another). However, if  $r$  is altered (as in folded or linear) either prior to analysis or during the separation (either spatially or temporally), resolution of mutation can be detected.

According to the unified separation equation (already discussed), most separation techniques have achieved separation from manipulating different parameters. To recap, for electrofocusing techniques, the unified separation equation describes the flux of analyte along the separation axis<sup>58,59</sup> as

$$J_i = -D_i \frac{\delta c_i}{\delta x} + c_i (U_x + \mu_i E_x) \quad (2)$$

where  $J_i$  is the molar flux,  $D_i$  is a dispersion term,  $c_i$  is ion concentration, and  $\mu_i$  is ion mobility of the  $i$ -th component of the system.  $U_x$  is total convective velocity (incorporating chromatographic velocities) and  $E_x$  is electric field strength along the  $x$ -axis. The derivative term accounts for diffusion and dispersion based spreading of the analyte band. The electrophoresis related terms can be further expanded:

$$J_i = -D_i \frac{\delta c_i}{\delta x} + c_i \left( U_x + z_i \omega_i \frac{I_x}{\sigma_x} \right) \quad (3)$$

where  $\omega_i$  is the absolute mobility (incorporating size and solvent viscosity effects), and  $z_i$  is ion charge of the  $i$ -th component of the system.  $I_x$  is current density and  $\sigma_x$  is the background electrolyte conductivity along the  $x$ -axis. Focusing is realized when  $J_i$  is equal to zero, which can occur by varying the other parameters (essentially velocity, charge, mobility, current, or conductivity).

Separation results by having different discrete parameter values or by employing a gradient of values so long as the analytes to be separated have differing properties, such as mobility. Focusing and separation in capillary and microfluidic mobility shift assays

use zonal methods (*i.e.*, a discrete injection slug of analyte is introduced on-column and allowed to resolve along the separation axis). The counteracting chromatographic electrophoresis (CACE) alters the chromatographic component of  $U_x$ .<sup>60</sup> Equilibrium gradient focusing methods<sup>62,63</sup> generates steady-state zones. IEF achieves focusing and separation through a pH gradient by altering  $z_i$  until the analytes reach null-velocity points and cease migrating. Electric field gradient focusing (EFGF) uses a spatial field gradient to manipulate  $I_x$ . Conductivity gradient focusing (CGF) and temperature gradient focusing (TGF) alter  $\sigma_x$ .<sup>61-63</sup>

Although not previously shown, TGDF using electrofocusing is expected to directly manipulation the electrophoretic mobility term  $\omega_i$  of Equation 3. Focusing under these conditions proceeds as discussed in chapter 3 (TGF Focusing); however, conductivity is independent of temperature. The electrophoretic velocity is altered by directly changing the frictional force of the analytes themselves. As with mobility shift assays for TGGE, the mobility due to conformational changes can be dramatically altered through temperature gradient.

## 4.4. Experimental

### 4.4.1. Chemicals and reagents

Boric acid, sodium hydroxide, and Tris-base of highest purity were obtained from ProPure, while tricine was from ICN Biomedical, Inc. (Solon, OH). Sodium chloride and ethylenediamine tetraacetic acid (EDTA) were obtained from Fisher. Custom made 10-mer (poly-G (Guanine), 11-mer (poly-C (Cytosine)) and 24-mer - wildtype (WT), mutant (Mut) single-stranded (ss) oligonucleotides purified by reverse phase HPLC, along with

Tris-HCl and bovine serum albumin (BSA) were purchased from Sigma-Aldrich Sigma-Aldrich (St. Louis, MO). Table 4.1 shows properties of strands 5' modified with fluorescein (Flc) tag (No. 1a, 1b, 2a, 3a, 4a, 5a) and unlabeled strands (No. 2b, 2c, 3b, 4b, 5b).

The oligonucleotide pellets were vortexed and individually resuspended in 1 ml of stabilizing buffer, 1X TE (Tris-EDTA) to give micromolar stock concentration (see Table 1). Stock of 1X TE buffer was prepared in 100 ml bottle as follows: 1mL of 1M Tris-HCL (pH range 7.5-8.0); 0.2 ml of 0.5 M EDTA (pH 8.0); 98.8 mL of Millipore water. Aliquots of 100  $\mu$ L were stored in microcentrifuges tubes wrapped with aluminum foil at 4°C until ready to use. The annealing buffer contained 0.5 M NaCl, 1mM EDTA dissolved in 50 mM Tricine-NaOH. Double stranded (ds) DNA were 250 nM stock prepared in annealing buffer; strands were annealed above their melting temperature, cooled and then stored in refrigerator until ready for use. For analysis, initially 10 nM dilutions were made from annealed stock in 50 mM Tricine-NaOH to ensure buffer in sample matrix was consistent with running buffer. Dilutions from unannealed stock were made directly in the running buffer. All solutions were made using Milli-Q (Millipore, Bedford, MA)  $\geq 18$  M $\Omega$  cm deionized (DI) water. Solutions were filter daily using 0.20  $\mu$ m Fisherbrand nylon syringe filters.

**Table 4.1. DNA oligonucleotides**

No.	Oligonucleotide	Sequence (5'-3')	Mol. Wt.	T <sub>m</sub> <sup>o</sup> (°C)	Stock Concentration (μM)
1a	Poly C (PC-11mer)*	5'[5Fle]-CCC GGG CCC CC 3'	3777	63.7	110.4
1b	Poly G (PG-10mer)*	5'[5Fle]-GGG GCC CGG G 3'	3647	58.5	38.9
2a	WT* (12mer)	5'[5Fle]-CTC ATG ATC ATA 3'	4141.8	24.8	36.6
2b	wt (12mer)	5' TAT GAT CAT GAG 3'	3684.4	24.8	175.4
2c	mut (12mer)	5' TAT GAT TAT GAG 3'	3699.4	21.0	96.6
3a	WT* (24mer)	5'[5Fle]- GCG ACT CTC ATG ATC ATA GAA CAC 3'	7843.1	63.7	21.7
3b	wt (24mer)	5'GTG TTC TAT GAT CAT GAG AGT CGC 3'	7398.6	63.7	103.7
4a	Mut* (24mer)	5'[5Fle]- GCG ACT CTC ATC ATC ATA GAA CAC 3'	7803.1	63.7	57.0
4b	mut (24mer)	5'GTG TTC TAT GAT GAT GAG AGT CGC 3'	7438.7	63.7	62.7
5a	GCWT*(24mer)	5'[5Fle]- GCG ACT CTC ATG GCG GGC GGG GCG 3'	7989.1	86.7	115.1
5b	gcwt (24mer)	5'CGC CCC GCC GCG CAT GAG AGT CGC 3'	7300.6	87.6	116.5

T<sub>m</sub><sup>o</sup> - melting temperature; asterisks (\*) indicates strand is labeled at 5' end.

#### 4.2.2. Instrumentation

TGDF was conducted on the same apparatus used for TGF. In summary, 7 cm of fused-silica capillary (25  $\mu\text{m}$  i.d.; 360  $\mu\text{m}$  o.d.; Polymicro Technologies, Phoenix, AZ) with a 2-mm optical window (Microsolv Window Maker, Eatontown, NJ) located 1.4 cm from the inlet was inserted into a machined 100- $\mu\text{L}$  Derlin sample reservoir (McMaster-Carr, Robbinsville, NJ) with a 400- $\mu\text{m}$  diameter hole sealed with a Teflon-backed silicon septum (Sigma). High voltage (CZE 3000, Spellman High Voltage Electronics, Hauppauge, NY) was applied to the sample reservoir ( $\pm 30$  kV) by platinum electrode. The capillary outlet was connected to a 750- $\mu\text{L}$  polymethyl methacrylate machined buffer reservoir (McMaster-Carr) *via* an Upchurch Nanoport (N-124S; Oak Harbor, WA); a grounding platinum electrode was also coupled to this reservoir *via* a Nanoport. The buffer reservoir was connected to a  $\pm 69$  kPa ( $\pm 10$  psi) precision pressure controller (Series 600, Mensor, San Marcos, TX) for hydrodynamic flow regulation through a removable Nylon Swagelok union (Penn Fluidic System Technologies, Huntingdon Valley, PA), which also was the access for fluid exchange.

Detection for capillary experiments was performed using an in-house modified Axio Observer A1 upright fluorescence microscope (Carl Zeiss, Thornwood, NY). The arc-lamp optical train was removed and the output of a 30-mW diode-pumped solid state 488-nm laser (Melles Griot, Carlsbad, CA) was directed onto a fluorescein-specific optical block containing a 500-nm longpass dichroic and 510- to 560-nm emission bandpass filter (QMAX Green series, Omega Optical, Battleboro, VT). Laser excitation was focused through a 20 $\times$  objective (0.4 numerical aperture, N.A., Carl Zeiss) into the capillary. Fluorescence emission was collected through the same objective and detected

through a 3-mm spatial filter with a Hamamatsu (Bridgewater, NJ, USA) H5784 photosensor module and C7169 power supply.

All instrument control and data acquisition was performed using LabVIEW software (National Instruments, Austin, TX) written in-house. Digitization of the UV output utilized a USB-6221 module (National Instruments) recording at 100 Hz. Data analysis was performed using Cutter software<sup>64</sup> with 1 Hz low-pass filtering of raw UV data. Plate number (N) was measured at width at half height,  $w_h$ . Peak identification of mixtures was accomplished through individual analyte runs and spiking of analytes.

## 4.5. Results and Discussion

### 4.5.1. Concept and Operation of TGDF

Although TGF and TGDF can be conducted on the same apparatus (Figs. 3.1 and 4.1), there are major differences between the two techniques. TGDF does not necessarily require a temperature dependent buffer, so conductivity is not a temperature dependent factor. Focusing in TGDF can result primarily from conformational changes which can be described by the analytes' electrophoretic mobility. The electrophoretic mobility is controlled mainly by frictional force of each analyte. The temperature dependent field strength and the temperature gradient (Figs. 3.1D and 4.1C) drive analytes electrophoretic velocity. The temperature gradient also facilitates conformational change leading to up to denaturing. Similarly, both TGDF and TGF achieve focusing and separation at a null point as a result of balancing effect between counterflows (bulk and  $\mu_{EP}$ ) on the column (Figs. 3.1C, 3.1E, 4.1B and D).

Sample (synthetic DNA) and background buffer are present at the microcolumn (Fig 4.1B) inlet at a negative potential (for anionic analyses). Upon application of voltage and current, sample is continuously loaded onto column being counter balanced by bulk flow. Once on column analytes move by electrophoretic velocity which is opposed by the EOF in the capillary, the applied pressure serves as referee between these counter exchanges until focusing is achieved at a steady state unique to each analyte. Both EOF and  $\Delta P$  move toward the sample reservoir (left to right) while  $\mu_{\text{Analyte}}$  is directed toward the  $\Delta P$  block (right to left).

The copper blocks maintain temperature regulation between 20 °C (cold) and 80 °C (hot). The temperature drop across the capillary spanning these blocks is defined by distance (gap) between the blocks. A smaller gap (usually 2-4 mm) minimizes the temperature drop per cross-sectional area of the capillary and increases peak efficiency. Unlike TGF, only the temperature gradient between the blocks creates the gradient on column. Analytes undergo conformational changes as a result of the temperature gradient imposed on the column. Their electrophoretic mobility generally increases in cold region (ds regime) and slows down in hot region (ss regime). DNA with a higher electrophoretic mobility will overcome the counter-flow ( $v_{\text{CF}}$ ) for focusing to occur. The double stranded complex begins to collapse and full melting occurs usually above the melting temperature of dsDNA. As the focused zone approaches the dsDNA melting temperature, counter-flow forces it back into the focus zone, this shifting persists until a dynamic equilibrium is reached (Fig. 4.1E). Once melting occurs, the ssDNA can travel past the focus zone. Since injection is continuous, the presence of labeled DNA (probe) along column increases the chance of the ssDNA reannealing (Fig. 4.1F). If the ssDNA

reanneals faster than it migrates through the gradient, focusing can be restored; however, signal intensity would be reduced in hotter regions. It is expected that for homo- and hetero- duplexes, separation would be achieved as a result of difference in their electrophoretic mobilities and focusing point; heteroduplex melts faster due to mutation or difference in sequence. LIF is used for sensitive detection of separate species.

#### *4.5.2. Ohm's Law Plot*

An Ohm's plot is a good predictor for estimating optimal field strength of a buffer. To generate the plot, both reservoirs were filled with buffer and upon applying voltage to the system, the current generated was recorded within five minutes intervals for each consecutive field strength change (increments of hundred). In Fig. 4.2, an example Ohm's plot is shown for 50 mM Tricine-NaOH balanced with 10 mM NaCl to pH 8.25 on 8.0 cm capillary (25  $\mu$ m i. d.), at a steep temperature gradient range (20-40°C). Below 900V/cm the plot is linear indicating that buffer can be tested using field strength within linear range to get optimized conditions. Above 900V/cm Joule heating is evident because of the deviation from linearity. An ohm's plot was not obtained for all the buffer systems tested; however, a quick test of current profile at different field strength was done instead.

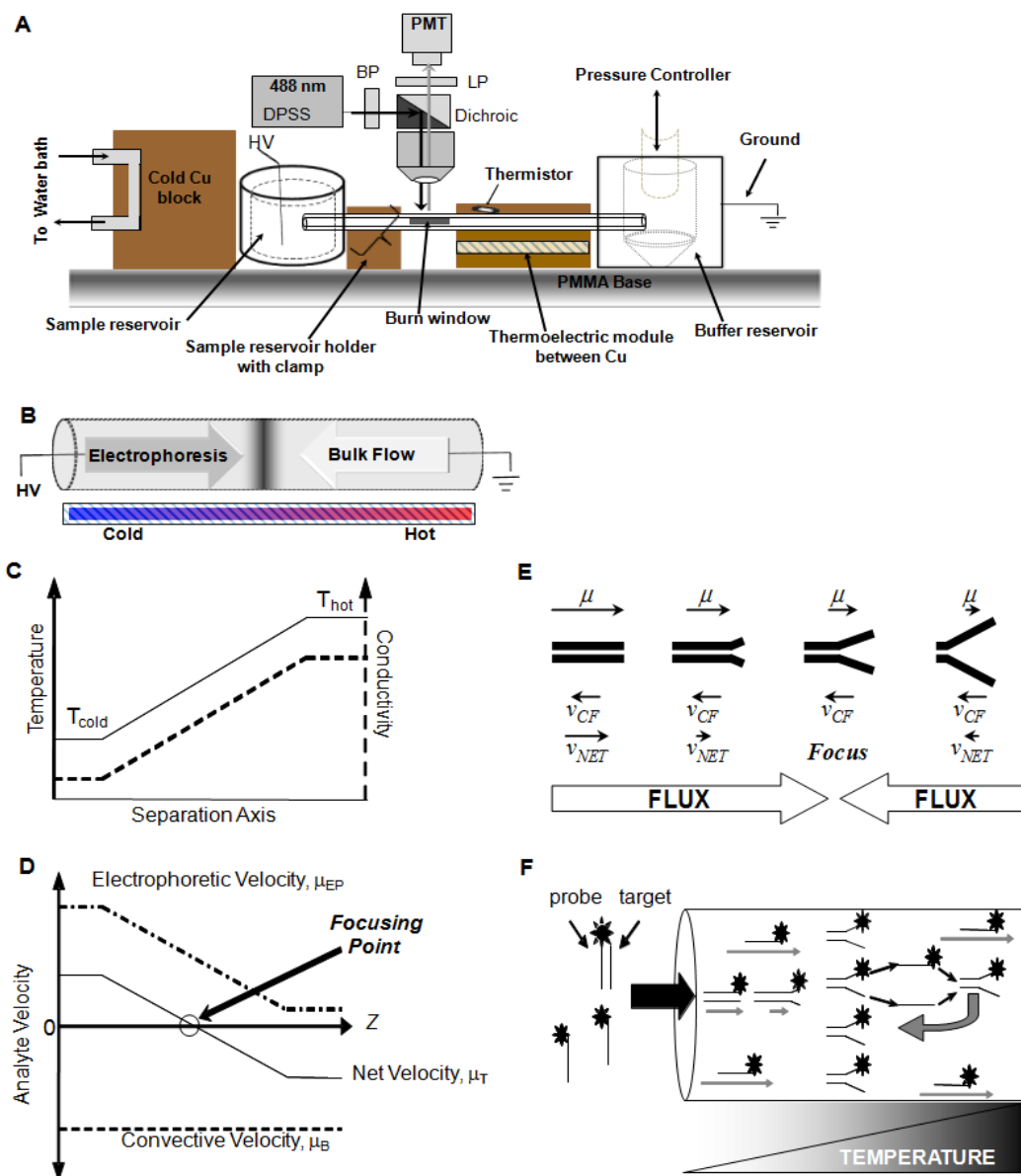


**Figure 4.1. TGDF Concept.** **A.** TGDF instrument. Assembly of the capillary format of TGF. 7.0 cm of capillary (1.4 cm from the sample inlet) connecting a pressure controlled and grounded 750  $\mu\text{L}$  reservoir containing background buffer to a 100  $\mu\text{L}$  open-air reservoir containing sample and background electrolyte matrix. Detection was performed by laser-induced fluorescence (LIF) microscopy. **B.** Schematic of TGDF in a microcolumn. **C.** Establishment of temperature gradient. **D.** Three major forces controlling focusing. The bulk velocity incorporates both hydrodynamic and EOF velocities. Focusing occurs at the equilibrium point where electrophoretic and bulk velocities balance to zero. **A-D** same as TGF. **E.** Focusing of dsDNA as it denatures. DNA to the left of the focus point has a higher electrophoretic mobility ( $\mu$ ) and will overcome the counter-flow ( $v_{CF}$ ) to move to the right. Should the DNA travel pass the focus zone,  $\mu$  continues to decrease and counter-flow forces it back into the focus zone. **F.** Recovery of melted DNA. As the focused zone approaches the dsDNA melting temperature, the likelihood for full melting increases. If the ssDNA reanneals faster than it migrates through the gradient, focusing can be restored. The continuous presence of labeled DNA (probe) increases the chances of recombination. Grey arrows show relative net velocities.

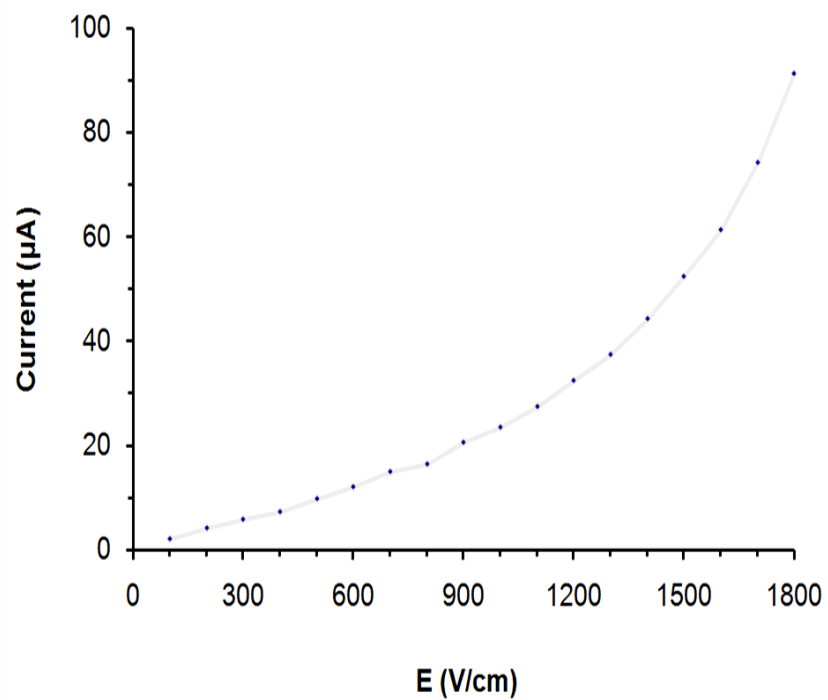


**Figure 4.2.** Ohm's Plot. Plot of 50 mM Tricine-NaOH buffer with 10 mM NaCl to pH 8.3; field strength range -100 to -1800 V/cm (in 100V/cm increments); 8.0 cm capillary (25 µm i. d.).

#### 4.5.3. TGDF enrichment

DNA in its native state is folded. To unfold a DNA complex heat treatment or denaturant is used. Here, solution containing labeled and unlabeled DNA strands (Tab. 4.1:3a-b) mixed to form a dsDNA complex was analyzed to observe enrichment efficiency and migration of ssDNA and dsDNA at different acceleration rates. Prior to analysis, DNA solution was annealed above melting temperature and stored in annealing buffer until ready for use. This was done to test single stranded and double stranded state of DNA. Complimentary single-stranded (ss) DNA under favorable conditions will normally hybridize to form double-stranded (ds) DNA. In Fig. 4.3, electropherograms from hot (80 °C) and cold (20 °C) sides were overlaid. Results confirmed an increase in enrichment efficiency as the scan rate was decreased from -10 to -2.5 Pa/s or with longer time on column in 50 mM Tricine-NaOH balance with 20 mM NaCl to pH 8.15. Generally, a bridged peak was observed on cold side which is probably indicative of dsDNA complex; on the hot side only a single peak was observed since the dsDNA complex collapses above its melting temperature ( $T_m^0$ ). Except at the slowest scan rate (-2.5 Pa/s), ssDNA migrated after dsDNA. The unexpected inversion in migration trend could be due to conformational changes; probably the rate of melting and focusing is faster than the rate of transforming from dsDNA to ssDNA. The change in acceleration rate is a parameter that can be used to tune sensitivity.<sup>65,66</sup>

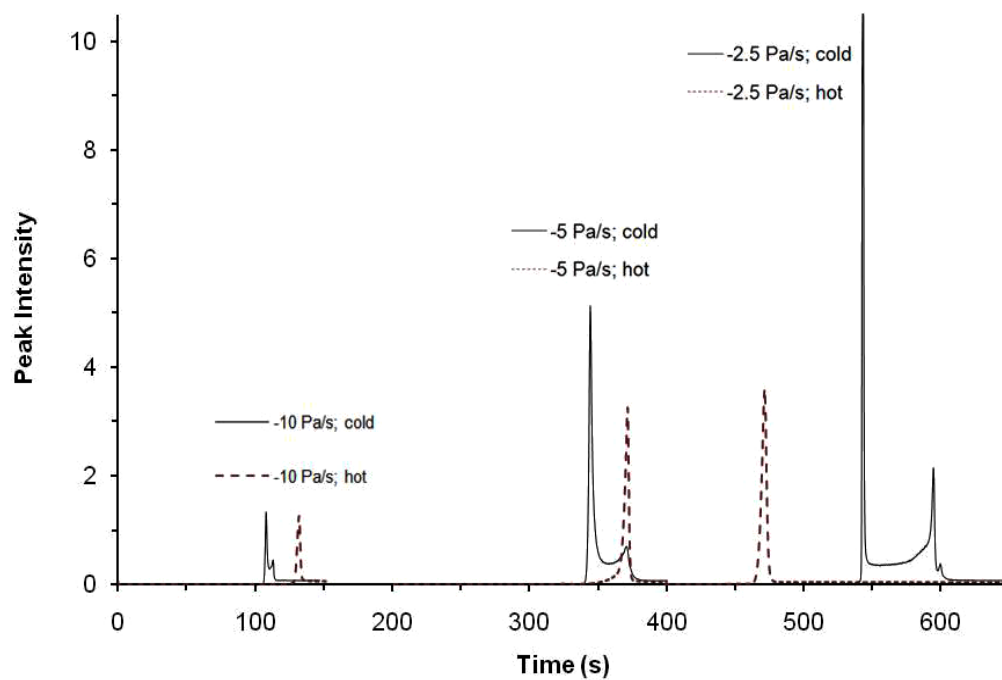


**Figure 4.3.** Enrichment Rates. Example electropherogram of 10 nM dsDNA (24mer WT\*/Wt; See Table 1 for DNA properties) focused on both hot (~80 °C) and cold (~20 °C) sides at -10, -5, -2.5 Pa/s acceleration rates, respectively. Running buffer: 50 mM Tricine-NaOH balance with 20 mM NaCl to pH 8.15; field strength, -250 V/cm; -2000 Pa start pressure; 8.0 cm capillary (25  $\mu$ m i. d.); temperature gradient between 80 °C - 20 °C (at 15 °C/mm).

#### 4.5.4. Evaluating trends in migration time

TGF has shown that steeper gradients can improve resolution. Figure 4.4 reflects change in temperature gradient along the separation column as follows: 80/15 °C, 80/20 °C, 80/30 °C, and 80/40 °C at different field strengths to observe peak profile and migration trend. In Fig. 4.2A, results show analysis of 10 nM perfectly matched (as in WT\*/wt), 10 nM wildtype mismatched (as in WT\*/mut) and a 5 nM mixture of both dsDNA strands. Individual runs from focusing on the cold side in 50 mM Tricine-NaOH balance with 20 mM NaCl to pH 8.17 showed migration time difference reduced with steeper gradients, and high enrichment was maintained throughout. Migration trend at temperature gradient was as follows: 80/20 °C, Mix-WT-WTMM; 80/30 °C, WT-Mix-WTMM; 80/40 °C, WTMM-WT-Mix. Generally, the peak profile was the similar for all run except at steeper gradient 80/40 °C (Fig. 4.2A) where 3 peaks were observed but the migration order was different at each gradient. All samples showed offscale peaks and it was unclear whether separation of DNA duplex was possible in mixture run; however, judging from other preliminary runs, on-scale peaks showed no separation.

In analyzing 2.5 nM perfectly matched (as in WT\*/wt), 2.5 nM GCWT\*/gcwt and a 2.5 nM mixture of both dsDNA strands (Fig 4.2B) the gradients used were: 80/15 °C, 80/20 °C, 80/30 °C, and 80/40 °C. Except for the 80/15 °C gradient, the migration order was the same (Mix-GCWT-WT) in 0.5M Tris-borate balanced with 20 mM NaCl to pH 8.3. The peak profile was different from previously observed, and the enriched decreased with steeper gradient. Also the secondary peak was inverted. The capillary lengths were different in Figs. 4.2A and B. Better enrichment was observed in 0.5M Tris-borate/20 mM NaCl buffer for dilute strand.

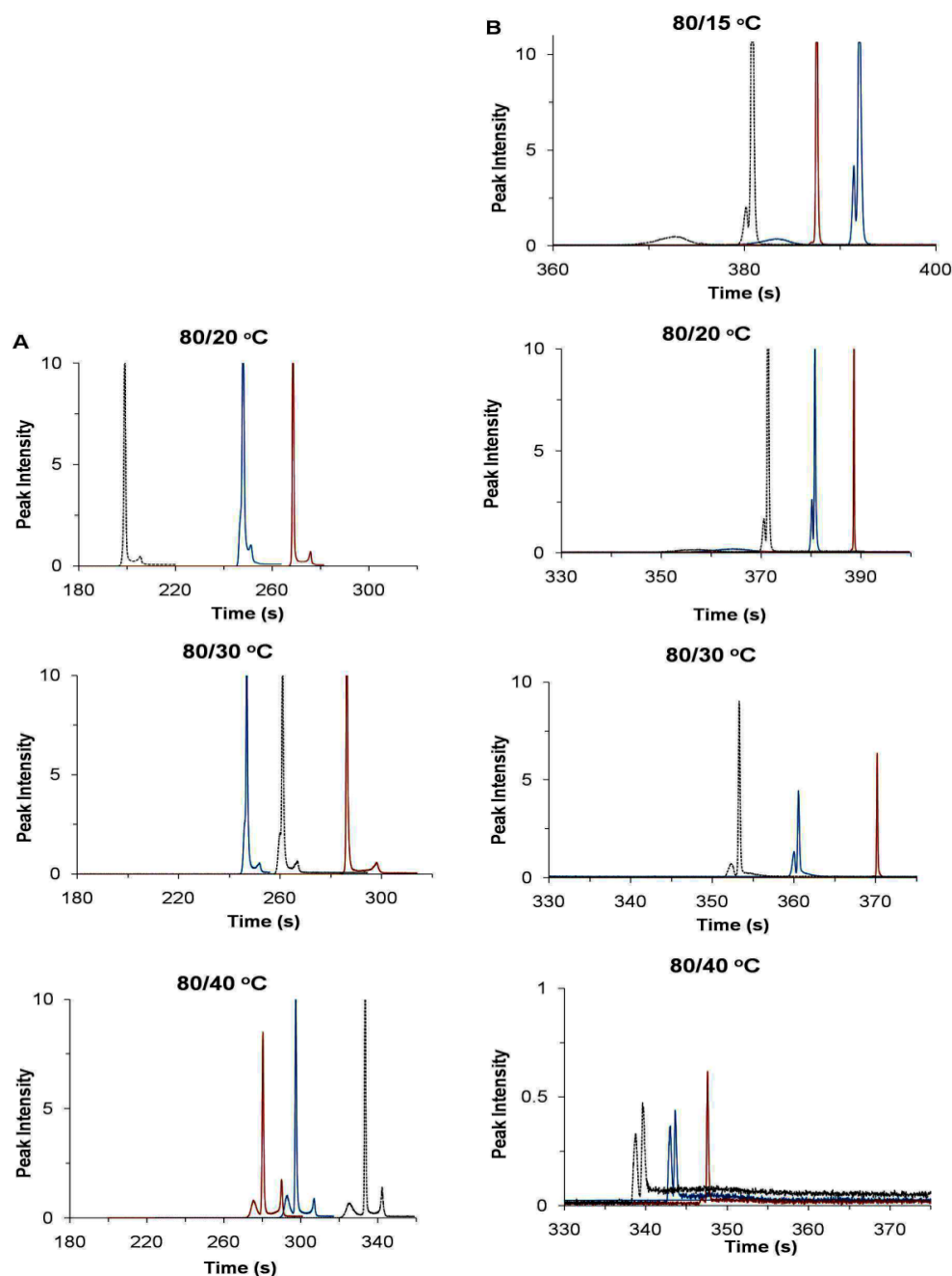


**Figure 4.4.** Trends in migration time. **A.** Example electropherogram of 10 nM dsDNA-24mer (WT\*/Wt; WT\*/mut) and 5 nM mixture of duplexes focused on cold side at different temperature gradients: 80/20 °C, 80/30 °C, 80/40 °C. Experiment conducted on 8.0 cm capillary (25 $\mu$ m i. d.). Conditions: -1400 Pa start  $\Delta$ P; -5 Pa/s acceleration; -350 V/cm field strength; PMT = 0.600V. Running buffer: 50 mM Tricine-NaOH balance with 20 mM NaCl to pH 8.17. **B.** Example electropherogram of 2.5 nM dsDNA-24mer (WT\*/Wt; GCWT\*/gcwt) and 5 nM mixture of duplexes focused on cold side at different temperature gradients: 80/15 °C, 80/20 °C, 80/30 °C, 80/40 °C. Experiment conducted on 7.0 cm capillary (25 $\mu$ m i. d.). Conditions: 2700 Pa start  $\Delta$ P; -20 Pa/s acceleration; -600 V/cm field strength; PMT = 0.600V. Running buffer: 0.5 M Tris borate balance with 20 mM NaCl to pH 8.3.

#### 4.5.5. Determination and comparison of buffer systems

The choice of buffer is a critical factor in achieving optimal focusing and separation. Although not shown, buffers of different properties: concentration, pH, buffer components, sodium and chloride content were evaluated at different field strengths for focusing and enrichment efficiency as well as reproducibility and repeatability in migration time, peak profile, and trends in migration order of strands/duplexes. It is unclear whether temperature dependence of buffer is a factor in TGDF.

Although high enrichment was possible in a number of buffers, separation of strands was questionable as profiles were constantly changing between runs and on a daily basis. Results summarized in Tab. 4.2 reflect analyses in two buffer systems: 0.5 M Tris-borate prepared in 20 mM NaCl, pH 8.29 (*sys A*), and 50 mM Tricine-NaOH prepared in 20 mM NaCl, pH 9.00 (*sys B*), respectively. In analyzing 10 nM perfectly matched strands (as in WT\*/wt, and GCWT\*/gcwt, respectively), and 5 nM mixture of both dsDNA strands/duplex, temperature gradient was gradually narrowed on the hot side by approximately 5 °C under constant run conditions (start  $\Delta P$ , 1400 Pa; acceleration, -5 Pa/s) to primarily observe trends in migration of strands, but also conformational changes and possible melting temperature of duplexes in mixture.

In *sys A* field strengths of 300V/cm, and 1000 V/cm, respectively, were applied under constant run conditions. At 300 V/cm the peaks migration order was the same but migration time for each run set of analyses was unstable. However, no resolution of mixture strands at each temperature gradient was observed. Between 45-60 °C temperature change the same trend was observed at both fields. In *sys B* analyses were performed at 350V/cm, and 500 V/cm. The migration order was the same at 350 V/cm

(GCWT-Mix-WT) and at 500V/cm (GCWT-WT-Mix); however, with each temperature change peaks shifted to lower (left) migration times.

No separation was achieved under experimental conditions with these buffer systems; however, at 1000 V/cm in *sys A*, slight resolution was observed between 60-50 °C. So as an alternative, steeper temperature gradient (gradual 1° C decrease) could possibly be used to achieve resolution. Buffer in *sys A* showed consistent trends.

**Table 4.2. Summary of comparison**

Hot Side Temp. (actual) °C	<i>Sys A: 0.5 M Tris-borate/20 mM NaCl, pH=8.29</i>		<i>Sys B: 50mM Tricine-NaOH/ 20 mM NaCl, pH= 9.00</i>	
	@ 300 V/cm (trend)	@ 1000 V/cm (trend)	@ 350 V/cm (trend)	@ 500 V/cm (trend)
80 (73.55)	GCWT-Mix- WT	GCWT/Mix- WT	GCWT- Mix- WT	GCWT- WT-Mix
75 (69.09)	GCWT-Mix- WT	GCWT/Mix- WT	skip	GCWT- WT-Mix
70 (64.63)	GCWT-Mix- WT	GCWT/Mix- WT	GCWT- Mix- WT	GCWT- WT-Mix
65(60.16)	GCWT-Mix- WT	GCWT- Mix- WT	GCWT- Mix- WT	GCWT- WT-Mix
60 (55.70)	GCWT-Mix- WT	GCWT- Mix- WT	GCWT- Mix- WT	GCWT- WT-Mix
55 (51.24)	GCWT-Mix- WT	GCWT- Mix- WT	FT	GCWT/ WT-Mix
50 (46.78)	GCWT-Mix- WT	GCWT- Mix- WT	No peak	GCWT/ WT-Mix
45 (42.31)	GCWT-Mix- WT	GCWT- Mix- WT	-	-
40 (37.85)	Mix(FT) - GCWT( FT)-WT	GCWT(FT)- Mix- WT	-	-

#### 4.5.6. Separation in BSA

Electrophoretic exclusion of molecules from separation channel using counterflow<sup>67</sup> provides a platform for analyzing biological samples. Bovine serum albumin (BSA), a high molecular weight, low mobility protein, has been used in many biological assays as a standard because of its purity and binding specificity. Here, the low mobility of BSA is exploited in an effort to improve reproducibility and repeatability in migration time, peak identity of DNA oligonucleotides being analyzed, also in resolution of strands in mixture. Similar to TGF counterflow rejection method,<sup>67</sup> a high enough counterflow is used to exclude BSA from the separation channel so that only DNA sample to be analyzed enters the column. Experimental conditions were determined after preliminary runs; focusing position was on the hot side prior to each run. A steep gradient of 55/20 °C was used for all runs under constant run conditions. Counterflow was held at 1400 Pa with acceleration rate of -10 Pa/s; a field strength of -600 V/cm was applied at the sample reservoir. Repeated analysis of samples: 10 nM GCWT, 10 nM WT and 5 nM mixture GCWT/WT, respectively, prepared in BSA of concentration ranging from 250 nM to 200 µM were performed in background buffer containing 0.5 M Tris borate balance with 20 mM NaCl to pH 8.3. Figure 4.2 shows a consistent migration order: *10nM GCWT-5nM Mix-10nM WT* for all runs; however, a fluctuation in the migration time under 7 minutes was observed for each particular strand. In Fig. 4.6B, multiple peak profiles were observed at high concentration (50-200 µM) of BSA. At lower concentration 1µM, and 250 nM, respectively, the mixture sample showed a slight resolution. Peak identification in mixture was not possible due to the large difference in

migration time for individual sample. Overall for all consecutive runs a shifts in migration time was observed.

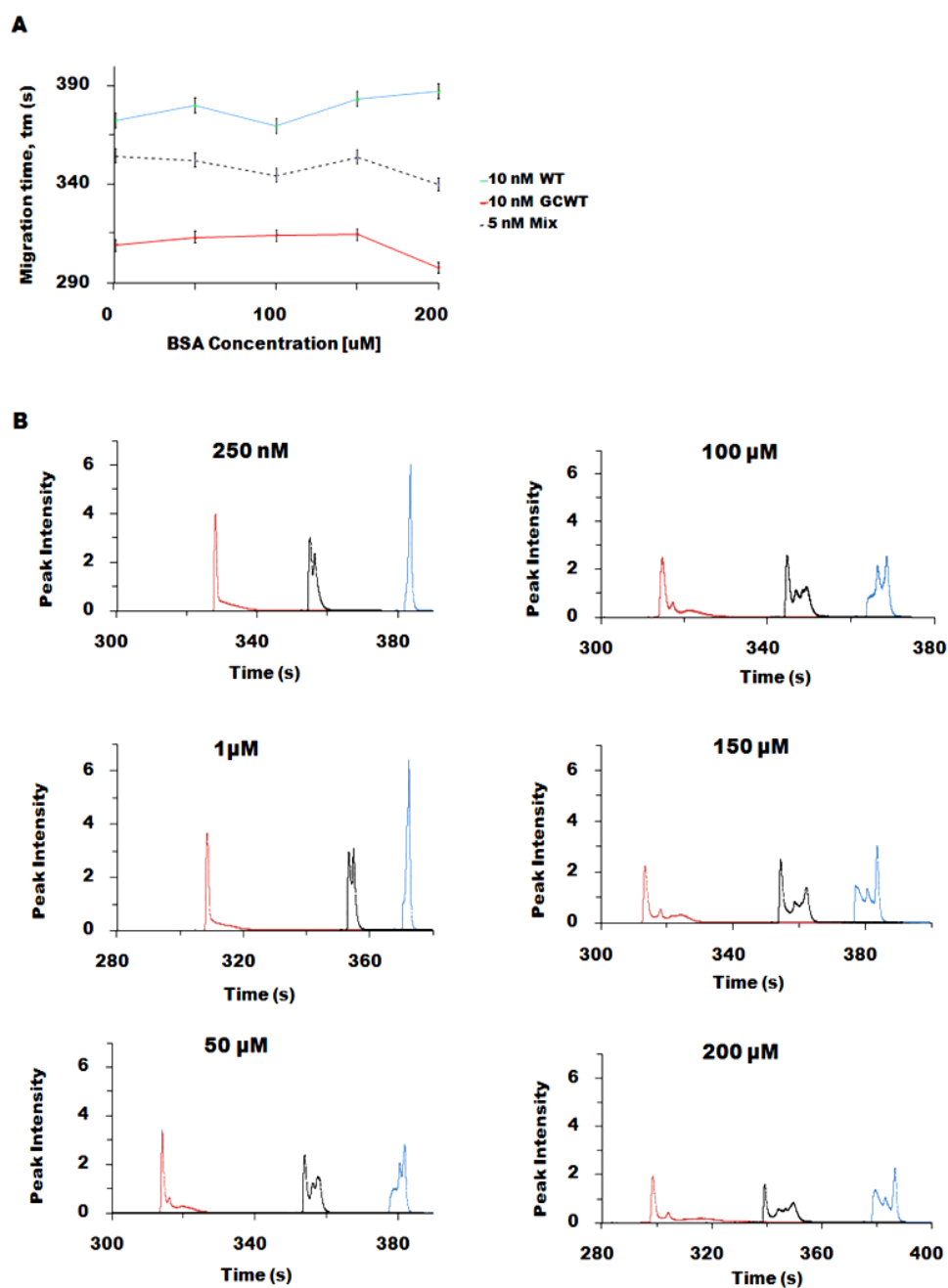


**Figure 4.5.** Separation in BSA. **A.** Plot of migration time versus concentration of BSA. **B.** Example electropherogram of 10 nM WT\*/Wt-24mer, 10 nM GCWT\*/gcwt-24mer, and 5 nM mixture of strands prepared in different concentrations of BSA (250 nM, 1, 50, 100, 150, and 200- $\mu\text{M}$ ): Focusing was on the hot side at 55/20  $^{\circ}\text{C}$  temperature gradient. Experiment was conducted on 7.0 cm capillary (25  $\mu\text{m}$  i. d.) at constant: -10 Pa/s acceleration, start  $\Delta P = 1400$  Pa, and -600 V/cm field strength; PMT = 0.475V. Running buffer was 0.5 M Tris borate balance with 20 mM NaCl to pH 8.3.

#### 4.5.7. Hardware modification

In addition to experimental operating procedures evaluation, some modifications were made to the hardware to address reproducibility issues. As shown in Fig. 4.6, larger volume pressure blocks and non-PMMA material were considered. The standard  $\Delta P$  block (#1) made from PMMA material was used in all laboratory hardware. Pressure block (#2) incorporates standard  $\Delta P$  block cured with 3 ml glass vial to allow easy replacement of buffer without readjust capillary alignment; entire block held up to 4 ml volume. Pressure block (#3) was a large volume (6 ml) reservoir to prevent possible precipitation at electrode as result of electrolysis of solution which could potentially cause arcing. Adjustable stage pressure block (#4) allows both large volume (3 ml) and longer capillary. Evaluation of  $\Delta P$  block compared to standard  $\Delta P$  block showed no difference in reproducibility; thus, the results presented only reflect the standard  $\Delta P$  block (#1).

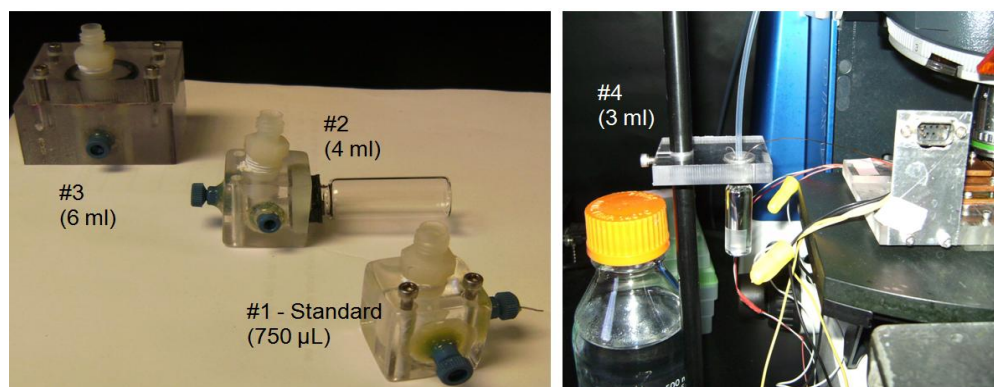


**Figure 4.6.** Generations of pressure blocks. #1: Standard  $\Delta P$  block, PMMA material; holds between 750-860  $\mu\text{L}$  volume; #2: standard  $\Delta P$  block cured with glass vial, 4 ml in volume; #3: 6 ml large volume reservoir, non-PMMA material; #4: stage vial attached to 20 cm (25  $\mu\text{m}$  i. d.) capillary.

#### 4.6. Conclusion

This work is a first demonstration of high level detection of synthetic 24mer DNA on a short length microcolumn using the TGDF method. On major difference compared the TGGE and DGGE is the exclusion of gel matrix effect. The TGDF method use counterflow to focus DNA undergoing conformational changes on a thermal separation column. High resolution detection of DNA is shown in a variety of matrices. Major drawbacks of the technique in ultimately achieving separation are repeatable for consecutive runs and irreproducibility in peak profile enrichment, migration time and migration order for same buffer, and validation of experimental conditions from day-to-day. The challenge remains in determining a suitable buffer and experimental condition for analysis. Although not shown, a number of peak identification experiments were conducted to determine whether the secondary peak generally observed was due to the dsDNA/duplex state or buffer system used. Preliminary experimental studies including varying ratio of label to unlabeled strand, different combinations and concentration of DNA strands, spiking, changing acceleration rate, changing temperature gradient, changing focusing point on column, and buffer components (including polymer).

Although focusing was achieved for 24-mer synthetic DNA (ss, homo- and hetero-duplexes), the results presented here are inconclusive. The evaluation of this work can be used for future studies of complex matrices. Future work can consider strands with significant difference in molecular weight, and melting temperature and using strands with different fluorescent probes to follow conformational changes along the column. Development of a suitable assay for the simultaneous enrichment and separation of synthetic DNA using the TGDF method has high potential for studying gene mutation

which could be easily transferred to microfluidic devices for multiplexing, and obtaining faster, sensitive detection.

#### 4.7. References Cited

1. Eisenberg, D.; Marcotte, E. M.; Xenarios, I.; Yeates, T. O. *Nature* **2000**, *405*, 823-826.
2. Ratain, M. J.; Relling, M. V. *Nat. Med.* **2001**, *7*, 283-285.
3. Peltonen, L.; McKusick, V. A. *Science* **2001**, *291*, 1224-1229.
4. Butcher, S. P. *Neurochem. Res.* **2003**, *28*, 367-371.
5. International HapMap Consortium; Frazer, K. A. ; Ballinger, D. G.; Cox, D. R.; Hinds, D. A.; Stuve, L. L.; Gibbs, R. A.; Belmont, J. W.; Boudreau, A.; Hardenbol, P.; Leal, S. M.; Pasternak, S.; Wheeler, D. A.; Willis, T. D.; Yu, F.; Yang, H.; Zeng, C.; Gao, Y.; Hu, H.; Hu, W.; Li, C.; Lin, W.; Liu, S.; Pan, H.; Tang, X.; Wang, J.; Wang, W.; Yu, J.; Zhang, B.; Zhang, Q.; Zhao, H.; Zhao, H.; Zhou, J.; Gabriel, S. B.; Barry, R.; Blumenstiel, B.; Camargo, A.; Defelice, M.; Faggart, M.; Goyette, M.; Gupta, S.; Moore, J.; Nguyen, H.; Onofrio, R. C.; Parkin, M.; Roy, J.; Stahl, E.; Winchester, E.; Ziaugra, L.; Altshuler, D.; Shen, Y.; Yao, Z.; Huang, W.; Chu, X.; He, Y.; Jin, L.; Liu, Y.; Shen, Y.; Sun, W.; Wang, H.; Wang, Y.; Wang, Y.; Xiong, X.; Xu, L.; Wayne, M. M.; Tsui, S. K.; Xue, H.; Wong, J. T.; Galver, L. M.; Fan, J. B.; Gunderson, K.; Murray, S. S.; Oliphant, A. R.; Chee, M. S.; Montpetit, A.; Chagnon, F.; Ferretti, V.; Leboeuf, M.; Olivier, J. F.; Phillips, M. S.; Roumy, S.; Sallee, C.; Verner, A.; Hudson, T. J.; Kwok, P. Y.; Cai, D.; Koboldt, D. C.; Miller, R. D.; Pawlikowska, L.; Taillon-Miller, P.; Xiao, M.; Tsui, L. C.; Mak, W.; Song,

Y. Q.; Tam, P. K.; Nakamura, Y.; Kawaguchi, T.; Kitamoto, T.; Morizono, T.; Nagashima, A.; Ohnishi, Y.; Sekine, A.; Tanaka, T.; Tsunoda, T.; Deloukas, P.; Bird, C. P.; Delgado, M.; Dermitzakis, E. T.; Gwilliam, R.; Hunt, S.; Morrison, J.; Powell, D.; Stranger, B. E.; Whittaker, P.; Bentley, D. R.; Daly, M. J.; de Bakker, P. I.; Barrett, J.; Chretien, Y. R.; Maller, J.; McCarroll, S.; Patterson, N.; Pe'er, I.; Price, A.; Purcell, S.; Richter, D. J.; Sabeti, P.; Saxena, R.; Schaffner, S. F.; Sham, P. C.; Varilly, P.; Altshuler, D.; Stein, L. D.; Krishnan, L.; Smith, A. V.; Tello-Ruiz, M. K.; Thorisson, G. A.; Chakravarti, A.; Chen, P. E.; Cutler, D. J.; Kashuk, C. S.; Lin, S.; Abecasis, G. R.; Guan, W.; Li, Y.; Munro, H. M.; Qin, Z. S.; Thomas, D. J.; McVean, G.; Auton, A.; Bottolo, L.; Cardin, N.; Eyheramendy, S.; Freeman, C.; Marchini, J.; Myers, S.; Spencer, C.; Stephens, M.; Donnelly, P.; Cardon, L. R.; Clarke, G.; Evans, D. M.; Morris, A. P.; Weir, B. S.; Tsunoda, T.; Mullikin, J. C.; Sherry, S. T.; Feolo, M.; Skol, A.; Zhang, H.; Zeng, C.; Zhao, H.; Matsuda, I.; Fukushima, Y.; Macer, D. R.; Suda, E.; Rotimi, C. N.; Adebamowo, C. A.; Ajayi, I.; Aniagwu, T.; Marshall, P. A.; Nkwodimmah, C.; Royal, C. D.; Leppert, M. F.; Dixon, M.; Peiffer, A.; Qiu, R.; Kent, A.; Kato, K.; Niikawa, N.; Adewole, I. F.; Knoppers, B. M.; Foster, M. W.; Clayton, E. W.; Watkin, J.; Gibbs, R. A.; Belmont, J. W.; Muzzy, D.; Nazareth, L.; Sodergren, E.; Weinstock, G. M.; Wheeler, D. A.; Yakub, I.; Gabriel, S. B.; Onofrio, R. C.; Richter, D. J.; Ziaugra, L.; Birren, B. W.; Daly, M. J.; Altshuler, D.; Wilson, R. K.; Fulton, L. L.; Rogers, J.; Burton, J.; Carter, N. P.; Clee, C. M.; Griffiths, M.; Jones, M. C.; McLay, K.; Plumb, R. W.; Ross, M. T.; Sims, S. K.; Willey, D. L.; Chen, Z.; Han, H.; Kang, L.; Godbout, M.; Wallenburg, J. C.; L'Archeveque, P.; Bellemare, G.; Saeki, K.; Wang,

- H.; An, D.; Fu, H.; Li, Q.; Wang, Z.; Wang, R.; Holden, A. L.; Brooks, L. D.; McEwen, J. E.; Guyer, M. S.; Wang, V. O.; Peterson, J. L.; Shi, M.; Spiegel, J.; Sung, L. M.; Zacharia, L. F.; Collins, F. S.; Kennedy, K.; Jamieson, R.; Stewart, J. *Nature* **2007**, *449*, 851-861.
6. Kwok, P. Y.; Gu, Z. *Mol. Med. Today* **1999**, *5*, 538-543.
  7. Cargill, M.; Altshuler, D.; Ireland, J.; Sklar, P.; Ardlie, K.; Patil, N.; Shaw, N.; Lane, C. R.; Lim, E. P.; Kalyanaraman, N.; Nemesh, J.; Ziaugra, L.; Friedland, L.; Rolfe, A.; Warrington, J.; Lipshutz, R.; Daley, G. Q.; Lander, E. S. *Nat. Genet.* **1999**, *22*, 231-238.
  8. Wang, Z.; Moulton, J. *Hum. Mutat.* **2001**, *17*, 263-270.
  9. Kim, S.; Misra, A. *Annu. Rev. Biomed. Eng.* **2001**, *9*, 289-320.
  10. Venter, J. C.; Adams, M. D.; Myers, E. W.; Li, P. W.; Mural, R. J.; Sutton, G. G.; Smith, H. O.; Yandell, M.; Evans, C. A.; Holt, R. A.; Gocayne, J. D.; Amanatides, P.; Ballew, R. M.; Huson, D. H.; Wortman, J. R.; Zhang, Q.; Kodira, C. D.; Zheng, X. H.; Chen, L.; Skupski, M.; Subramanian, G.; Thomas, P. D.; Zhang, J.; Gabor Miklos, G. L.; Nelson, C.; Broder, S.; Clark, A. G.; Nadeau, J.; McKusick, V. A.; Zinder, N.; Levine, A. J.; Roberts, R. J.; Simon, M.; Slayman, C.; Hunkapiller, M.; Bolanos, R.; Delcher, A.; Dew, I.; Fasulo, D.; Flanigan, M.; Florea, L.; Halpern, A.; Hannenhalli, S.; Kravitz, S.; Levy, S.; Mobarry, C.; Reinert, K.; Remington, K.; Abu-Threideh, J.; Beasley, E.; Biddick, K.; Bonazzi, V.; Brandon, R.; Cargill, M.; Chandramouliswaran, I.; Charlab, R.; Chaturvedi, K.; Deng, Z.; Di Francesco, V.; Dunn, P.; Eilbeck, K.; Evangelista, C.; Gabrielian, A. E.; Gan, W.; Ge, W.; Gong, F.; Gu, Z.; Guan, P.; Heiman, T. J.; Higgins, M. E.; Ji, R. R.; Ke, Z.; Ketchum, K.

A.; Lai, Z.; Lei, Y.; Li, Z.; Li, J.; Liang, Y.; Lin, X.; Lu, F.; Merkulov, G. V.; Milshina, N.; Moore, H. M.; Naik, A. K.; Narayan, V. A.; Neelam, B.; Nusskern, D.; Rusch, D. B.; Salzberg, S.; Shao, W.; Shue, B.; Sun, J.; Wang, Z.; Wang, A.; Wang, X.; Wang, J.; Wei, M.; Wides, R.; Xiao, C.; Yan, C.; Yao, A.; Ye, J.; Zhan, M.; Zhang, W.; Zhang, H.; Zhao, Q.; Zheng, L.; Zhong, F.; Zhong, W.; Zhu, S.; Zhao, S.; Gilbert, D.; Baumhueter, S.; Spier, G.; Carter, C.; Cravchik, A.; Woodage, T.; Ali, F.; An, H.; Awe, A.; Baldwin, D.; Baden, H.; Barnstead, M.; Barrow, I.; Beeson, K.; Busam, D.; Carver, A.; Center, A.; Cheng, M. L.; Curry, L.; Danaher, S.; Davenport, L.; Desilets, R.; Dietz, S.; Dodson, K.; Doup, L.; Ferriera, S.; Garg, N.; Gluecksmann, A.; Hart, B.; Haynes, J.; Haynes, C.; Heiner, C.; Hladun, S.; Hostin, D.; Houck, J.; Howland, T.; Ibegwam, C.; Johnson, J.; Kalush, F.; Kline, L.; Koduru, S.; Love, A.; Mann, F.; May, D.; McCawley, S.; McIntosh, T.; McMullen, I.; Moy, M.; Moy, L.; Murphy, B.; Nelson, K.; Pfannkoch, C.; Pratts, E.; Puri, V.; Qureshi, H.; Reardon, M.; Rodriguez, R.; Rogers, Y. H.; Romblad, D.; Ruhfel, B.; Scott, R.; Sitter, C.; Smallwood, M.; Stewart, E.; Strong, R.; Suh, E.; Thomas, R.; Tint, N. N.; Tse, S.; Vech, C.; Wang, G.; Wetter, J.; Williams, S.; Williams, M.; Windsor, S.; Winn-Deen, E.; Wolfe, K.; Zaveri, J.; Zaveri, K.; Abril, J. F.; Guigo, R.; Campbell, M. J.; Sjolander, K. V.; Karlak, B.; Kejariwal, A.; Mi, H.; Lazareva, B.; Hatton, T.; Narechania, A.; Diemer, K.; Muruganujan, A.; Guo, N.; Sato, S.; Bafna, V.; Istrail, S.; Lippert, R.; Schwartz, R.; Walenz, B.; Yooseph, S.; Allen, D.; Basu, A.; Baxendale, J.; Blick, L.; Caminha, M.; Carnes-Stine, J.; Caulk, P.; Chiang, Y. H.; Coyne, M.; Dahlke, C.; Mays, A.; Dombroski, M.; Donnelly, M.; Ely, D.; Esparham, S.; Fosler, C.; Gire, H.; Glanowski, S.; Glasser, K.; Glodek, A.;

- Gorokhov, M.; Graham, K.; Gropman, B.; Harris, M.; Heil, J.; Henderson, S.; Hoover, J.; Jennings, D.; Jordan, C.; Jordan, J.; Kasha, J.; Kagan, L.; Kraft, C.; Levitsky, A.; Lewis, M.; Liu, X.; Lopez, J.; Ma, D.; Majoros, W.; McDaniel, J.; Murphy, S.; Newman, M.; Nguyen, T.; Nguyen, N.; Nodell, M.; Pan, S.; Peck, J.; Peterson, M.; Rowe, W.; Sanders, R.; Scott, J.; Simpson, M.; Smith, T.; Sprague, A.; Stockwell, T.; Turner, R.; Venter, E.; Wang, M.; Wen, M.; Wu, D.; Wu, M.; Xia, A.; Zandieh, A.; Zhu, X. *Science* **2001**, *291*, 1304-1351.
11. Brookes, A. J. *Gene* **1999**, *234*, 177-186.
  12. Waterfall, C. M.; Cobb, B. D. *Nucleic Acids Res.* **2001**, *29*, E119.
  13. Kan, Y. W.; Dozy, A. M. *Proc. Natl. Acad. Sci. U. S. A.* **1978**, *75*, 5631-5635.
  14. Kieseewetter, S.; Macek, M., Jr.; Davis, C.; Curristin, S. M.; Chu, C. S.; Graham, C.; Shrimpton, A. E.; Cashman, S. M.; Tsui, L. C.; Mickle, J. *Nat. Genet.* **1993**, *5*, 274-278.
  15. Kerem, E.; Corey, M.; Kerem, B. S.; Rommens, J.; Markiewicz, D.; Levison, H.; Tsui, L. C.; Durie, P. N. *Engl. J. Med.* **1990**, *323*, 1517-1522.
  16. Medintz, I.; Wong, W. W.; Berti, L.; Shiow, L.; Tom, J.; Scherer, J.; Sensabaugh, G.; Mathies, R. A. *Genome Res.* **2001**, *11*, 413-421.
  17. Jazwinska, E. C.; Powell, L. W. *Hepatology* **1997**, *25*, 495-496.
  18. Ward, C. P.; Fensom, A. H.; Green, P. M. *Genet. Test.* **2000**, *4*, 351-358.
  19. Navon, R.; Proia, R. L. *Science* **1989**, *243*, 1471-1474.
  20. Shen, Y.; Wu, B. L. *Clin. Chem.* **2009**, *55*, 659-669.
  21. Hengen, P. N. *Trends Biochem. Sci.* **1995**, *20*, 324-325.
  22. Eckert, K. A.; Kunkel, T. A. *PCR Methods Appl.* **1991**, *1*, 17-24.

23. Kan, C. W.; Fredlake, C. P.; Doherty, E. A.; Barron, A. E. *Electrophoresis* **2004**, *25*, 3564-3588.
24. Pettersson, E.; Lundeberg, J.; Ahmadian, A. *Genomics* **2009**, *93*, 105-111.
25. Collins, F. S.; Morgan, M.; Patrinos, A. *Science* **2003**, *300*, 286-290.
26. Collins, F. S.; Patrinos, A.; Jordan, E.; Chakravarti, A.; Gesteland, R.; Walters, L. R. *Science* **1998**, *282*, 682-689.
27. Andersen, P. S.; Jespersgaard, C.; Vuust, J.; Christiansen, M.; Larsen, L. A. *Hum. Mutat.* **2003**, *21*, 455-465.
28. Kakavas, V. K.; Plageras, P.; Vlachos, T. A.; Papaioannou, A.; Noulas, V. A. *Mol. Biotechnol.* **2008**, *38*, 155-163.
29. Orita, M.; Suzuki, Y.; Sekiya, T.; Hayashi, K. *Genomics* **1989**, *5*, 874-879.
30. Nataraj, A. J.; Olivos-Glander, I.; Kusukawa, N.; Highsmith, W. E., Jr. *Electrophoresis* **1999**, *20*, 1177-1185.
31. White, M. B.; Carvalho, M.; Derse, D.; O'Brien, S. J.; Dean, M. *Genomics* **1992**, *12*, 301-306.
32. Hestekin, C. N.; Barron, A. E. *Electrophoresis* **2006**, *27*, 3805-3815.
33. Wartell, R. M.; Hosseini, S.; Powell, S.; Zhu, J. *J. Chromatogr. A* **1998**, *806*, 169-185.
34. Gianazza, E.; Eberini, I.; Santi, O.; Vignati, M. *Anal. Chim. Acta* **1989**, *372*, 99-120.
35. Fischer, S. G.; Lerman, L. S. *Cell* **1979**, *16*, 191-200.
36. Riesner, D.; Steger, G.; Zimmat, R.; Owens, R. A.; Wagenhofer, M.; Hillen, W.; Vollbach, S.; Henco, K. *Electrophoresis* **1989**, *10*, 377-389.

37. Ekstrom, P. O.; BJORHEIM, J.; THILLY, W. G. *BMC Genet.* **2007**, *8*, 54.
38. BJORHEIM, J.; GAUDERNACK, G.; GIERCKSKY, K. E.; EKSTROM, P. O. *Electrophoresis* **2003**, *24*, 63-69.
39. HINSELWOOD, D. C.; ABRAHAMSEN, T. W.; EKSTROM, P. O. *Electrophoresis* **2005**, *26*, 2553-2561.
40. HINSELWOOD, D. C.; WARREN, D. J.; EKSTROM, P. O. *Electrophoresis* **2005**, *26*, 2562-2566.
41. EKSTROM, P. O.; KHRAPKO, K.; LI-SUCHOLEIKI, X. C.; HUNTER, I. W.; THILLY, W. G. *Nat. Protoc.* **2008**, *3*, 1153-1166.
42. MINARIK, M.; BENESOVA, L.; FANTOVA, L.; HORACEK, J.; HERACEK, J.; LOUKOLA, A. *Electrophoresis* **2006**, *27*, 3856-3863.
43. EKSTROM, P. O.; BJORHEIM, J. *Electrophoresis* **2006**, *27*, 1878-1885.
44. HSIA, A. P.; WEN, T. J.; CHEN, H. D.; LIU, Z.; YANDEAU-NELSON, M. D.; WEI, Y.; GUO, L.; SCHNABLE, P. S. *Theor. Appl. Genet.* **2005**, *111*, 218-225.
45. CHOU, L. S.; GEDGE, F.; LYON, E. *J. Mol. Diagn.* **2005**, *7*, 111-120.
46. ZHU, L.; LEE, H. K.; LIN, B.; YEUNG, E. S. *Electrophoresis* **2001**, *22*, 3683-3687.
47. SCHELL, J.; WULFERT, M.; RIESNER, D. *Electrophoresis* **1999**, *20*, 2864-2869.
48. FUNG, E. N.; PANG, H. M.; YEUNG, E. S. *J. Chromatogr. A* **1998**, *806*, 157-164.
49. RIGHETTI, P. G.; GELFI, C. *J. Chromatogr. B Biomed. Sci. Appl.* **1997**, *697*, 195-205.
50. GELFI, C.; RIGHETTI, P. G.; TRAVI, M.; FATTORE, S. *Electrophoresis* **1997**, *18*, 724-731.
51. GELFI, C.; CREMONESI, L.; FERRARI, M.; RIGHETTI, P. G. *BioTechniques* **1996**, *21*, 926-930, 932.

52. Gelfi, C.; Righetti, P. G.; Cremonesi, L.; Ferrari, M. *Electrophoresis* **1994**, *15*, 1506-1511.
53. Buch, J. S.; Rosenberger, F.; Highsmith, W. E., Jr.; Kimball, C.; DeVoe, D. L.; Lee, C. S. *Lab. Chip* **2005**, *5*, 392-400.
54. Buch, J. S.; Kimball, C.; Rosenberger, F.; Highsmith, W. E., Jr.; DeVoe, D. L.; Lee, C. S. *Anal. Chem.* **2004**, *76*, 874-881.
55. Zhang, H. D.; Zhou, J.; Xu, Z. R.; Song, J.; Dai, J.; Fang, J.; Fang, Z. L. *Lab. Chip* **2007**, *7*, 1162-1170.
56. Giddings, J. C. *Unified Separation Science*, Wiley, New York, 1991.
57. Landers, J. P. *Handbook of Capillary Electrophoresis, 2nd ed.*, CRC Press, Boca Raton, 1997.
58. Ivory, C. F. *Electrophoresis* **2007**, *28*, 15-28.
59. Ivory, C. F. *Sep. Sci. Technol.* **2000**, *35*, 1777-1793.
60. O'farrell, P. H. *Science* **1985**, *227*, 1586-1589.
61. Wang, Q.; Tolley, H. D.; LeFebvre, D. A.; Lee, M. L. *Anal. Bioanal. Chem.* **2002**, *373*, 125-135.
62. Shackman, J. G.; Ross, D. *Electrophoresis* **2007**, *28*, 556-571.
63. Ross, D.; Locascio, L. E. *Anal. Chem.* **2002**, *74*, 2556-2564.
64. Shackman, J. G.; Watson, C. J.; Kennedy, R. T. *J. Chromatogr. A* **2004**, *1040*, 273-282.
65. Balss, K. M.; Ross, D.; Begley, H. C.; Olsen, K. G.; Tarlov, M. J. *J. Am. Chem. Soc.* **2004**, *126*, 13474-13479.

66. Hoebel, S. J.; Balss, K. M.; Jones, B. J.; Malliaris, C. D.; Munson, M. S.; Vreeland, W. N.; Ross, D. *Anal. Chem.* **2006**, *78*, 7186-7190.
67. Munson, M. S.; Meacham, J. M.; Locascio, L. E.; Ross, D. *Anal. Chem.* **2008**, *80*, 172-178.

**BIBLIOGRAPHY**

1. Acevedo, F. J. *Chromatogr. A* **1991**, *545*, 391-396.
2. Andersen, P. S.; Jespersgaard, C.; Vuust, J.; Christiansen, M.; Larsen, L. A. *Hum. Mutat.* **2003**, *21*, 455-465.
3. Bada, J. L.; Glavin, D. P.; McDonald, G. D.; Becker, L. *Science* **1998**, *279*, 362-365.
4. Baker, D. R. *Capillary Electrophoresis*, John Wiley & Sons, Inc.: New York, NY; **1995**.
5. Balss, K. M.; Ross, D.; Begley, H. C.; Olsen, K. G.; Tarlov, M. J. *J. Am. Chem. Soc.* **2004**, *126*, 13474-13479.
6. Balss, K. M.; Vreeland, W. N.; Howell, P. B.; Henry, A. C.; Ross, D. *J. Am. Chem. Soc.* **2004**, *126*, 1936-1937.
7. Balss, K. M.; Vreeland, W. N.; Phinney, K. W.; Ross, D. *Anal. Chem.* **2004**, *76*, 7243-7249.
8. Bayle, C.; Siri, N.; Poinso, V.; Treilhou, M.; Causse, E.; Couderc, F. *J. Chromatogr. A* **2003**, *1013*, 123-130.
9. Becker, M.; Mansouri, A.; Beilein, C.; Janasek, D. *Electrophoresis* **2009**, *30*, 4206-4212.
10. Beckers, J. L.; Bocek, P. *Electrophoresis* **2000**, *21*, 2747-2767.
11. Bercovici, M.; Kaigala, G. V.; Santiago, J. G. *Anal. Chem.* **2010**, *82*, 2134-2138.
12. Bergmann, J.; Jaehde, U.; Schunack, W. *Electrophoresis* **1998**, *19*, 305-310.

13. Bjorheim, J.; Gaudernack, G.; Giercksky, K. E.; Ekstrom, P. O. *Electrophoresis* **2003**, *24*, 63-69.
14. Bocek, P., Deml, M., Gebauer, P. and Dolnik, V. *Analytical Isotachopheresis*, VCH: New York; **1988**.
15. Breadmore, M. C.; Thabano, J. R.; Dawod, M.; Kazarian, A. A.; Quirino, J. P.; Guijt, R. M. *Electrophoresis* **2009**, *30*, 230-248.
16. Breadmore, M. C. *Electrophoresis* **2007**, *28*, 254-281.
17. Breadmore, M. C.; Quirino, J. P. *Anal. Chem.* **2008**, *80*, 6373-6381.
18. Brookes, A. J. *Gene* **1999**, *234*, 177-186.
19. Bruno, T. J. *Chromatographic and Electrophoretic Methods*, Prentice Hall: Englewood Cliffs, NJ; **1991**.
20. Buch, J. S.; Kimball, C.; Rosenberger, F.; Highsmith, W. E., Jr.; DeVoe, D. L.; Lee, C. S. *Anal. Chem.* **2004**, *76*, 874-881.
21. Buch, J. S.; Rosenberger, F.; Highsmith, W. E., Jr.; Kimball, C.; DeVoe, D. L.; Lee, C. S. *Lab. Chip* **2005**, *5*, 392-400.
22. Busnel, J. M.; Descroix, S.; Godfrin, D.; Hennion, M. C.; Kasicka, V.; Peltre, G. *Electrophoresis* **2006**, *27*, 3591-3598.
23. Butcher, S. P. *Neurochem. Res.* **2003**, *28*, 367-371.
24. Cao, C. X.; Zheng, Q. S.; Chen, W. K.; Zhu, J. H. *J. Chromatogr. A* **1999**, *863*, 219-226.
25. Cargill, M.; Altshuler, D.; Ireland, J.; Sklar, P.; Ardlie, K.; Patil, N.; Shaw, N.; Lane, C. R.; Lim, E. P.; Kalyanaraman, N.; Nemesh, J.; Ziaugra, L.; Friedland, L.;

- Rolfe, A.; Warrington, J.; Lipshutz, R.; Daley, G. Q.; Lander, E. S. *Nat. Genet.* **1999**, *22*, 231-238.
26. Castro-Puyana, M.; Crego, A. L.; Marina, M. L. *Electrophoresis.* **2010**, *31*, 229-250.
27. Chartogne, A.; Reeuwijk, B.; Hofte, B.; van der Heijden, R.; Tjaden, U. R.; van der Greef, J. *J.Chromatogr. A* **2002**, *959*, 289-298.
28. Chen, L.; Prest, J. E.; Fielden, P. R.; Goddard, N. J.; Manz, A.; Day, P. J. *Lab. Chip* **2006**, *6*, 474-487.
29. Chen, S.; Lee, M. L. *Anal. Chem.* **1998**, *70*, 3777-3780.
30. Chiesl, T. N.; Chu, W. K.; Stockton, A. M.; Amashukeli, X.; Grunthaner, F.; Mathies, R. A. *Anal. Chem.* **2009**, *81*, 2537-2544.
31. Chou, L. S.; Gedge, F.; Lyon, E. *J. Mol. Diagn.* **2005**, *7*, 111-120.
32. Chu, Q.; Guan, Y.; Geng, C.; Ye, J. *Anal. Lett.* **2006**, *39*, 729-749.
33. Cohen, A. S.; Karger, B. L. *J. Chromatogr.* **1987**, *397*, 409-417.
34. Collins, F. S.; Morgan, M.; Patrinos, A. *Science* **2003**, *300*, 286-290.
35. Collins, F. S.; Patrinos, A.; Jordan, E.; Chakravarti, A.; Gesteland, R.; Walters, L. *Science* **1998**, *282*, 682-689.
36. Culbertson, C. T.; Jorgenson, J. W. *Anal. Chem.* **1994**, *66*, 955-962.
37. Danger, G.; Ross, D. *Electrophoresis* **2008**, *29*, 3107-3114.
38. Dankova, M.; Kaniansky, D.; Fanali, S.; Ivanyi, F. *J.Chromatogr. A* **1999**, *838*, 31-43.
39. Davis, N. I.; Mamunooru, M.; Vyas, C. A.; Shackman, J. G. *Anal.Chem.* **2009**, *81*, 5452-5459.

40. Dolnik, V. *Electrophoresis* **2008**, *29*, 143-156.
41. Eckert, K. A.; Kunkel, T. A. *PCR Methods Appl.* **1991**, *1*, 17-24.
42. Eisenberg, D.; Marcotte, E. M.; Xenarios, I.; Yeates, T. O. *Nature* **2000**, *405*, 823-826.
43. Ekstrom, P. O.; Bjorheim, J. *Electrophoresis* **2006**, *27*, 1878-1885.
44. Ekstrom, P. O.; Bjorheim, J.; Thilly, W. G. *BMC Genet.* **2007**, *8*, 54.
45. Ekstrom, P. O.; Khrapko, K.; Li-Sucholeiki, X. C.; Hunter, I. W.; Thilly, W. G. *Nat. Protoc.* **2008**, *3*, 1153-1166.
46. Everaerts, F. M.; Vacik, J.; Verheggen, T. P. E. M.; Zuska, J. *J. Chromatogr. A.* **1970**, *49*, 262-268.
47. Everaerts, F. M.; Vacik, J.; Verheggen, Th. P. E. M.; Zuska, J. *J. Chromatogr. A.* **1971**, *60*, 397-405.
48. Everaerts, F. M.; Verheggen, T. P. E. M.; van de Venne, J. L. M. *J. Chromatogr. A.* **1976**, *123*, 139-148.
49. Fang, X.; Wang, W.; Yang, L.; Chandrasekaran, K.; Kristian, T.; Balgley, B. M.; Lee, C. S. *Electrophoresis* **2008**, *29*, 2215-2223.
50. Fischer, S. G.; Lerman, L. S. *Cell* **1979**, *16*, 191-200.
51. Flanigan, P. M.; Ross, D.; Shackman, J. G. *Electrophoresis* **2010**, *31*, 3466-3474.
52. Fu, L. M.; Leong, J. C.; Lin, C. F.; Tai, C. H.; Tsai, C. H. *Biomed. Microdevices* **2007**, *9*, 405-412.
53. Fung, E. N.; Pang, H. M.; Yeung, E. S. *J. Chromatogr. A.* **1998**, *806*, 157-164.
54. Gareil, P. *Chromatographia* **1990**, *30*, 195-200.
55. Gebauer, P.; Mala, Z.; Bocek, P. *Electrophoresis* **2007**, *28*, 26-32.

56. Gebauer, P.; Bocek, P. *Electrophoresis* **2002**, *23*, 3858-3864.
57. Gebauer, P.; Bocek, P. *Electrophoresis* **2000**, *21*, 3898-3904.
58. Gebauer, P.; Mala, Z.; Bocek, P. *Electrophoresis* **2009**, *30*, 29-35.
59. Gelfi, C.; Cremonesi, L.; Ferrari, M.; Righetti, P. G. *BioTechniques* **1996**, *21*, 926-28, 930, 932.
60. Gelfi, C.; Righetti, P. G.; Cremonesi, L.; Ferrari, M. *Electrophoresis* **1994**, *15*, 1506-1511.
61. Gelfi, C.; Righetti, P. G.; Travi, M.; Fattore, S. *Electrophoresis* **1997**, *18*, 724-731.
62. Ghowsi, K.; Foley, J. P.; Gale, R. J. *Anal. Chem.* **1990**, *30*, 195-200.
63. Gianazza, E.; Eberini, I.; Santi, O.; Vignati, M. *Anal. Chim. Acta.* **1989**, *372*, 99-120.
64. Giddings, J. C. *Unified Separation Science*, John Wiley & Sons, Inc.: New York; 1991.
65. Giddings, J. C.; Dahlgren, K. *Sep. Sci. Technol.* **1971**, *6*, 345-356.
66. Glavin, D. P.; Schubert, M.; Botta, O.; Kminek, G.; Bada, J. L. *Earth and Planetary Science Letters* **2001**, *185*, 1-5.
67. Gotz, S.; Karst, U. *Anal. Bioanal Chem.* **2007**, *387*, 183-192.
68. Guttman, A. *Electrophoresis* **1995**, *16*, 611-616.
69. Ha, P. T.; Hoogmartens, J.; Van Schepdael, A. *J. Pharm. Biomed. Anal.* **2006**, *41*, 1-11.
70. Hahn, T.; O'Sullivan, C. K.; Drese, K. S. *Anal. Chem.* **2009**, *81*, 2904-2911.

71. Harris, D. C. *Quantitative Chemical Analysis*, 7<sup>th</sup> ed.; W. H. Freeman and Co.: New York, NY; 2006.
72. Hawkins, K. R.; Yager, P. *Lab. Chip.* **2003**, *3*, 248-252.
73. Hengen, P. N. *Trends Biochem. Sci.* **1995**, *20*, 324-325.
74. Herrero, M.; García-Cañas, V.; Simo, C.; Cifuentes, A. *Electrophoresis* **2010**, *31*, 205-228.
75. Hestekin, C. N.; Barron, A. E. *Electrophoresis* **2006**, *27*, 3805-3815.
76. Hinselwood, D. C.; Abrahamsen, T. W.; Ekstrom, P. O. *Electrophoresis* **2005**, *26*, 2553-2561.
77. Hinselwood, D. C.; Warren, D. J.; Ekstrom, P. O. *Electrophoresis* **2005**, *26*, 2562-2566.
78. Hiraoka, A.; Miura, I.; Tominaga, I.; Hattori, M. *Clin. Biochem.* **1989**, *22*, 293-296.
79. Hjertén, S. *J. Chromatogr. A.* **1985**, *347*, 191-198.
80. Hjertén, S. *J. Chromatogr. A.* **1983**, *270*, 1-6.
81. Hjertén, S. *J. Chromatogr.* **1972**, *65*, 345-348.
82. Hjertén, S. *Chromatogr. Rev.* **1967**, *9*, 122-219.
83. Hjertén, S.; Zhu, M. D. *J. Chromatogr. A.* **1985**, *346*, 265-270.
84. Hoebel, S. J.; Balss, K. M.; Jones, B. J.; Malliaris, C. D.; Munson, M. S.; Vreeland, W. N.; Ross, D. *Anal. Chem.* **2006**, *78*, 7186-7190.
85. Hruska, V.; Gas, B. *Electrophoresis* **2007**, *28*, 3-14.
86. Hsia, A. P.; Wen, T. J.; Chen, H. D.; Liu, Z.; Yandea-Nelson, M. D.; Wei, Y.; Guo, L.; Schnable, P. S. *Theor. Appl. Genet.* **2005**, *111*, 218-225.

87. Huang, Z.; Ivory, C. F. *Anal. Chem.* **1999**, *71*, 1628-1632.
88. Huber, D. E.; Santiago, J. G. *Electrophoresis* **2007**, *28*, 2333-2344.
89. Huber, D. E.; Santiago, J. G. *Proc. R. Soc. A.* **2008**, *464*, 595-612.
90. Humble, P. H.; Kelly, R. T.; Woolley, A. T.; Tolley, H. D.; Lee, M. L. *Anal. Chem.* **2004**, *76*, 5641-5648.
91. Hutt, L. D.; Glavin, D. P.; Bada, J. L.; Mathies, R. A. *Anal. Chem.* **1999**, *71*, 4000-4006.
92. Inano, K.; Tezuka, S.; Miida, T.; Okada, M. *Ann. Clin. Biochem.* **2000**, *37*, 708-716.
93. International HapMap Consortium; Frazer, K. A.; Ballinger, D. G.; Cox, D. R.; Hinds, D. A.; Stuve, L. L.; Gibbs, R. A.; Belmont, J. W.; Boudreau, A.; Hardenbol, P.; Leal, S. M.; Pasternak, S.; Wheeler, D. A.; Willis, T. D.; Yu, F.; Yang, H.; Zeng, C.; Gao, Y.; Hu, H.; Hu, W.; Li, C.; Lin, W.; Liu, S.; Pan, H.; Tang, X.; Wang, J.; Wang, W.; Yu, J.; Zhang, B.; Zhang, Q.; Zhao, H.; Zhao, H.; Zhou, J.; Gabriel, S. B.; Barry, R.; Blumenstiel, B.; Camargo, A.; Defelice, M.; Faggart, M.; Goyette, M.; Gupta, S.; Moore, J.; Nguyen, H.; Onofrio, R. C.; Parkin, M.; Roy, J.; Stahl, E.; Winchester, E.; Ziaugra, L.; Altshuler, D.; Shen, Y.; Yao, Z.; Huang, W.; Chu, X.; He, Y.; Jin, L.; Liu, Y.; Shen, Y.; Sun, W.; Wang, H.; Wang, Y.; Wang, Y.; Xiong, X.; Xu, L.; Wayne, M. M.; Tsui, S. K.; Xue, H.; Wong, J. T.; Galver, L. M.; Fan, J. B.; Gunderson, K.; Murray, S. S.; Oliphant, A. R.; Chee, M. S.; Montpetit, A.; Chagnon, F.; Ferretti, V.; Leboeuf, M.; Olivier, J. F.; Phillips, M. S.; Roumy, S.; Sallee, C.; Verner, A.; Hudson, T. J.; Kwok, P. Y.; Cai, D.; Koboldt, D. C.; Miller, R. D.; Pawlikowska, L.; Taillon-Miller, P.; Xiao,

M.; Tsui, L. C.; Mak, W.; Song, Y. Q.; Tam, P. K.; Nakamura, Y.; Kawaguchi, T.; Kitamoto, T.; Morizono, T.; Nagashima, A.; Ohnishi, Y.; Sekine, A.; Tanaka, T.; Tsunoda, T.; Deloukas, P.; Bird, C. P.; Delgado, M.; Dermitzakis, E. T.; Gwilliam, R.; Hunt, S.; Morrison, J.; Powell, D.; Stranger, B. E.; Whittaker, P.; Bentley, D. R.; Daly, M. J.; de Bakker, P. I.; Barrett, J.; Chretien, Y. R.; Maller, J.; McCarroll, S.; Patterson, N.; Pe'er, I.; Price, A.; Purcell, S.; Richter, D. J.; Sabeti, P.; Saxena, R.; Schaffner, S. F.; Sham, P. C.; Varilly, P.; Altshuler, D.; Stein, L. D.; Krishnan, L.; Smith, A. V.; Tello-Ruiz, M. K.; Thorisson, G. A.; Chakravarti, A.; Chen, P. E.; Cutler, D. J.; Kashuk, C. S.; Lin, S.; Abecasis, G. R.; Guan, W.; Li, Y.; Munro, H. M.; Qin, Z. S.; Thomas, D. J.; McVean, G.; Auton, A.; Bottolo, L.; Cardin, N.; Eyheramendy, S.; Freeman, C.; Marchini, J.; Myers, S.; Spencer, C.; Stephens, M.; Donnelly, P.; Cardon, L. R.; Clarke, G.; Evans, D. M.; Morris, A. P.; Weir, B. S.; Tsunoda, T.; Mullikin, J. C.; Sherry, S. T.; Feolo, M.; Skol, A.; Zhang, H.; Zeng, C.; Zhao, H.; Matsuda, I.; Fukushima, Y.; Macer, D. R.; Suda, E.; Rotimi, C. N.; Adebamowo, C. A.; Ajayi, I.; Aniagwu, T.; Marshall, P. A.; Nkwodimmah, C.; Royal, C. D.; Leppert, M. F.; Dixon, M.; Peiffer, A.; Qiu, R.; Kent, A.; Kato, K.; Niikawa, N.; Adewole, I. F.; Knoppers, B. M.; Foster, M. W.; Clayton, E. W.; Watkin, J.; Gibbs, R. A.; Belmont, J. W.; Muzzy, D.; Nazareth, L.; Sodergren, E.; Weinstock, G. M.; Wheeler, D. A.; Yakub, I.; Gabriel, S. B.; Onofrio, R. C.; Richter, D. J.; Ziaugra, L.; Birren, B. W.; Daly, M. J.; Altshuler, D.; Wilson, R. K.; Fulton, L. L.; Rogers, J.; Burton, J.; Carter, N. P.; Clee, C. M.; Griffiths, M.; Jones, M. C.; McLay, K.; Plumb, R. W.; Ross, M. T.; Sims, S. K.; Willey, D. L.; Chen, Z.; Han, H.; Kang, L.; Godbout,

- M.; Wallenburg, J. C.; L'Archeveque, P.; Bellemare, G.; Saeki, K.; Wang, H.; An, D.; Fu, H.; Li, Q.; Wang, Z.; Wang, R.; Holden, A. L.; Brooks, L. D.; McEwen, J. E.; Guyer, M. S.; Wang, V. O.; Peterson, J. L.; Shi, M.; Spiegel, J.; Sung, L. M.; Zacharia, L. F.; Collins, F. S.; Kennedy, K.; Jamieson, R.; Stewart, J. *Nature* **2007**, *449*, 851-861.
94. Ivory, C. F. *Electrophoresis* **2007**, *28*, 15-28.
95. Ivory, C. F. *Electrophoresis* **2004**, *28*, 15-25.
96. Ivory, C. F. *Sep. Sci. Technol.* **2000**, *35*, 1777-1793.
97. Iwata, T.; Kurosu, Y. *Anal. Sci.* **1995**, *11*, 131-133.
98. Janasek, D.; Schilling, M.; Franzke, J.; Manz, A. *Anal. Chem.* **2006**, *78*, 3815-3819.
99. Jazwinska, E. C.; Powell, L. W. *Hepatology* **1997**, *25*, 495-496.
100. Johnson, M. E.; Landers, J. P. *Electrophoresis* **2004**, *25*, 3513-3527.
101. Jorgenson, J. W.; Lukacs, K. D. *Science* **1983**, *222*, 266-272.
102. Jorgenson, J. W.; Lukacs, K. D. *Anal. Chem.* **1981**, *53*, 1298-1302.
103. 102 Jung, B.; Bharadwaj, R.; Santiago, J. G. *Anal. Chem.* **2006**, *78*, 2319-2327.
104. Jung, B.; Zhu, Y.; Santiago, J. G. *Anal. Chem.* **2007**, *79*, 345-349.
105. Kaigala, G. V.; Bercovici, M.; Behnam, M.; Elliott, D.; Santiago, J. G.; Backhouse, C. J. *Lab. Chip* **2010**, *10*, 2242-2250.
106. Kakavas, V. K.; Plageras, P.; Vlachos, T. A.; Papaioannou, A.; Noulas, V. A. *Mol. Biotechnol.* **2008**, *38*, 155-163.

107. Kamande, M. W.; Ross, D.; Locascio, L. E.; Lowry, M.; Warner, I. M. *Anal. Chem.* **2007**, *79*, 1791-1796.
108. Kan, C. W.; Fredlake, C. P.; Doherty, E. A.; Barron, A. E. *Electrophoresis* **2004**, *25*, 3564-3588.
109. Kan, Y. W.; Dozy, A. M. *Proc. Natl. Acad. Sci. U. S. A.* **1978**, *75*, 5631-5635.
110. Kar, S.; Dasgupta, P. K. *J. Microchem.* **199**, *62*, 128-137.
111. Kartsova, L. A.; Bessonova, E. A. *J. Anal. Chem.* **2009**, *64*, 326-337.
112. Kašička, V. *Electrophoresis* **2010**, *31*, 122-146.
113. Kasicka, V. *Electrophoresis* **2008**, *29*, 179-206.
114. Kerem, E.; Corey, M.; Kerem, B. S.; Rommens, J.; Markiewicz, D.; Levison, H.; Tsui, L. C.; Durie, P. N. *Engl. J. Med.* **1990**, *323*, 1517-1522.
115. Khurana, T. K.; Santiago, J. G. *Anal. Chem.* **2008**, *80*, 6300-6307.
116. Kiesewetter, S.; Macek, M., Jr; Davis, C.; Curristin, S. M.; Chu, C. S.; Graham, C.; Shrimpton, A. E.; Cashman, S. M.; Tsui, L. C.; Mickle, J. *Nat. Genet.* **1993**, *5*, 274-278.
117. Kilar, F. *Electrophoresis* **2003**, *24*, 3908-3916.
118. Kim, S. M.; Sommer, G. J.; Burns, M. A.; Hasselbrink, E. F. *Anal. Chem.* **2006**, *78*, 8028-8035.
119. Kim, S.; Misra, A. *Annu. Rev. Biomed. Eng.* **2001**, *9*, 289-320.
120. Kjellin, K. G.; Hallander, L. *J. Neurol.* **1979**, *221*, 235-244.
121. Klampfl, C. W. *Electrophoresis* **2009**, *30*, S83-91.
122. Koegler, W. S.; Ivory, C. F. *J. Chromatogr. A.* **1996**, *726*, 229-236.

123. Kohlheyer, D.; Eijkel, J. C.; van den Berg, A.; Schasfoort, R. B. *Electrophoresis* **2008**, *29*, 977-993.
124. Kohlrausch, F. *Ann. Phys. Chem.* **1897**, *62*, 209-239.
125. Kok, W. T. *Anal. Chem.* **1993**, *65*, 1853-1860.
126. Kolin, A. *J. Chem. Phys.* **1954**, *22*, 1628-1629.
127. Kondratova, V. N.; Botezatu, I. V.; Shelepov, V. P.; Lichtenstein, A. V. *Anal. Biochem.* **2011**, *408*, 304-308.
128. Kopwille, A.; Merriman, W. G.; Cuddeback, R. M.; Smolka, A. J.; Bier, M. J. *J. Chromatogr.* **1976**, *118*, 34-46.
129. Krivankova, L.; Bocek, P. *J. Chromatogr. B Biomed. Sci. Appl.* **1997**, *689*, 13-34.
130. Kuhr, W. G.; Monnig, C. A. *Anal. Chem.* **1992**, *64*, 389-407.
131. Kwok, P. Y.; Gu, Z. *Mol. Med. Today* **1999**, *5*, 538-543.
132. Landers, J. P. *Handbook of Capillary Electrophoresis, 2nd Ed.*; CRC Press: Boca Raton, FL.; **1997**.
133. Lewis, G. N. *J. Am. Chem. Soc.* **1910**, *32*, 862-869.
134. Lin, C. H.; Kaneta, T. *Electrophoresis* **2004**, *25*, 4058-4073.
135. Lin, H.; Shackman, J. G.; Ross, D. *Lab. Chip* **2008**, *8*, 969-978.
136. Liu, D.; Chen, B.; Wang, L.; Zhou, X. *Electrophoresis* **2009**, *30*, 4300-4305.
137. Liu, D.; Ou, Z.; Xu, M.; Wang, L. *J. Chromatogr. A* **2008**, *1214*, 165-170.
138. Majors, R. E. *LG-GC.* **1997**, *15*, 412, 413, 416-420, 422.
139. Mala, Z.; Slampova, A.; Gebauer, P.; Bocek, P. *Electrophoresis* **2009**, *30*, 215-229.

140. Mamunooru, M.; Jenkins, R. J.; Davis, N. I.; Shackman, J. G. *J. Chromatogr. A* **2008**, *1202*, 203-211.
141. Matsui, T.; Franzke, J.; Manz, A.; Janasek, D. *Electrophoresis* **2007**, *28*, 4606-4611.
142. Mazereeuw, M.; Tjaden, U. R.; Reinhoud, N. J. *J. Chromatogr. Sci.* **1995**, *33*, 686-697.
143. Mazereeuw, M.; Tjaden, U. R.; van der Greef, J. *J. Chromatogr. A* **1994**, *677*, 151-157.
144. Mazereeuw, M.; Spikmans, V.; Tjaden, U. R.; van der Greef, J. *J. Chromatogr. A* **2000**, *879*, 219-233.
145. McDonald, G. D.; Storrie-Lombardi, M. C. *Astrobiology* **2006**, *6*, 17-33.
146. Medintz, I.; Wong, W. W.; Berti, L.; Shiow, L.; Tom, J.; Scherer, J.; Sensabaugh, G.; Mathies, R. A. *Genome Res.* **2001**, *11*, 413-421.
147. Meighan, M. M.; Staton, S. J.; Hayes, M. A. *Electrophoresis* **2009**, *30*, 852-865.
148. Mikkers, F. E. P.; Everaerts, F. M.; Verheggen, T. P. E. *J. Chromatogr. A* **1979**, *169*, 11-20.
149. Mikkers, F.; Ringoir, S.; De Smet, R. *J. Chromatogr.* **1979**, *162*, 341-350.
150. Minarik, M.; Benesova, L.; Fantova, L.; Horacek, J.; Heracek, J.; Loukola, A. *Electrophoresis* **2006**, *27*, 3856-3863.
151. Mohan, D.; Lee, C. S. *Electrophoresis* **2002**, *23*, 3160-3167.
152. Munson, M. S.; Danger, G.; Shackman, J. G.; Ross, D. *Anal. Chem.* **2007**, *79*, 6201-6207.

153. Munson, M. S.; Meacham, J. M.; Locascio, L. E.; Ross, D. *Anal. Chem.* **2008**, *80*, 172-178.
154. Munson, M. S.; Meacham, J. M.; Ross, D.; Locascio, L. E. *Electrophoresis* **2008**, *29*, 3456-3465.
155. Nataraj, A. J.; Olivos-Glander, I.; Kusukawa, N.; Highsmith, W. E., Jr. *Electrophoresis* **1999**, *20*, 1177-1185.
156. Navon, R.; Proia, R. L. *Science* **1989**, *243*, 1471-1474.
157. Neue, U. D. *J. Chromatogr. A* **2005**, *1079*, 153-161.
158. Oefner, P.; Hafele, R.; Bartsch, G. *J. Chromatogr.* **1990**, *516*, 251-262.
159. O'farrell, P. H. *Science* **1985**, *227*, 1586-1589.
160. Orita, M.; Suzuki, Y.; Sekiya, T.; Hayashi, K. *Genomics* **1989**, *5*, 874-879.
161. Osbourn, D. M.; Weiss, D. J.; Lunte, C. E. *Electrophoresis* **2000**, *21*, 2768-2779.
162. Pang, H. M.; Kenseth, J.; Coldiron, S. *Drug Discov. Today* **2004**, *9*, 1072-1080.
163. Peltonen, L.; McKusick, V. A. *Science* **2001**, *291*, 1224-1229.
164. Peric, I.; Kenndler, E. *Electrophoresis* **2003**, *24*, 2924-2934.
165. Petr, J.; Maier, V.; Horakova, J.; Sevcik, J.; Stransky, Z. *J. Sep. Sci.* **2006**, *29*, 2705-2715.
166. Petsev, D. N.; Lopez, G. P.; Ivory, C. F.; Sibbett, S. S. *Lab. Chip* **2005**, *5*, 587-597.
167. Pettersson, E.; Lundeberg, J.; Ahmadian, A. *Genomics* **2009**, *93*, 105-111.
168. Poinot, V.; Gavard, P.; Feurer, B.; Couderc, F. *Electrophoresis* **2010**, *31*, 105-121.

169. Poinso, V.; Rodat, A.; Gavard, P.; Feurer, B.; Couderc, F. *Electrophoresis* **2008**, *29*, 207-223.
170. Pospichal, J.; Gebauer, P.; Bocek, P. *Chem. Rev.* **1989**, *89*, 419-430.
171. Prest, J. E.; Baldock, S. J.; Day, P. J.; Fielden, P. R.; Goddard, N. J.; Treves Brown, B. J. *J. Chromatogr. A* **2007**, *1156*, 154-159.
172. Prochazkova, B.; Glovinova, E.; Pospichal, J. *Electrophoresis* **2007**, *28*, 2168-2173.
173. Qu, Q.; Liu, Y.; Tang, X.; Wang, C.; Yang, G.; Hu, X.; Yan, C. *Electrophoresis*. **2006**, *27*, 4500-4507.
174. Quirino, J. P.; Terabe, S. *J. Capillary Electrophor.* **1997**, *4*, 233-245.
175. Quirino, J. P.; Terabe, S. *J. Chromatogr. A* **2000**, *902*, 119-135.
176. Quirino, J. P.; Terabe, S. *J. Chromatogr. A* **2000**, *902*, 119-135.
177. Ratain, M. J.; Relling, M. V. *Nat. Med.* **2001**, *7*, 283-285.
178. Reinhoud, N. J.; Tjaden, U. R.; van der Greef, J. *J. Chromatogr. A* **1993**, *641*, 155-162.
179. Reinhoud, N. J.; Tjaden, U. R.; van der Greef, J. *J. Chromatogr. A* **1993**, *653*, 303-312.
180. Reinhoud, N. J.; Tjaden, U. R.; van der Greef, J. *J. Chromatogr. A* **1993**, *653*, 303-312.
181. Ren, L.; Masliyah, J.; Li, D. *J. Colloid Interface Sci.* **2003**, *257*, 85-92.
182. Riesner, D.; Steger, G.; Zimmat, R.; Owens, R. A.; Wagenhofer, M.; Hillen, W.; Vollbach, S.; Henco, K. *Electrophoresis* **1989**, *10*, 377-389.
183. Righetti, P. G.; Bossi, A. *Anal. Chim. Acta.* **1998**, *372*, 1-19.

184. Righetti, P. G.; Gelfi, C. *J. Chromatogr. B Biomed. Sci. Appl.* **1997**, *697*, 195-205.
185. Rodriguez-Diaz, R.; Wehr, T.; Zhu, M. *Electrophoresis* **1997**, *18*, 2134-2144.
186. Ross, D.; Locascio, L. E. *Anal. Chem.* **2002**, *74*, 2556-2564.
187. Ross, D.; Kralj, J. G. *Anal. Chem.* **2008**, *80*, 9467-9474.
188. Ross, D.; Romantseva, E. F. *Anal. Chem.* **2009**, *81*, 7326-7335.
189. Ryslavý, Z.; Bocek, P.; Deml, M.; Janak, J. *J. Chromatogr. A* **1978**, *147*, 446-448.
190. Schell, J.; Wulfert, M.; Riesner, D. *Electrophoresis* **1999**, *20*, 2864-2869.
191. Shackman, J. G.; Munson, M. S.; Kan, C. W.; Ross, D. *Electrophoresis* **2006**, *27*, 3420-3427.
192. Shackman, J. G.; Munson, M. S.; Ross, D. *Anal. Bioanal Chem.* **2007**, *387*, 155-158.
193. Shackman, J. G.; Ross, D. *Electrophoresis* **2007**, *28*, 556-571.
194. Shackman, J. G.; Watson, C. J.; Kennedy, R. T. *J. Chromatogr. A* **2004**, *1040*, 273-282.
195. Shackman, J. G.; Munson, M. S.; Ross, D. *Anal. Chem.* **2007**, *79*, 565-571.
196. Shackman, J. G.; Ross, D. *Anal. Chem.* **2007**, *79*, 6641-6649.
197. Shen, Y.; Wu, B. L. *Clin. Chem.* **2009**, *55*, 659-669.
198. Shimura, K. *Electrophoresis* **2002**, *23*, 3847-3857.
199. Simpson, S. L., Jr.; Quirino, J. P.; Terabe, S. *J. Chromatogr. A* **2008**, *1184*, 504-541.
200. Sjoback, R.; Nygren, J.; Kubista, M. *Biopolymers* **1998**, *46*, 445-453.

201. Skelley, A. M.; Scherer, J. R.; Aubrey, A. D.; Grover, W. H.; Ivester, R. H.; Ehrenfreund, P.; Grunthaner, F. J.; Bada, J. L.; Mathies, R. A. *PNAS*. **2005**, *102*, 1041-1046.
202. Smuts, H. E.; Russell, B. W.; Moodie, J. W. *J. Neurol. Sci.* **1982**, *56*, 283-292.
203. Sommer, G. J.; Kim, S. M.; Littrell, R. J.; Hasselbrink, E. F. *Lab. Chip* **2007**, *7*, 898-907.
204. Sueyoshi, K.; Kitagawa, F.; Otsuka, K. *J. Sep. Sci.* **2008**, *31*, 2650-2666.
205. Tang, G.; Yang, C. *Electrophoresis* **2008**, *29*, 1006-1012.
206. Tanyanyiwa, J.; Abad-Villar, E. M.; Fernandez-Abedul, M. T.; Costa-Garcia, A.; Hoffmann, W.; Guber, A. E.; Herrmann, D.; Gerlach, A.; Gottschlich, N.; Hauser, P. C. *Analyst* **2003**, *128*, 1019-1022.
207. Terabe, S. *Annu. Rev. Anal. Chem.* **2009**, *2*, 99-120.
208. Terabe, S.; Otsuka, K.; Ando, T. *Anal. Chem.* **1985**, *57*, 834-841.
209. Tulp, A.; Verwoerd, D.; Hart, A. A. *Electrophoresis* **1997**, *18*, 767-773.
210. Tůma, P.; Samcova, E.; Andelova, K. *J. Chromatogr. B.* **2006**, *839*, 12-18.
211. Vacik, J.; Zuska, J. *J. Chromatogr. A* **1974**, *91*, 795-808.
212. Van Deemter, J. J.; Zuiderweg, F. J.; Klinkenberg, A. *Chem. Eng. Sci.* **1956**, *5*, 271-289.
213. Venter, J. C.; Adams, M. D.; Myers, E. W.; Li, P. W.; Mural, R. J.; Sutton, G. G.; Smith, H. O.; Yandell, M.; Evans, C. A.; Holt, R. A.; Gocayne, J. D.; Amanatides, P.; Ballew, R. M.; Huson, D. H.; Wortman, J. R.; Zhang, Q.; Kodira, C. D.; Zheng, X. H.; Chen, L.; Skupski, M.; Subramanian, G.; Thomas, P. D.; Zhang, J.; Gabor Miklos, G. L.; Nelson, C.; Broder, S.; Clark, A. G.; Nadeau, J.; McKusick,

V. A.; Zinder, N.; Levine, A. J.; Roberts, R. J.; Simon, M.; Slayman, C.;  
Hunkapiller, M.; Bolanos, R.; Delcher, A.; Dew, I.; Fasulo, D.; Flanigan, M.;  
Florea, L.; Halpern, A.; Hannenhalli, S.; Kravitz, S.; Levy, S.; Mobarry, C.;  
Reinert, K.; Remington, K.; Abu-Threideh, J.; Beasley, E.; Biddick, K.; Bonazzi,  
V.; Brandon, R.; Cargill, M.; Chandramouliswaran, I.; Charlab, R.; Chaturvedi,  
K.; Deng, Z.; Di Francesco, V.; Dunn, P.; Eilbeck, K.; Evangelista, C.;  
Gabrielian, A. E.; Gan, W.; Ge, W.; Gong, F.; Gu, Z.; Guan, P.; Heiman, T. J.;  
Higgins, M. E.; Ji, R. R.; Ke, Z.; Ketchum, K. A.; Lai, Z.; Lei, Y.; Li, Z.; Li, J.;  
Liang, Y.; Lin, X.; Lu, F.; Merkulov, G. V.; Milshina, N.; Moore, H. M.; Naik, A.  
K.; Narayan, V. A.; Neelam, B.; Nusskern, D.; Rusch, D. B.; Salzberg, S.; Shao,  
W.; Shue, B.; Sun, J.; Wang, Z.; Wang, A.; Wang, X.; Wang, J.; Wei, M.; Wides,  
R.; Xiao, C.; Yan, C.; Yao, A.; Ye, J.; Zhan, M.; Zhang, W.; Zhang, H.; Zhao, Q.;  
Zheng, L.; Zhong, F.; Zhong, W.; Zhu, S.; Zhao, S.; Gilbert, D.; Baumhueter, S.;  
Spier, G.; Carter, C.; Cravchik, A.; Woodage, T.; Ali, F.; An, H.; Awe, A.;  
Baldwin, D.; Baden, H.; Barnstead, M.; Barrow, I.; Beeson, K.; Busam, D.;  
Carver, A.; Center, A.; Cheng, M. L.; Curry, L.; Danaher, S.; Davenport, L.;  
Desilets, R.; Dietz, S.; Dodson, K.; Doup, L.; Ferriera, S.; Garg, N.;  
Gluecksmann, A.; Hart, B.; Haynes, J.; Haynes, C.; Heiner, C.; Hladun, S.;  
Hostin, D.; Houck, J.; Howland, T.; Ibegwam, C.; Johnson, J.; Kalush, F.; Kline,  
L.; Koduru, S.; Love, A.; Mann, F.; May, D.; McCawley, S.; McIntosh, T.;  
McMullen, I.; Moy, M.; Moy, L.; Murphy, B.; Nelson, K.; Pfannkoch, C.; Pratts,  
E.; Puri, V.; Qureshi, H.; Reardon, M.; Rodriguez, R.; Rogers, Y. H.; Romblad,  
D.; Ruhfel, B.; Scott, R.; Sitter, C.; Smallwood, M.; Stewart, E.; Strong, R.; Suh,

E.; Thomas, R.; Tint, N. N.; Tse, S.; Vech, C.; Wang, G.; Wetter, J.; Williams, S.; Williams, M.; Windsor, S.; Winn-Deen, E.; Wolfe, K.; Zaveri, J.; Zaveri, K.; Abril, J. F.; Guigo, R.; Campbell, M. J.; Sjolander, K. V.; Karlak, B.; Kejariwal, A.; Mi, H.; Lazareva, B.; Hatton, T.; Narechania, A.; Diemer, K.; Muruganujan, A.; Guo, N.; Sato, S.; Bafna, V.; Istrail, S.; Lippert, R.; Schwartz, R.; Walenz, B.; Yooseph, S.; Allen, D.; Basu, A.; Baxendale, J.; Blick, L.; Caminha, M.; Carnes-Stine, J.; Caulk, P.; Chiang, Y. H.; Coyne, M.; Dahlke, C.; Mays, A.; Dombroski, M.; Donnelly, M.; Ely, D.; Esparham, S.; Fosler, C.; Gire, H.; Glanowski, S.; Glasser, K.; Glodek, A.; Gorokhov, M.; Graham, K.; Gropman, B.; Harris, M.; Heil, J.; Henderson, S.; Hoover, J.; Jennings, D.; Jordan, C.; Jordan, J.; Kasha, J.; Kagan, L.; Kraft, C.; Levitsky, A.; Lewis, M.; Liu, X.; Lopez, J.; Ma, D.; Majoros, W.; McDaniel, J.; Murphy, S.; Newman, M.; Nguyen, T.; Nguyen, N.; Nodell, M.; Pan, S.; Peck, J.; Peterson, M.; Rowe, W.; Sanders, R.; Scott, J.; Simpson, M.; Smith, T.; Sprague, A.; Stockwell, T.; Turner, R.; Venter, E.; Wang, M.; Wen, M.; Wu, D.; Wu, M.; Xia, A.; Zandieh, A.; Zhu, X. *Science* **2001**, *291*, 1304-1351.

214. Verheggen, Th. P. E. M.; Mikkers, F. E. P.; Everaerts, F. M. J. *Chromatogr. A* **1977**, *132*, 205-215.
215. Vesterberg, O. *Methods Enzymol.* **1971**, *22*, 389-412.
216. Vesterberg, O. *Electrophoresis* **1993**, *14*, 1243-1249.
217. Vesterberg, O. *J.Chromatogr.* **1989**, *480*, 3-19.
218. Vyas, C. A.; Mamunooru, M.; Shackman, J. G. *Chromatographia* **2009**, *70*, 151-156.

219. Vyas, C. A.; Flanigan, P. M.; Shackman, J. G. *Bioanalysis* **2010**, *2*, 815-827.
220. Wang, Q.; Tolley, H. D.; LeFebre, D. A.; Lee, M. L. *Anal. Bioanal Chem.* **2002**, *373*, 125-135.
221. Wang, Q.; Yu, H.; Li, H.; Ding, F.; He, P.; Fang, Y. *Food Chem.* **2003**, *83*, 311-317.
222. Wang, Z.; Moulton, J. *Hum. Mutat.* **2001**, *17*, 263-270.
223. Wang, J.; Zhang, Y.; Mohamadi, M. R.; Kaji, N.; Tokeshi, M.; Baba, Y. *Electrophoresis* **2009**, *30*, 3250-3256.
224. Ward, C. P.; Fensom, A. H.; Green, P. M. *Genet. Test.* **2000**, *4*, 351-358.
225. Wartell, R. M.; Hosseini, S.; Powell, S.; Zhu, J. *J. Chromatogr. A* **1998**, *806*, 169-185.
226. Waterfall, C. M.; Cobb, B. D. *Nucleic Acids Res.* **2001**, *29*, E119.
227. Weinberger, R. *Practical Capillary Electrophoresis*, Academic Press, Inc.: New York; **1993**.
228. White, M. B.; Carvalho, M.; Derse, D.; O'Brien, S. J.; Dean, M. *Genomics* **1992**, *12*, 301-306.
229. Xu, Z. Q.; Hirokawa, T.; Nishine, T.; Arai, A. *J. Chromatogr. A* **2003**, *990*, 53-61.
230. Zhang, H. D.; Zhou, J.; Xu, Z. R.; Song, J.; Dai, J.; Fang, J.; Fang, Z. L. *Lab. Chip* **2007**, *7*, 1162-1170.
231. Zhang, W.; Jin, J.; Fan, L. Y.; Li, S.; Shao, J.; Cao, C. X. *J. Sep. Sci.* **2009**, *32*, 2123-2131.
232. Zhao, S.; Liu, Y. M. *Electrophoresis* **2001**, *22*, 2769-2774.
233. Zhu, L.; Lee, H. K.; Lin, B.; Yeung, E. S. *Electrophoresis* **2001**, *22*, 3683-3687.